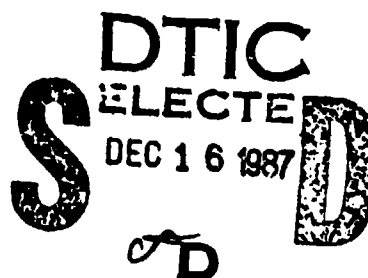


# STRAIN RATE EFFECTS FOR CONCRETE AND FIBER REINFORCED CONCRETE SUBJECTED TO IMPACT LOADING

Final Report



By : Surendra P. Shah

October 1987

Prepared for : U. S. Army Research Office  
Metallurgy and Materials Science Division

Grant Number : DAAG29-82-K-0171

Center for Concrete and Geomaterials  
Department of Civil Engineering  
Northwestern University  
Evanston, IL 60201



Approved for public release ; Distribution Unlimited

87 12 9 008

AD-A188 659

THE VIEW, OPINIONS, AND/OR FINDINGS CONTAINED IN THIS REPORT ARE THOSE OF THE AUTHOR(S) AND SHOULD NOT BE CONSTRUED AS AN OFFICIAL DEPARTMENT OF THE ARMY POSITION, POLICY, OR DECISION, UNLESS SO DESIGNATED BY OTHER DOCUMENTATION.

# **STRAIN RATE EFFECTS FOR CONCRETE AND FIBER REINFORCED CONCRETE SUBJECTED TO IMPACT LOADING**

**Final Report**

**By : Surendra P. Shah**

**October 1987**

**Prepared for : U. S. Army Research Office  
Metallurgy and Materials Science Division**

**Grant Number : DAAG29-82-K-0171**

**Center for Concrete and Geomaterials  
Department of Civil Engineering  
Northwestern University  
Evanston, IL 60201**



**Approved for public release ; Distribution Unlimited**

UNCLASSIFIED

SECURITY CLASSIFICATION OF THIS PAGE (When Data Entered)

AD-A188 659

| REPORT DOCUMENTATION PAGE  |                       | READ INSTRUCTIONS<br>BEFORE COMPLETING FORM                                   |
|--|-----------------------|---|
| 1. REPORT NUMBER   | 2. GOVT ACCESSION NO. | 3. RECIPIENT'S CATALOG NUMBER   |
|  | N/A                   | N/A   |
| 4. TITLE (and Subtitle)<br>Strain Rate Effects for Concrete and Fiber Reinforced Concrete Subjected to Impact Loading  |                       | 5. TYPE OF REPORT & PERIOD COVERED<br>Final Report<br>Sept. 1982 - Aug. 1987. |
|  |                       | 6. PERFORMING ORG. REPORT NUMBER  |
| 7. AUTHOR(s)<br>SHAH, Surendra P.  |                       | 8. CONTRACT OR GRANT NUMBER(s)<br>DAAG29 - 82 - K - 0171                      |
| 9. PERFORMING ORGANIZATION NAME AND ADDRESS<br>Northwestern University<br>Evanston, IL 60201   |                       | 10. PROGRAM ELEMENT, PROJECT, TASK AREA & WORK UNIT NUMBERS                   |
| 11. CONTROLLING OFFICE NAME AND ADDRESS<br>U. S. Army Research Office<br>Post Office Box 12211<br>Research Triangle Park, NC 27709   |                       | 12. REPORT DATE<br>October 1987   |
|  |                       | 13. NUMBER OF PAGES<br>82   |
| 14. MONITORING AGENCY NAME & ADDRESS (if different from Controlling Office)  |                       | 15. SECURITY CLASS. (of this report)<br>Unclassified                          |
|  |                       | 15a. DECLASSIFICATION/DOWNGRADING SCHEDULE                                    |
| 16. DISTRIBUTION STATEMENT (of this Report)<br><br>Approved for public release; distribution unlimited.  |                       |   |
| 17. DISTRIBUTION STATEMENT (of the abstract entered in Block 20, if different from Report)<br><br>NA   |                       |   |
| 18. SUPPLEMENTARY NOTES<br><br>The view, opinions, and/or findings contained in this report are those of the author(s) and should not be construed as an official Department of the Army position, policy, or decision, unless so designated by other documentation.   |                       |   |
| 19. KEY WORDS (Continue on reverse side if necessary and identify by block number)<br>Charpy test ; damage ; flexural fracture;<br>cracks ; dynamic, fracture mechanics;<br>concrete ; experiments ; impact;<br>constitutive fiber composite; instrumented testing,<br>modeling; fiber reinforced concrete, microcracks (cont'd) |                       |   |
| 20. ABSTRACT (Continue on reverse side if necessary and identify by block number)<br><br>see 2. SUMMARY  |                       |   |

DD FORM 1 JAN 73 1473

EDITION OF 1 NOV 65 IS OBSOLETE

UNCLASSIFIED

SECURITY CLASSIFICATION OF THIS PAGE (When Data Entered)

UNCLASSIFIED

SECURITY CLASSIFICATION OF THIS PAGE(When Data Entered)

19. KEYWORDS (cont'd)

|                |                  |                        |
|----------------|------------------|------------------------|
| micromechanics | rate-sensitivity | tensile fracture       |
| nonlinear      | steel fibers     | high strength concrete |
| pullout        | strain rate      |                        |

UNCLASSIFIED

SECURITY CLASSIFICATION OF THIS PAGE(When Data Entered)

# CONTENTS

|  |    |
|--|----|
| 1. RESEARCH OBJECTIVE .....  | 1  |
| 2. SUMMARY .....   | 1  |
| 3. LIST OF PUBLICATIONS .....  | 3  |
| Refreed Articles .....   | 3  |
| Symposium Proceedings Articles .....   | 4  |
| Theses .....   | 5  |
| 4. LIST OF PRINCIPAL PROFESSIONAL COLLABORATORS .....  | 6  |
| 5. ADDITIONAL INFORMATION .....  | 6  |
| Paper I. Constitutive Modeling of Concrete Under Impact Loading .  | 7  |
| Paper II. Strength, Deformation and Fracture Toughness of Fiber<br>Cement Composites at Different Rates of Loading ..... | 39 |



|  |   |
|--|---|
| Accession For                                      |   |
| NTIS   | CRA&I <input checked="" type="checkbox"/> |
| DTIC   | TAB <input type="checkbox"/>              |
| Unannounced Justification <input type="checkbox"/> |   |
| By   |   |
| Distribution                                       |   |
| Availability Codes                                 |   |
| Disa   | Acad and/or Special                       |
| A-1  |   |

## 1. RESEARCH OBJECTIVE

It is known that increase in rate of loading alters the fracture strength and cracking behavior of cement based composites such as concrete and steel fiber reinforced concrete. The main objectives of this research were: (1) development of a rational and accurate experimental procedure for evaluating impact properties of cementitious materials, (2) experimental observations of impact behavior of plain and steel fiber reinforced concrete, and (3) development of damage based rate sensitive constitutive laws and fracture mechanics based model for predicting the response of concrete under impact loading.



## 2. SUMMARY

Despite its extensive use, low tensile strength has been recognized as one of the major drawbacks of concrete. Although one has learned to avoid exposing concrete structures to adverse static tensile loads, these structures cannot be shielded from short duration dynamic tensile loads. Such loads originate from sources such as impact from missiles and projectiles, wind gusts, earthquakes and machine vibrations. In addition, modern computer-aided analysis and use of concrete for special structures such as reactor containment vessels, missile storage silos and fall-out shelters, has led to a growing interest in the cracking behavior of concrete. Experimental results indicate that the fracture strength and cracking behavior of concrete are affected by the rate of loading. To accurately predict the structural response under impact conditions, the knowledge of behavior of concrete at high rates of loading is essential.

One method to improve the resistance of concrete when subjected to impact and/or impulsive loading is by the incorporation of randomly distributed short .

steel fibers. Concrete (or mortar) so reinforced is termed steel fiber reinforced concrete (SFRC). As yet no standard test methods are available to quantify the impact resistance of such composites, although several investigators have employed a variety of tests including drop weight, swinging pendulums and the detonation of explosives. These tests though useful in ascertaining the relative merits of different composites do not yield basic material characteristics which can be used for design.

→ Using a two degree of freedom model guidelines were developed for designing an impact test setup, thus enabling one to conduct impact tests free of adverse inertial effects. Based on these guidelines, the author has developed an instrumented modified Charpy impact testing system. This experimental test setup was used to obtain basic information such as load-deflection relationship, fracture toughness, crack velocity (measured using 'Kraak Gages'), and load-strain history during an impact fracture event of plain concrete and SFRC. (keywords: go to DD1473)

Some of the main experimental results are listed below:

- (1) the fracture strength and fracture toughness of concrete and SFRC increase at impact rates,
- (2) Young's modulus of elasticity can be considered rate independent for the strain rate range of  $10^{-7}$  to 1.0 per second,
- (3) prepeak nonlinearity may be attributed to prepeak crack growth (also termed fracture process zone or slow crack growth). This prepeak crack growth and hence prepeak nonlinearity decreases at impact rates, and
- (4) stress intensity factor calculations and crack velocity observations at impact rates indicate that stress corrosion type models and dynamic crack models may be inapplicable at such rates of loading.

Based on the experimental evidence from this and other investigations, two analytical models were developed.

The first model was a continuum damage based rate sensitive constitutive theory developed to predict the behavior of concrete under dynamic loading conditions. This model was based on the observation that the prepeak nonlinearity could be attributed to microcracking and that the extent of microcracking is rate dependent. The proposed model could predict the impact loading effect on concrete under uniaxial stress (compression or tension) and biaxial compression-tension stress states. A fracture mechanics approach was adopted for the second model. This model was based on the observation that to obtain size and geometry independent fracture parameter(s) one should include prepeak crack growth in the evaluation of this parameter(s) and that this prepeak crack growth decreases with increase in rate of loading. The second model could predict all the observed rate effect phenomena in mode I fracture, i.e. tensile and flexural failure.

For more details regarding this investigation, the reader is referred to the attached copies of two papers.

### 3. LIST OF PUBLICATIONS

#### Refereed Articles:

1. Suaris, W., and Shah, S. P., "Properties of Concrete Subjected to Impact," Journal of Structural Engineering, ASCE, Vol. 109, No. 7, pp. 1727-1741, July 1983.
2. Suaris, W., and Shah, S. P., "Test Methods for Impact Resistance of Fiber Reinforced Concrete," Fiber Reinforced Concrete, ACI, SP-81, 1984.
3. Suaris, W., and Shah, S. P., "Rate-Sensitive Damage Theory for Brittle Solids," Journal of Engineering Mechanics, ASCE, Vol. 110, No. 6, pp. 985-997, June 1984.
4. Gopalaratnam, V. S., Shah, S. P., and John, R., "A Modified Instrumented Charpy Test for Cement Based Composites," Experimental Mechanics, SEM, Vol. 24, No. 2, pp. 102-111, June 1984.

5. Suaris, W., and Shah, S. P., "Constitutive Model for Dynamic Loading of Concrete." ASCE, Journal of Structural Engineering, Vol. 111, No. 3, pp. 563-576, March 1985.
6. Gopalaratnam, V. S., and Shah, S. P., "Properties of Steel-Fiber Reinforced Concrete Subjected to Impact Loading," ACI Journal, Vol. 83, No. 1, pp. 117-126, January - February 1986.
7. John, R. and Shah, S. P., "Fracture of Concrete Subjected to Impact Loading," Journal of Cement, Concrete and Aggregates, ASTM, Vol. 8, No. 1, pp. 24-32, Summer 1986.
8. Gopalaratnam, V. S., and Shah, S. P., "Failure Mechanisms and Fracture of Fiber Reinforced Concrete," ACI Fiber Reinforced Concrete Symposium, Baltimore, Special Publication 105 (eds. G. Batson and S. P. Shah), November 1986.
9. John, R., Shah, S. P., and Jenq, Y. S., "A Fracture Mechanics Model to Predict the Rate Sensitivity of Mode I Fracture of Concrete," Journal of Cement and Concrete Research, Vol. 17, No. 2, pp. 249-262, March 1987.
10. Gopalaratnam, V. S., and Shah, S. P., "Tensile Failure of Steel Fiber Reinforced Mortar," Journal of the Engineering Mechanics Division, ASCE, Vol. 113, No. 5, pp. 635-652, May 1987.

#### **Symposium Proceedings Articles:**

1. Shah, S. P., "Constitutive Relations of Concrete Subjected to a Varying Strain Rate," Proceedings, Symposium on the Interaction of Nonnuclear Munitions with Structures, U.S. Air Force Academy, Colorado, May 10-13, pp. 81-84, 1983.
2. Suaris, W. and Shah, S. P., "A Strain Rate Dependent Damage Model for Concrete," Proceedings of the Fourth Engineering Mechanics Conference, Purdue University, pp. 977-980, May 1983.
3. Suaris, W., and Shah, S. P., "Mechanical Properties of Concrete at High Strain Rates," Proceedings, SMIRT-7, Chicago, 1983.
4. Suaris, W., and Shah, S. P., "A Strain Rate Sensitive Damage Model for the Biaxial Behavior of Concrete," Proceedings, RILEM-CEB Conference on Multiaxial Loading of Concrete, Vol. II, Toulouse, France, May 1984.
5. Gopalaratnam, V. S., and Shah, S. P., "Instrumented Impact Testing of Brittle Materials," Proceedings 5th ASCE Engineering Mechanics Division Specialty Conference, University of Wyoming, pp. 635-638, August 1984.
6. Gopalaratnam, V. S., and Shah, S. P., "Micromechanical Model for the Tensile Fracture of Steel Fiber Reinforced Concrete," Proceedings of the 3rd International Fiber Concrete Symposium, University of Sheffield, U.K., July 1986.

7. Shah, S. P., and Gopalaratnam, V. S., "Impact Resistance Measurements for Fiber Cement Composites," Proceedings of the 3rd International Fiber Concrete Symposium, University of Sheffield, U.K., July 1986.
8. Shah, S. P., and John, R., "Rate Sensitivity of Mode I and Mode II Fracture of Concrete, in Cement Based Composites: Strain Rate Effects on Fracture (eds. S. Mindess and S. P. Shah) MRS Symposia Proceedings, Vol. 64, pp. 21-37, 1986.
9. Shah, S. P., "Concrete and Fiber Reinforced Concrete Subjected to Impact Loading," in Cement Based Composites: Strain Rate Effects on Fracture (eds. S. Mindess and S. P. Shah) MRS Symposia Proceedings, Vol. 64, pp. 181-201, 1986.
10. Gopalaratnam, V. S., and Shah, S. P., "Strength, Deformation and Fracture Toughness of Fiber Cement Composites at Different Rates of Flexural Loading," Steel Fiber Concrete, Proceedings of U.S.-Sweden Seminar (NSF-STU), (eds. S. P. Shah and A. Skarendahl) Stockholm, Sweden, Elsevier Applied Science Publishers, U.K., pp. 299-331, October 1986.
11. Shah, S. P., and John, R., "Strain Rate Effects on Mode I Crack Propagation in Concrete," Fracture Toughness and Fracture Energy of Concrete, (ed. F. H. Wittmann), Elsevier Publishers, The Netherlands, pp. 453-465, 1986.
12. Jenq, Y. S., and Shah, S. P., "Fracture Mechanics and Constitutive Modeling of Concrete," Proceedings, Constitutive Laws for Engineering Materials, Tucson, AZ, Elsevier, (eds. Desai, et al.), January 1987.
13. John, R., and Shah, S. P., "Effect of High Strength and Rate of Loading on Fracture Parameters of Concrete," Proceedings of RILEM - SEM International Conference on Fracture of Concrete and Rock, Houston, June 1987.
14. John, R., and Shah, S. P., "Constitutive Modeling of Concrete Under Impact Loading," Proceedings of SMIRT - 9 - Post - Conference-Seminar: Impact, Lausanne, Switzerland, August 1987.

#### Theses:

1. Gopalaratnam, V. S., "Fracture and Impact Resistance of Steel Fiber Reinforced Concrete," Ph.D. Thesis, Department of Civil Engineering, Northwestern University, Evanston, IL, June 1985.
2. Jenq, Y. S., "Fracture Mechanics of Cementitious Composites," Ph.D. Thesis, Department of Civil Engineering, Northwestern University, Evanston, IL, June 1987.
3. John, R., "Strain Rate Effects on Fracture of Cement Based Composites," Ph.D. Thesis, Department of Civil Engineering, Northwestern University, Evanston, IL, Nov. 1987 (to be submitted).

#### **4. LIST OF PRINCIPAL PROFESSIONAL COLLABORATORS**

|                    |                              |
|--------------------|------------------------------|
| Reji John          | Ph.D. Candidate              |
| Y. S. Jenq         | Ph.D. (1987)                 |
| V. S. Gopalaratnam | Ph.D. (1985)                 |
| J. Schmidt         | Technician, Instrument Maker |
| C. Nkani           | Technician, Electronics      |
| M. Hagen           | Technician, Machinist        |

#### **5. ADDITIONAL INFORMATION**

The results of this investigation are summarized in the attached papers.

**Proceedings, SMiRT-9-Post-Conference-Seminar: Impact, Lausanne,  
Switzerland, August 26-27, 1987.**

**Constitutive Modeling of Concrete  
Under Impact Loading**

*by*

**Reji John and Surendra P. Shah**

**Center for Concrete and Geomaterials  
Department of Civil Engineering  
The Technological Institute  
Northwestern University  
Evanston, IL 60201, USA**

**August 1987**

# Constitutive Modeling of Concrete Under Impact Loading

R. John

Graduate Research Assistant, Department of Civil Engineering,  
Northwestern University, Evanston, IL, USA

S. P. Shah

Professor of Civil Engineering, and Director, Center for Concrete and  
Geomaterials, Northwestern University, Evanston, IL, USA

## 1 INTRODUCTION

Modern computer-aided analysis and use of concrete for special structures such as reactor containment vessels and missile storage silos, has led to a growing interest in the cracking behavior of concrete (1-4). Such concrete structures are also likely to be subjected to short duration impulsive and impact loads in addition to static loads. Experimental results indicate that tensile, flexural and compressive strength of concrete increase with increase in rate of loading (5-7). This implies that neglecting the 'rate effect' in structural design might result in underestimation of the strength of structures and hence uneconomical designs. On the other hand, there is experimental evidence to suggest that higher rate of loading might result in a brittle failure of concrete structures as compared to ductile failure at slow rate of loading (8-10).

In order to accurately evaluate the overall structural response under impact loading, a knowledge of the constitutive relationships and failure criteria of concrete, steel, and interface properties, over a wide range of strain rates (i. e., rates of loading) is essential. In this report, some relevant experimental results and analytical models of concrete, and concrete-steel bond behavior at different rates of loading are discussed.

## 2 REVIEW OF DYNAMIC TEST METHODS

The effect of impact loading on mechanical properties of concrete has been reviewed in detail by Suaris and Shah (7), Mindess (11), Sierakowski (12), and Reinhardt (13). Many investigators (see for example Ref. 6) have studied the rate sensitivity of fracture strength of concrete in tension, flexure, and compression. Various test methods have been used for this purpose, as discussed next.

### 2.1 Test Methods

**Conventional Drop weight test:** This is a simple qualitative test. In this test, a known weight is dropped on a specimen and the impact resistance is characterized by the number of blows required to either

initiate visible cracking in the specimen or cause complete failure of the specimen. Evidently this method is dependent on the weight, size, and shape of hammer, drop height, and size of specimen. ACI Committee 544 recommends this test to evaluate the impact resistance of fiber reinforced concrete. Ramakrishnan et al. (14) used this technique to determine the performance of steel fiber reinforced concrete.

**Explosive test:** This method involves use of explosive shocks for applying high rates of loading. This test is useful for studying scabbing and fragmentation. Bhargava and Rehnstrom (15) used explosives and high speed photography to study dynamic cracking behavior of plain and polymer modified concrete. Mayrhofer and Thor (16) used a blast-simulator to study the dynamic response of fibre and conventional reinforced concrete.

**Charpy impact test:** The Charpy Impact Test consists of a pendulum-type hammer striking a specimen, simulating either a cantilever beam or a three-point bend specimen. This test was originally recommended for metals (ASTM). The impact toughness is characterized in terms of the energy required for total fracture of the specimen. The energy required for fracture is evaluated from the travel of the pendulum after the impact. The measured energy value includes the energy to fracture the specimen, energy absorbed by the testing system, and the kinetic energy imparted to the specimen (17, 18). Krenchel (19) and Johnston (20) used this test to evaluate the impact performance of steel fiber reinforced concrete in terms of energy absorption capacity relative to unreinforced matrix. The next step involved the use of an instrumented hammer in the conventional Charpy test. Thus the hammer load - time history could be obtained. Based on such Charpy impact tests of silicon carbide specimens, Abe, Chandan and Bradt (21) concluded that the energy calculated from the Charpy test is higher than the true fracture energy of the specimen and that the lower the true fracture energy, the higher is the discrepancy obtained from the Charpy test. Since the strength to weight ratio of concrete is much lower than that of metals, the conventional Charpy impact test could overestimate the energy absorption values of unreinforced matrix.

The above test methods do not facilitate rigorous quantitative analysis of the impact behavior of cement composites. One cannot obtain useful parameters for constitutive modeling purposes using the above experimental methods.

**Instrumented drop weight test:** The instrumented drop weight test consists of instrumented hammer and supports so that these serve as load cells. With the aid of adequate data acquisition systems, one can obtain load, displacement and strain versus time response of the specimen during the impact event. These results can be used to obtain design parameters such as modulus of rupture (MOR), Young's modulus, cracking strain, and energy absorbed (directly evaluated from load-deflection response) as functions of strain rate. Suaris and Shah (22) developed this test for studying the impact behavior of plain and fiber reinforced concrete, Fig. 1. Naaman and Gopalaratnam (23) used this method to investigate the effect of impact loading on steel fiber reinforced concrete. Recently, Bentur, Mindess and Banthia (24) developed a similar test setup for testing large-sized concrete specimens.

**Modified Instrumented Charpy Impact Test:** Gopalaratnam, Shah and John (17) developed the modified instrumented Charpy impact testing

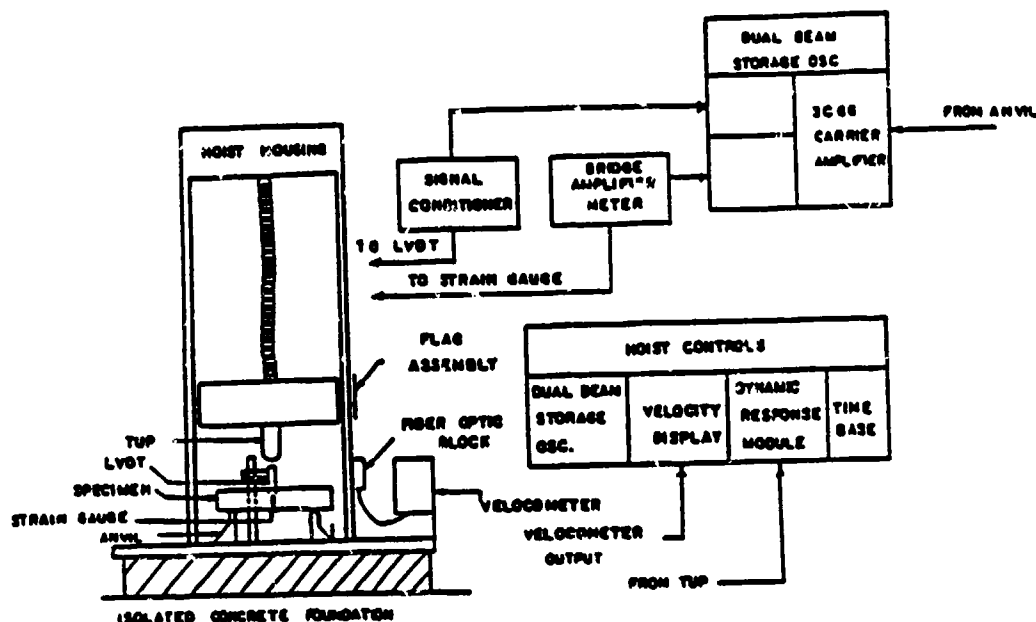


Figure 1. Schematic of instrumented drop weight system (22).

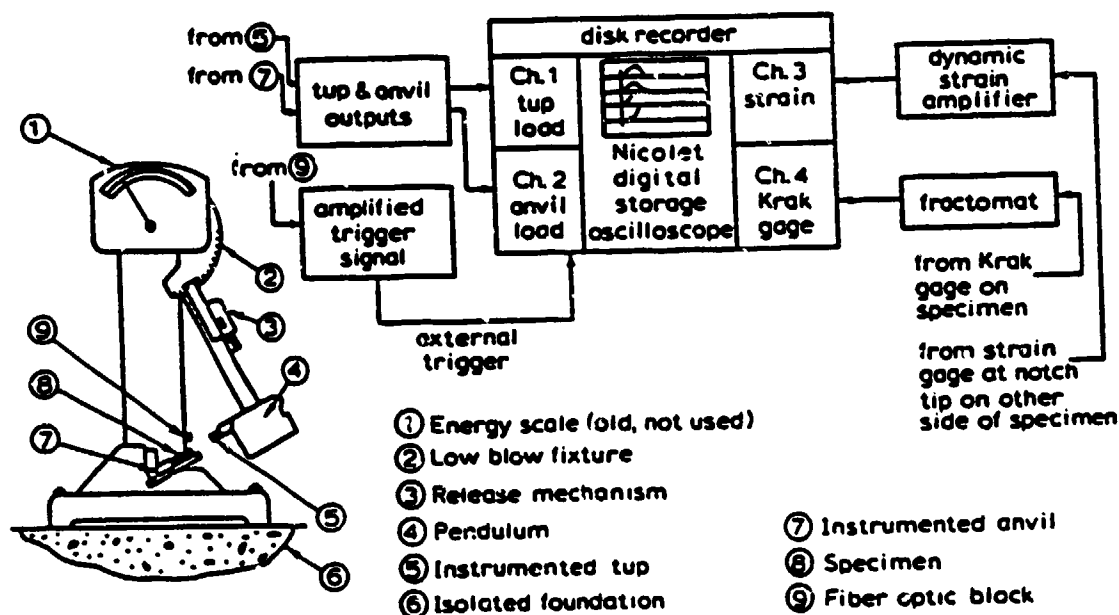


Figure 2. Modified instrumented Charpy impact testing system (17, 25, 26).

system, Fig. 2. As the name suggests, the conventional Charpy machine was modified to include the following features among others (17, 25, 26):

1. concrete specimens larger than the conventional metal specimens could be tested;
2. hammer and support loads could be recorded independently;
3. deflections, strains, and crack growth could also be recorded.

This test setup has been used for studying impact behavior of steel and glass fiber reinforced cement composites (18, 27), and fracture mechanics investigation of effect of impact loading on concrete (25,

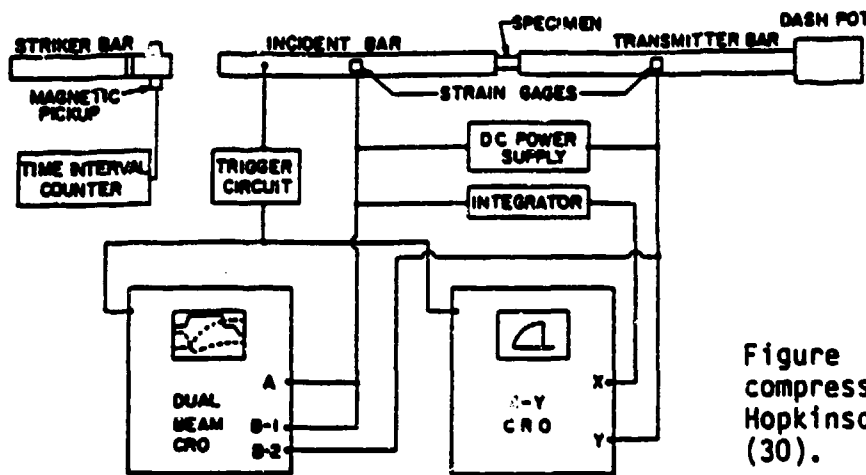


Figure 3. Schematic of compression split Hopkinson bar test setup (30).

26, 28). Similar to the instrumented drop weight test, this method also yields parameters useful for constitutive modeling of concrete under impact loading.

**Split Hopkinson Bar Test:** The split Hopkinson bar test enables determination of stress-strain responses in compression and tension at high strain rates. The test was originally developed by Kolsky (29). A schematic of this test setup is shown in Fig. 3. The specimen is located between two long bars, namely incident and transmitter bars. The specimen may be held in such a way that either a tensile or a compressive stress pulse, as desired, could pass through the specimen. The stress pulse is generated at the free end of the incident bar by an explosive charge or an impacting bullet. An excellent summary of the split Hopkinson bar technique is given in Ref. 30. Reinhardt et al. (31) and Malvern et al. (32) used this method to study the high strain rate behavior of cement composites in uniaxial tension and compression, respectively.

**Constant Strain Rate Test:** Constant strain rate tests are deflection-controlled tests (see for example Refs. 22, 25 and 26). Constant strain rate tests can be done in tension, flexure, and compression. This is an ideal test suitable for strain-softening materials such as concrete. But it may be difficult to achieve high strain rates in such tests.

## 2.2 Inertial effects in high strain rate tests

Inertial effects could become significant at higher rates of loading. Using a two degree of freedom model to represent the impact test setup (see Fig. 4), Suaris and Shah (33) analyzed in detail the inertial effects in impact tests. The use of the hammer load signal alone can lead to erroneous results. The inertial loads could be neglected only if the hammer load cell response was identical to the support load cells. This required the use of a rubber pad to soften the contact zone between the hammer and the specimen. Suaris and Shah (33) validated this approach analytically using the model shown in Fig. 4. Gopalaratnam, Shah and John (17) used this model to obtain guidelines for designing an impact test setup, as discussed earlier.

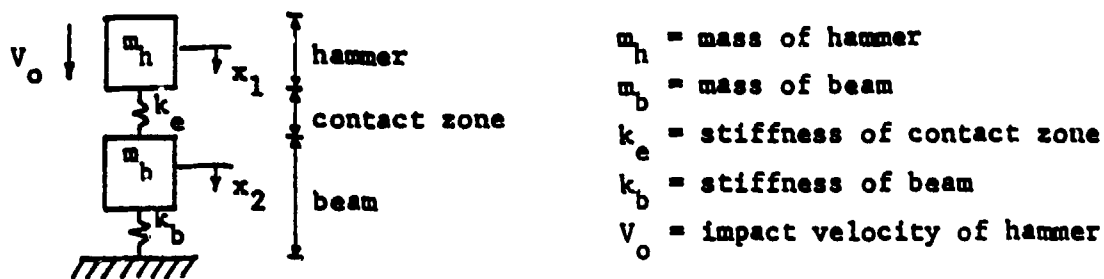


Figure 4. Two degree of freedom model (17, 33).

Bentur et al. (24) conducted instrumented drop weight impact tests on large-sized concrete specimens. The acceleration of the specimen was measured using accelerometers glued on the specimen. This enabled direct evaluation of the inertial effects experienced by the specimen. They reported that the inertial loads could be as high as 90% for concrete specimens. They also concluded that though the use of rubber pad decreased the inertial effects, it also reduced the rate of loading, as expected. It should be noted that this was also observed by Suaris and Shah (33) and Gopalaratnam et al. (17). John (25) showed that the model shown in Fig. 4 could be used to accurately predict the acceleration experienced by the specimen and hence the inertial effects observed by Bentur et al. (24).

### 2.3 Discussion

The test methods used by different investigators for achieving high strain rates are listed in Tables I, II and III, for tension, flexure, and compression respectively (see Appendix). Based on the above review of dynamic test methods the following remarks can be made:

1. Instrumented impact tests (drop weight or Charpy) and split Hopkinson bar tests can be used for developing constitutive models for concrete at impact rates.
2. Inertial effects have to be considered while analyzing the experimental results. In some cases direct measurements using accelerometers may be required.
3. To obtain the rate sensitivity of mechanical properties useful for constitutive modeling over a wide range of strain rates, instrumented impact (drop weight or Charpy) tests or split Hopkinson bar tests should be coupled with constant strain tests.

## 3. EXPERIMENTAL RESULTS OBTAINED FROM HIGH STRAIN RATE TESTS

### 3.1 Plain Concrete - Tension, Compression and Flexure

Typical experimental load-deformation responses are shown in Figs. 5-7. Fig. 5 corresponds to uniaxial tension (37), Fig. 6 to flexure (18), and Fig. 7 to uniaxial compression (48). The relevant conclusions regarding high strain rate behavior of concrete are listed below:

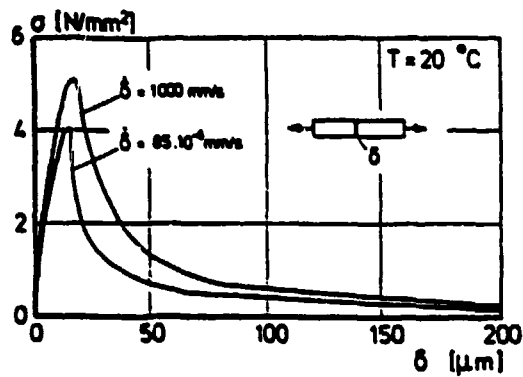


Figure 5. Uniaxial tension stress-strain curves of concrete at two different rates of loading (13).

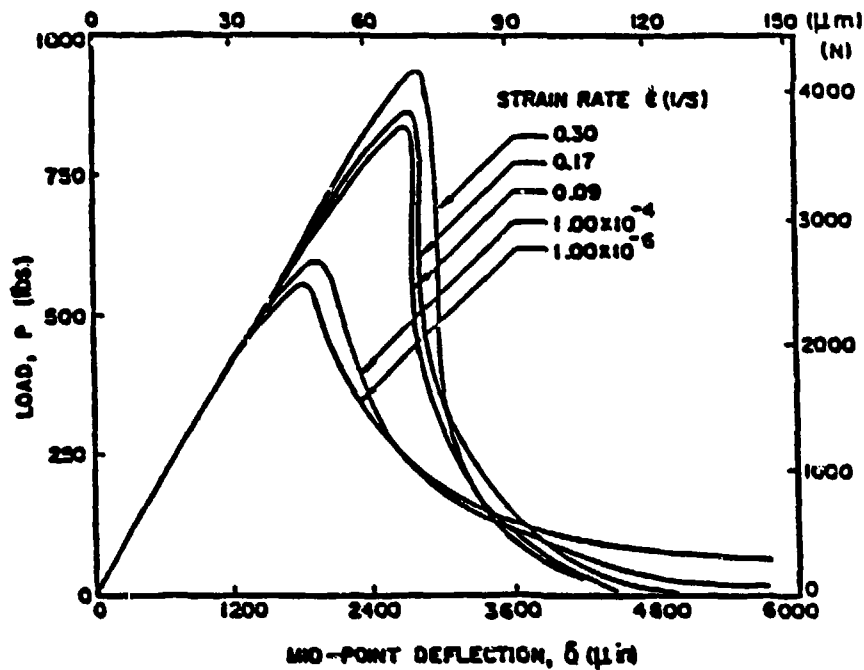


Figure 6. Typical load-deflection response of concrete in bending at different rates of loading (18).

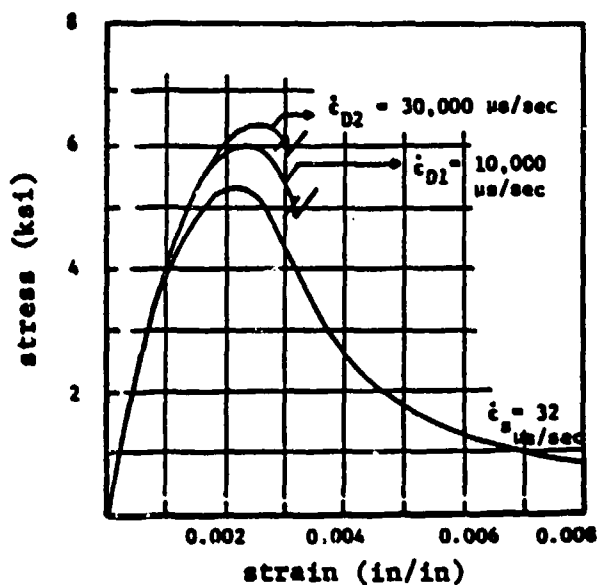


Figure 7. Typical effect of strain rate on the compression stress-strain curve of concrete (48)

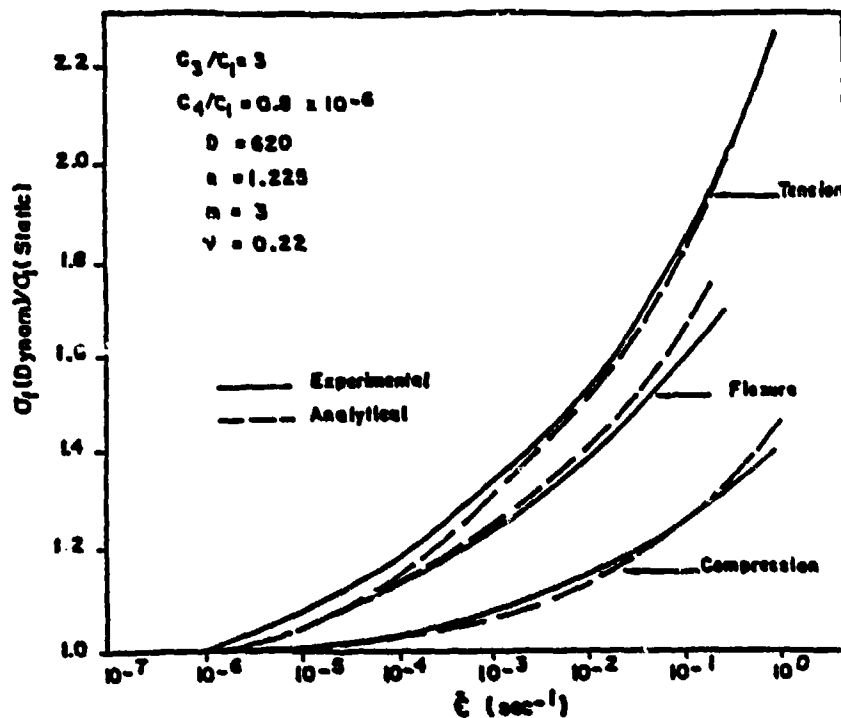


Figure 8. Analytical and experimental curves for the effect of strain rate on the ultimate strength (49, 50).

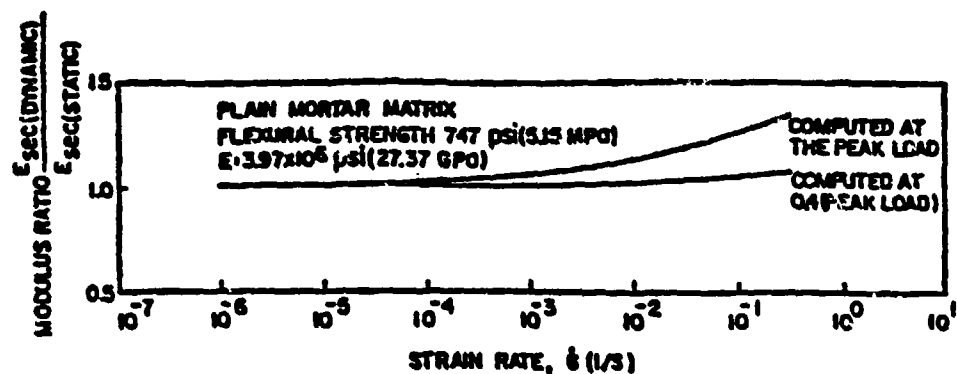


Figure 9. Effect of strain rate on the elastic moduli of mortar (18).

1. The peak strength increases with increase in rate of loading in tension, flexure, and compression, Fig. 8 (49, 50).
2. The rate sensitivity (ratio of impact strength to static strength) is highest for tension and lowest for compression, Fig. 8. Rate sensitivity in flexure is between that of tension and compression. This implies that rate sensitivity of mode I (tensile) cracking is probably responsible for the observed rate effects (49, 50).
3. Young's modulus ( $E$ ) is relatively rate independent from strain rate of  $10^{-6}$  to 1.0 per second. This is shown in Fig. 9, which was reported by Gopalaratnam and Shah (18) based on flexural impact results. This trend of relatively rate independent  $E$  was also observed by:

- a. Tinic and Bruhwiler (38) in uniaxial tension,
- b. Suaris and Shah (49), and Ahmad and Shah (48) in compression, and
- c. John (25) in flexure based on load-crack mouth opening responses of notched beams at impact rates.

In contrast, Reinhardt (13) reported that  $E$  increases with increasing strain rate based on impact tensile tests. The results indicated that the increase was about 25% at a strain rate of 1.0 per second.

4. Secant modulus evaluated at the peak load increases, see Fig. 9. This was also observed by others in tension and compression (38, 48, 49). This implies that the material behaves more linearly at high strain rates, i. e. prepeak nonlinearity decreases with increase in rate of loading.
5. John and Shah (26) used special brittle Krak Gages for studying the effect of impact loading on mode I crack growth in concrete. Fig. 10. The experimental results indicate that prepeak nonlinearity in concrete is due to prepeak crack growth and this prepeak crack growth decreases with increasing strain rates, Fig. 11.
6. The average crack velocity at strain rate of 0.4/sec. is less than 5% (about 100 m/sec.) of Rayleigh wave velocity in concrete, as observed by John and Shah (26). Bhargava and Rehnstrom (15) and Mindess et al. (52) also reported similar crack velocities.
7. The deflection or strain at peak load also increases with the rate of loading (7, 13, 38, 48, 49).
8. The rate sensitivity of lower strength concrete is higher than that of higher strength concrete, Fig. 12 (7, 8, 17, 28).
9. Most of the reported data correspond to strain rate less than or equal to 20 per sec. except those of Malvern et al. (32) and Jawed et al. (47) (see Tables I-III in Appendix).

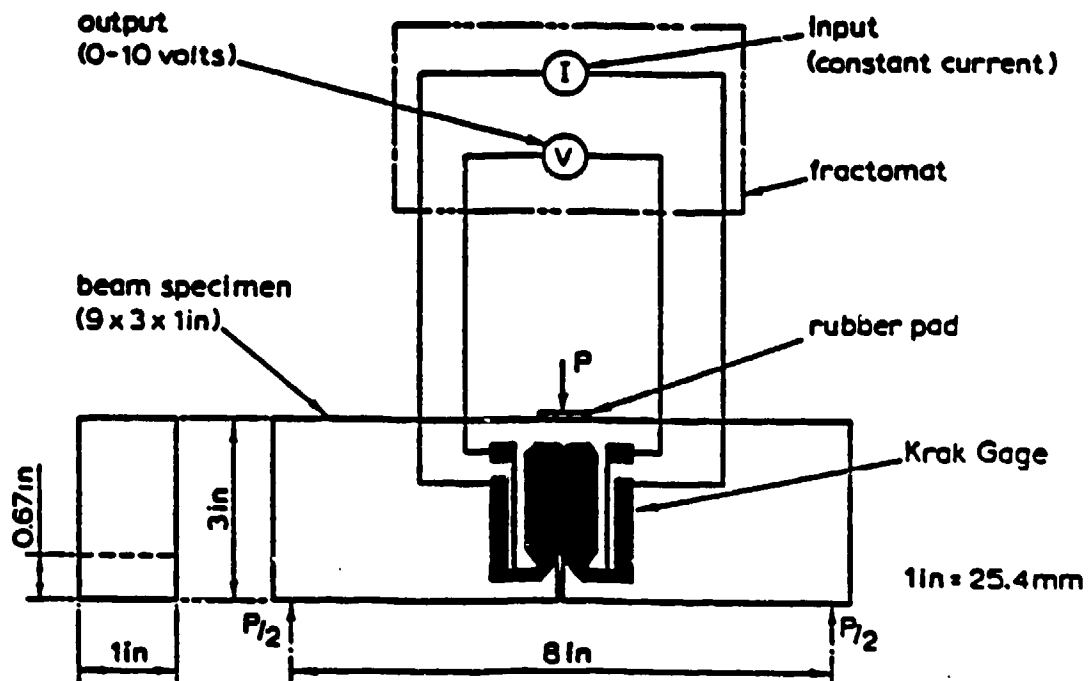


Figure 10. Crack growth measurement using Krak gages (26).

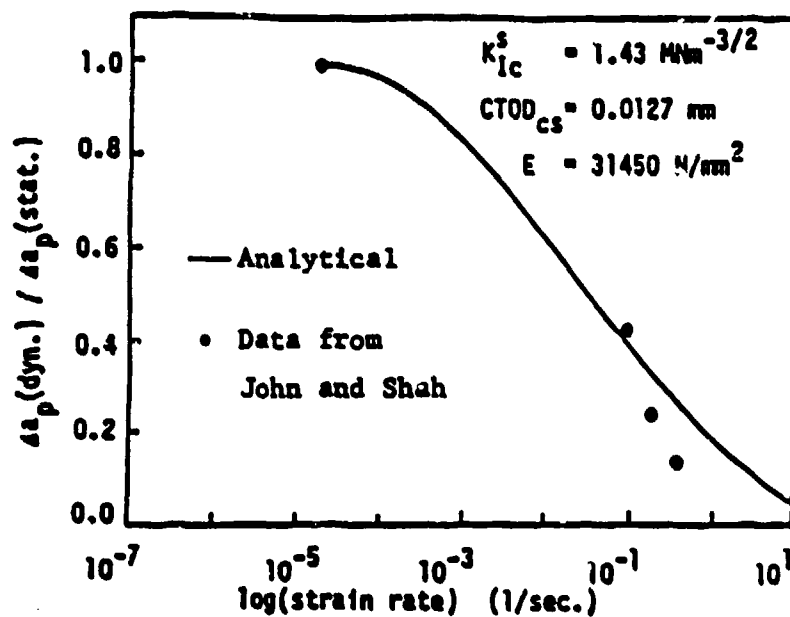


Figure 11. Strain rate effect on precritical crack growth (15, 16).

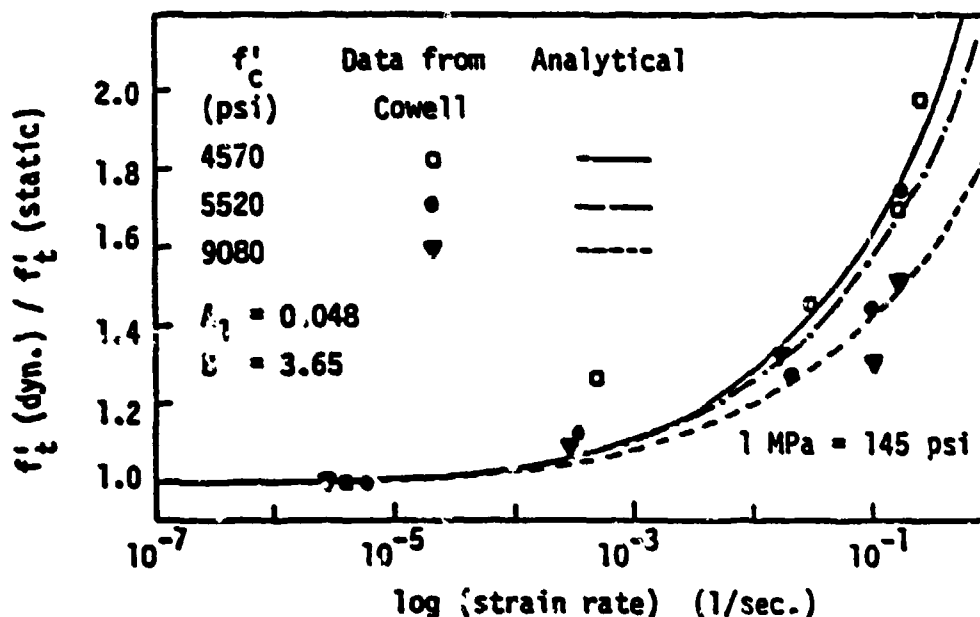


Figure 12. Strain rate effect on tensile strength of concrete (28).

Recently, Jawed et al. (47) reported very high strain rate results for cement paste specimens (up to strain rate = 1000/sec.) based on split Hopkinson pressure bar tests in the compressive mode. Compressive strength increased with increasing rates of loading up to strain rate of 250/sec., Fig. 13. But it appeared to reach a limiting value between strain rate of 250/sec. and 1000/sec., Fig. 13. This implies apparent rate independent behavior at very high rates of loading (strain rate > 250/sec.). It should be noted that they tested small cylindrical specimens of diameters 0.25, 0.50, 0.75 inches. Size effect in cement based composites has been shown to be significant at both static (1-4, 53-55) and impact rates (28, 51), although it has also been shown that size effect is minimum for cement paste (53).

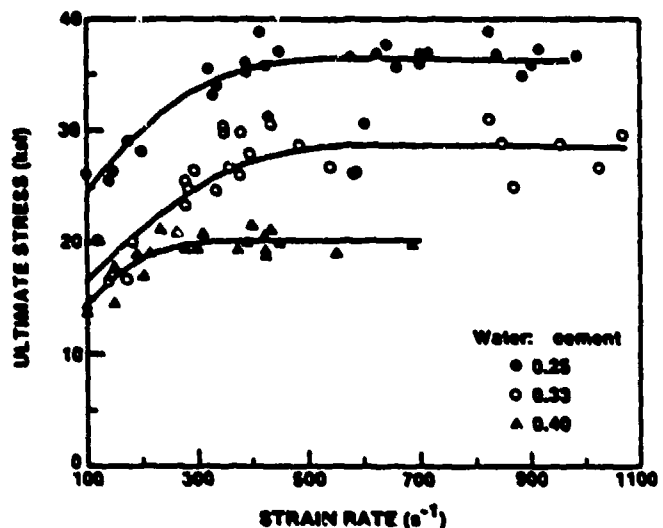
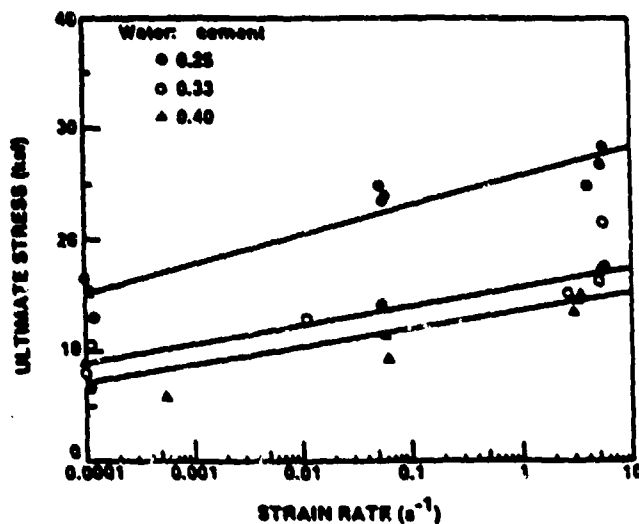


Figure 13. Strain rate effect on compressive strength (47).

### 3.2 Plain Concrete - Complex Stress States and Shear

All the above conclusions are based on uniaxial stress states. In actual practice the structures may be subjected to preloading prior to application of dynamic tensile loads. Tinc and Bruhwiler (38) investigated the effect of compressive preloading. Compressive loads up to certain strain levels were applied to specimens (at slow rates) and subsequently subjected to different rates of tensile loading. Compressive and tensile loads were applied along the longitudinal axis of the specimen. The tensile strength was sensitive to the initial compressive load. The tensile rate sensitivity was approximately independent of the initial compressive load (38).

Zielinski (39) studied the effect of biaxial compressive loading on impact tensile behavior of concrete. Specimens were subjected to different levels of compression and thereafter subjected to different rates of tensile loading. The results indicated that the increase in tensile strength due to impact rates of loading of concrete subjected to biaxial compression-impact tension is similar to that of concrete subjected to uniaxial tension. These results are similar to the observations of Takeda et al. (56) based on results of dynamic triaxial tests on concrete cylinders loaded by axial compressive and tensile loads.

Malakar et al. (57) investigated the behavior of concrete under dy-

namic tensile-compressive loading using hollow cylinder specimens subjected to simultaneous axial compression and internal pressure loads. They concluded that peak failure stresses increased with increasing strain rates while the failure strain in compression, tension and biaxial tension-compression was independent of rate of loading. Other studies have shown that failure strains increase at higher rates of loading (7, 13, 38). This discrepancy could perhaps be due to the occurrence of the fracture plane outside the gage length (58). It should be noted that the measured strain values are dependent on whether the failure took place inside or outside the gage length (38-58).

The rate effects in mode I (tensile) and mode II (shear) fractures may be different. Based on shear tests, Takeda et al. (59) reported that the shear displacement at peak shear load decreases with increase in rate of loading, Fig. 14. This is contrary to the usual observations that deformation at peak load increases with increase in rate of loading under tensile, flexural and compressive loading.

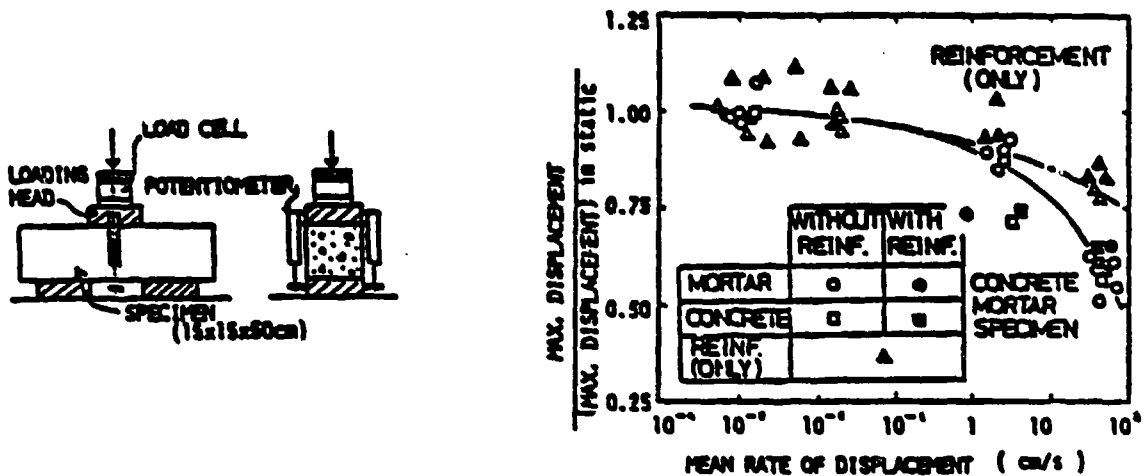


Figure 14. Decrease of shear displacement with increase in rate of loading (59).

### 3.3 Bond between concrete and steel

Explosive tests conducted by the U. S. Army Waterways Experiment Station on buried reinforced structures (60), impact tests conducted by Mutsuyoshi and Machida (9) on reinforced concrete beams, and fast rate cyclic tests conducted by Chung and Shah (10) on reinforced concrete beam-column joint specimens, showed that concrete structures designed to fail in a ductile (flexural type) manner under slower rates of loading may fail in a brittle manner (shear type) at higher rates of loading, Fig. 15. This could be attributed to the following mechanisms:

1. decrease in shear strain of concrete at peak shear load with increasing strain rates (see Fig. 14), and
2. localization of bond stress distribution along the reinforcement bar at higher rates of loading (see Fig. 16).

These mechanisms usually act simultaneously.

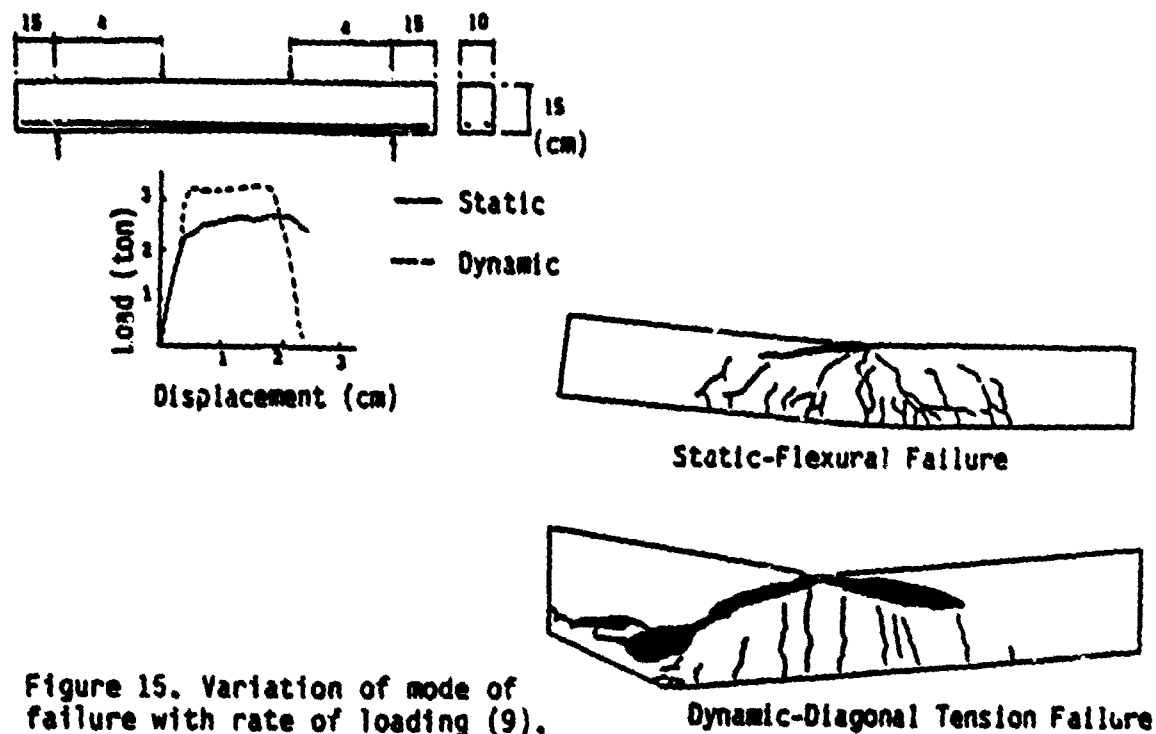


Figure 15. Variation of mode of failure with rate of loading (9).

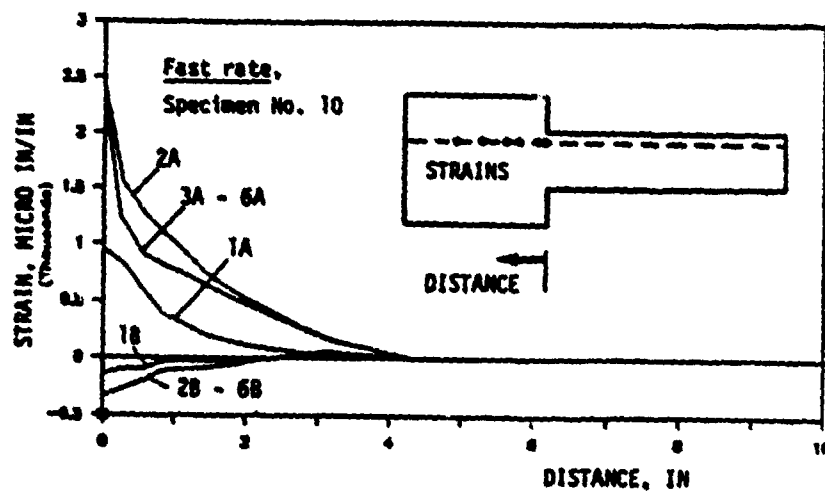
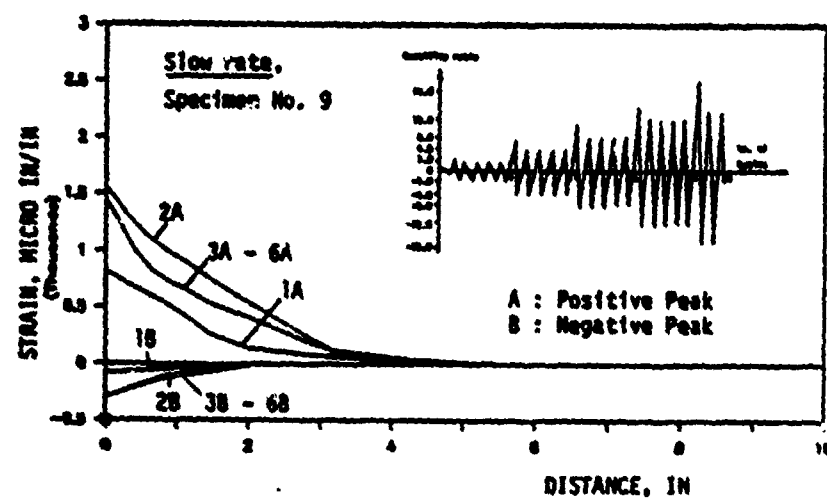


Figure 16. Localization of bond stress at higher rates of loading (10).

Based on impact loading study of concrete-steel bond behavior, Vos and Reinhardt (61) concluded that deformed bars exhibited rate dependent bond-slip response as opposed to rate independent behavior of smooth bars. Average bond stress increased with increasing strain rates. This rate sensitivity was lesser for higher strength concrete (61). The rate effect on deformed bars is probably due to the rate dependent crushing and splitting of concrete that occurs due to the bearing of ribs (7). Using the bond-slip relationship, Vos and Reinhardt (61) calculated the steel stress distribution along the bar and reported that the higher the rate of loading the more localized is the steel stress distribution. Using the relationship between bond stress and steel stress, it can be shown that under high rates of loading bond stress distribution along the reinforcement bar is also more localized compared to the corresponding static behavior. Takeda et al. (59), and Chung and Shah (10) observed this by direct strain measurements along the reinforcement bar (Fig. 16).

#### 4. MODELING OF CONCRETE BEHAVIOR UNDER HIGH STRAIN RATES

Some of the models proposed for predicting the rate sensitivity of fracture of concrete are discussed in this section.

##### 4.1 Fracture mechanics models

**Thermally Activated Flaw Growth Models:** Many investigators have used thermally activated flaw growth models to predict the strain rate effects on fracture strength of materials such as concrete, ceramics and rocks. For example, Evans (62) assumed that the crack velocity is a power function of stress intensity factor (Eqn. 1) and derived a relationship between the fracture stress and rate of stress application as given by Eqn. 2. Note that Eqn. 2 was also derived by Charles (63).

$$(1) \quad V \sim K_I^N$$

$$(2) \quad \sigma_f \sim (\dot{\sigma})^{1/N+1}$$

in which  $K_I$  = mode I stress intensity factor,  $V$  = crack velocity,  $\sigma_f$  = fracture strength,  $\dot{\sigma}$  = rate of stress application, and  $N$  is assumed to be rate independent. Mindess (11) reported a value of  $N = 30$  for crack velocities up to  $10^{-1}$  cm/sec. Based on impact crack growth measurements, John and Shah (26) concluded that  $\log K_I$  versus  $\log V$  relationship is nonlinear at higher rates of loading and hence Eqn. 1 is invalid at impact rates. Mihashi and Wittmann (64)

derived an expression similar to Eqn. 2 (see equation in Fig. 17) by combining rate process theory and stochastic principles.

The rate process theory models were developed to predict crack growth under a constant load or a slowly increasing monotonically applied load. Under such loads crack growth is slow (crack velocity less than 1 mm/sec.). Hence this theory may not be valid at impact rates where crack growth is at much higher rate (15, 26, 51, 52), as shown in Fig. 17. Kormeling (65) used the rate theory to derive relations between fracture energy ( $G_f$ ), deformation rate and temperature.

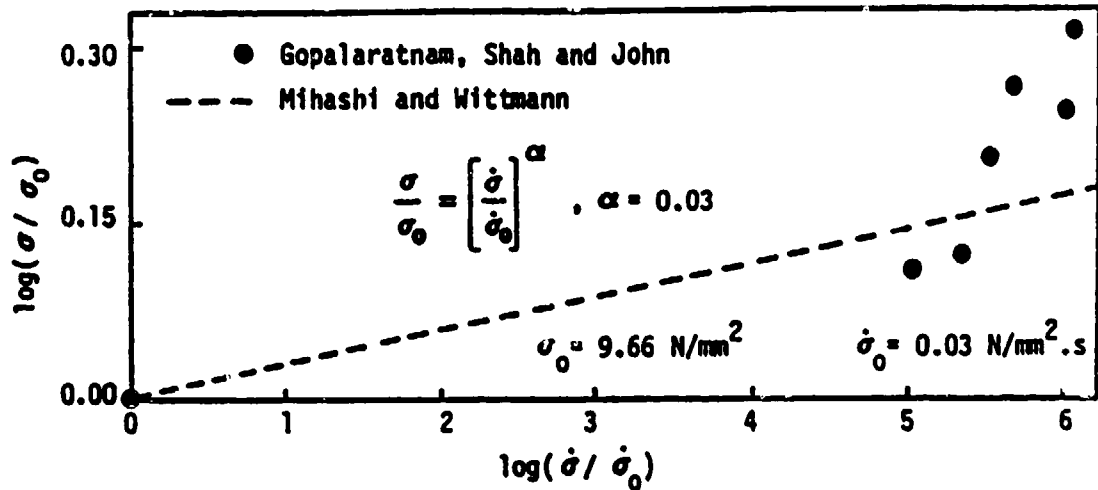


Figure 17. Comparison of data from Ref. 17 with rate theory equation.

**Dynamic Crack Models:** To determine the dynamic stress distribution around a fast moving crack tip, one can use equations of motion including the inertia terms. Freund (66) obtained dynamic elastic solutions for crack growth due to general loading. He concluded that the dynamic stress intensity factor decreases with increasing crack velocity as given by the following equations:

$$(3) \quad K_{ID} = k(V) \cdot K_{IS}$$

in which  $K_{ID}$  = dynamic  $K_I$ ,  $K_{IS}$  = static  $K_I$  for the same loading, and  $k(V)$  = velocity correction factor, similar to the results of Broberg (67). The variation of  $k(V)$  with crack velocity ( $V$ ) is shown in Fig. 18. The maximum observed crack velocity at impact rates (strain rates about 1.0/sec.) is less than 5% of Rayleigh wave velocity ( $C_R$ ) (26, 51). For this small value of  $V/C_R$ , it can be seen in Fig. 18 that the value  $k(V)$  is close to 1.0 and hence  $K_{ID} = K_{IS}$  in Eqn. 3.

Using the theory of linear elastic dynamic fracture mechanics for Heaviside loading of an isolated crack, Grady and Kipp (68) derived the following relationship between fracture strength,  $\sigma_f$  and strain rate,  $\dot{\epsilon}$ , Eqn. 4.

$$(4) \quad \sigma_f \sim (\dot{\epsilon})^{1/3}$$

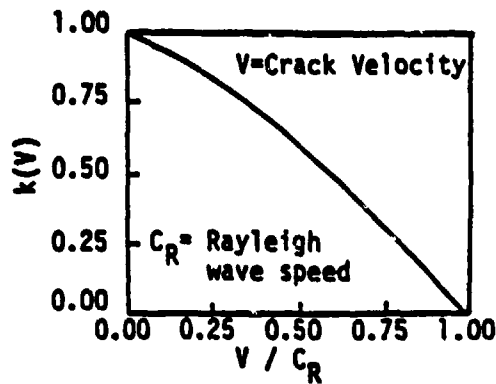


Figure 18. Variation of velocity correction factor  $k(V)$  with crack velocity,  $V$  (66).

Note that Eqn. 4 is similar to Eqn. 2 with  $N = 2$ . This cubic rate dependence of fracture stress on strain rate was experimentally observed for a rock sample (Arkansas novaculite) at  $\dot{\epsilon} = 0.8 \times 10^4$  to  $2.5 \times 10^4$  / sec. Eqn. 4 is applicable at very high rates only because it was derived assuming that the crack travels at terminal velocity (acoustic velocity) after initiation. As discussed earlier, the observed crack velocity ( $V$ ) is very low ( $V/C_R < 5\%$ ) even at strain rates  $\sim 1.0/\text{sec}$  (26,51). Hence Eqn. 4 may not be applicable for concrete at strain rates observed so far.

From the above two sections, one can conclude that neither the rate process theory nor the elastic dynamic theory is capable of predicting the rate sensitivity of a nonlinear material such as concrete in the strain rate regime of  $10^{-7}$  to  $10/\text{sec}$ .

**Nonlinear Fracture Mechanics Model:** For conditions where LEFM (linear elastic fracture mechanics) is applicable, one can calculate the critical stress intensity factor,  $K_{Ic}$ , from the notched beam tests using the measured peak load and initial notch depth,  $a_0$ . For cement based composites there is significant precritical (prepeak) nonlinear crack extension (also called "slow crack growth" or "process zone") (53 - 55). This can be seen in Fig. 19. Crack growth was measured using Krak gages (see Fig. 10) on one side of the specimen and strain was measured at the notch tip on the other side of the same specimen. The strain gage reading shows extensive

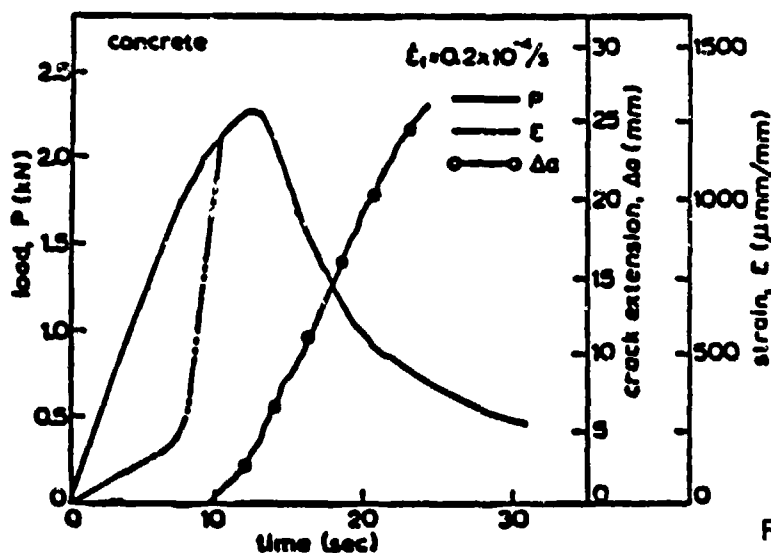
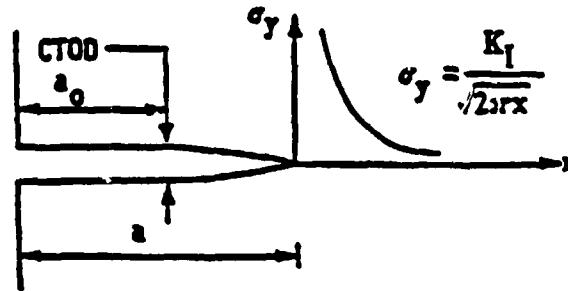


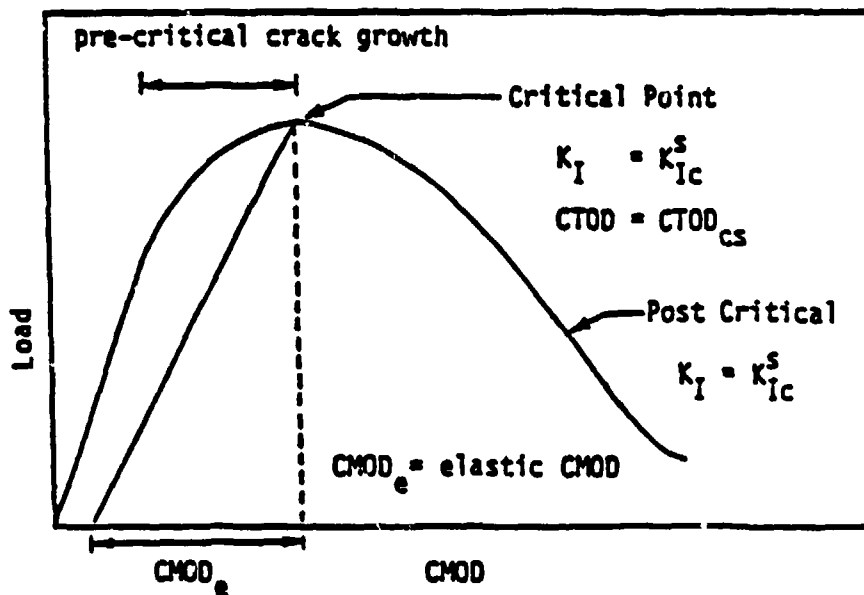
Figure 19. Typical crack growth test data (26).

"straining" (strain  $> 150 \mu \text{ str}$ ) when the load response deviates from linearity. Close to this the Krak gage indicates crack initiation. One should include this prepeak crack growth for determining size independent  $K_{IC}$ . It is very difficult to estimate the crack length based on surface measurements since the crack front is tortuous and discontinuous (26, 69 - 71).

To overcome this difficulty Jenq and Shah (53, 72) proposed an effective crack length approach to obtain a valid fracture toughness value. The effective crack length  $a_e$  was defined such that the measured elastic crack mouth opening displacement was the same as that calculated using LEFM, Fig. 20. They observed that  $K_{IC}$  and  $CTOD_c$  (critical crack tip opening displacement, Fig. 20) determined thus is essentially independent of size of beam. Note that  $CTOD_c$  is the elastic opening at the location of the initial notch tip when the initial notch,  $a_0$ , is assumed to grow to an effective crack,  $a_e$ , at the peak load. Note that  $K_{IC}$  defined by them is termed  $K_{IC}^s$ . Jenq and Shah used this Two Parameter Fracture model (TPFM) to explain the various size effect related phenomena in plain concrete (53, 72), fracture of steel fiber reinforced concrete (73), size effect in shear failure of reinforced concrete beams (74), and mixed mode fracture of concrete (75).



Effective Griffith Crack



Typical Plot of Load vs. Crack Mouth Opening Displacement

Figure 20. Two parameter fracture model (53, 72).

Based on the Two Parameter Fracture model, John, Shah and Jenq (51) proposed a model to predict the rate sensitivity of mode I fracture of concrete.  $K_{Ic}$  and  $E$  were assumed to be rate independent and  $CTOD_c$  was assumed to decrease with increasing strain rates. John and Shah (28) used this model for studying high strength concrete, and the interaction of static strength and rate of loading. The proposed model predicts the generally observed trends in rate effect in tension (Figs. 12, 21), and flexure (Figs. 22, 23). The model also predicts the decrease of prepeak nonlinearity with increase in rate of loading, as shown in Fig. 11. The difference in rate sensitivity in tension and flexure is predicted to be due to the size effect involved in the determination of flexural strength as shown in Fig. 24. Note that a large beam has the same rate sensitivity as uniaxial tension, Fig. 24.

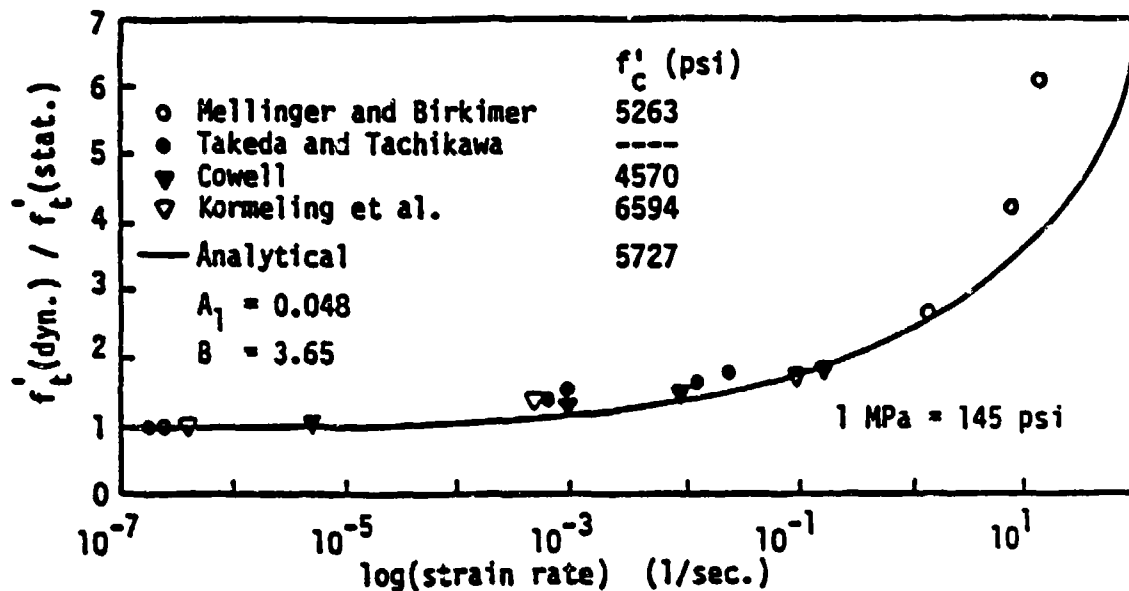


Figure 21. Strain rate effect on tensile strength of concrete (28).

This model seems to be valid in the range  $10^{-7}$  to 1.0/sec. Note that this model was developed for fracture due to a single macrocrack (as in the case of uniaxial tensile (76, 77) and flexural failure (26, 70, 72)). In actual failures, the fracture will be mixed mode (mode I, tensile, and mode II, shear) in nature. Experimental and theoretical study is in progress at Northwestern University to investigate the effect of rate of loading on mixed mode fracture of concrete (25). This study would be helpful in assessing the potential variation of mode of failure of reinforced concrete structures with increasing strain rates as discussed in section 3.3.

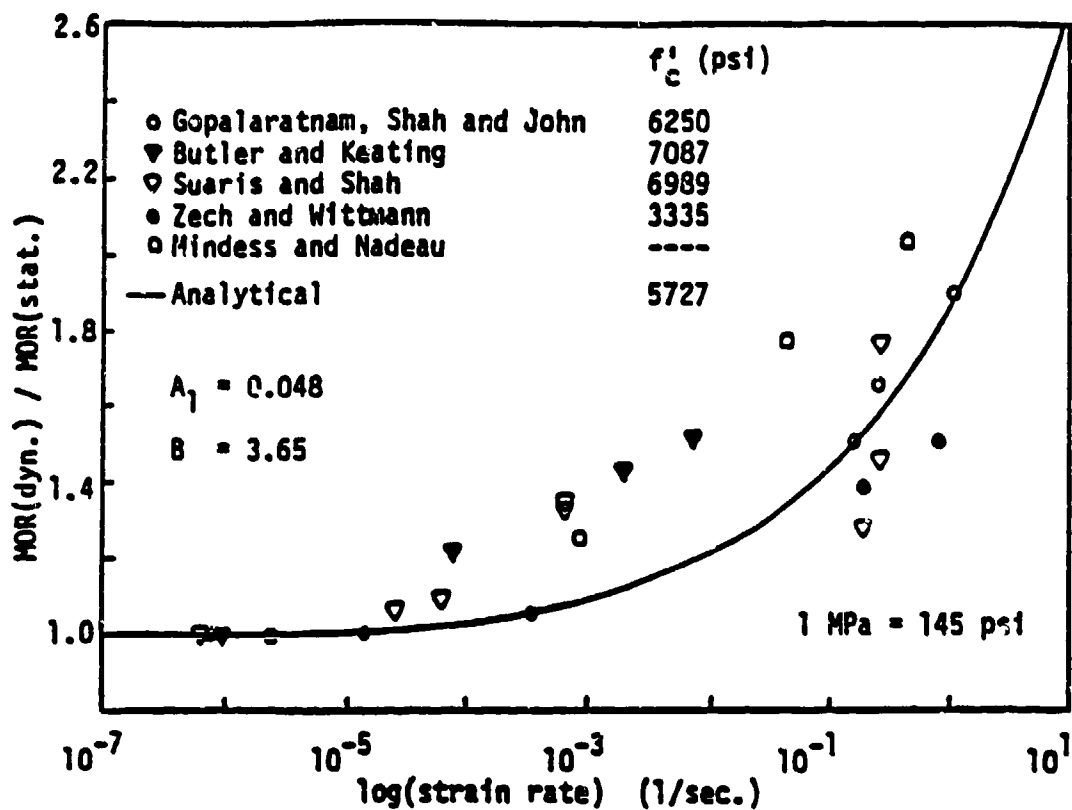


Figure 22. Strain rate effect on flexural strength of concrete (28).

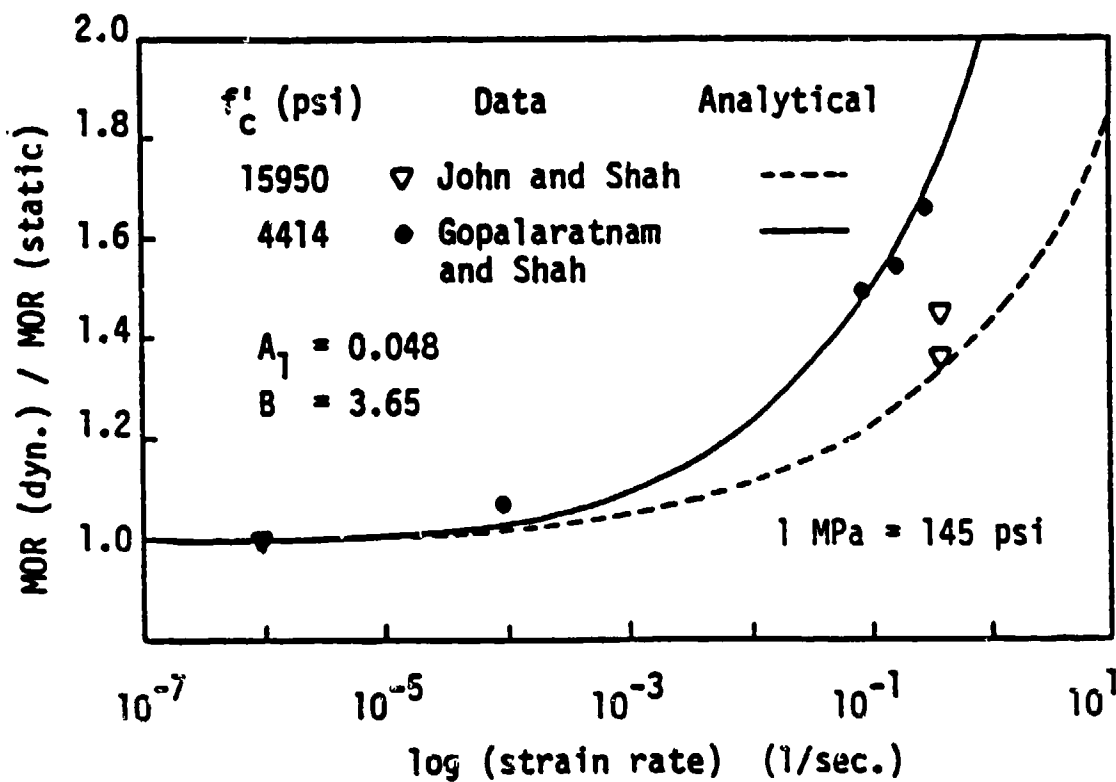


Figure 23. Interaction of strain rate and compressive strength on flexural strength (28).

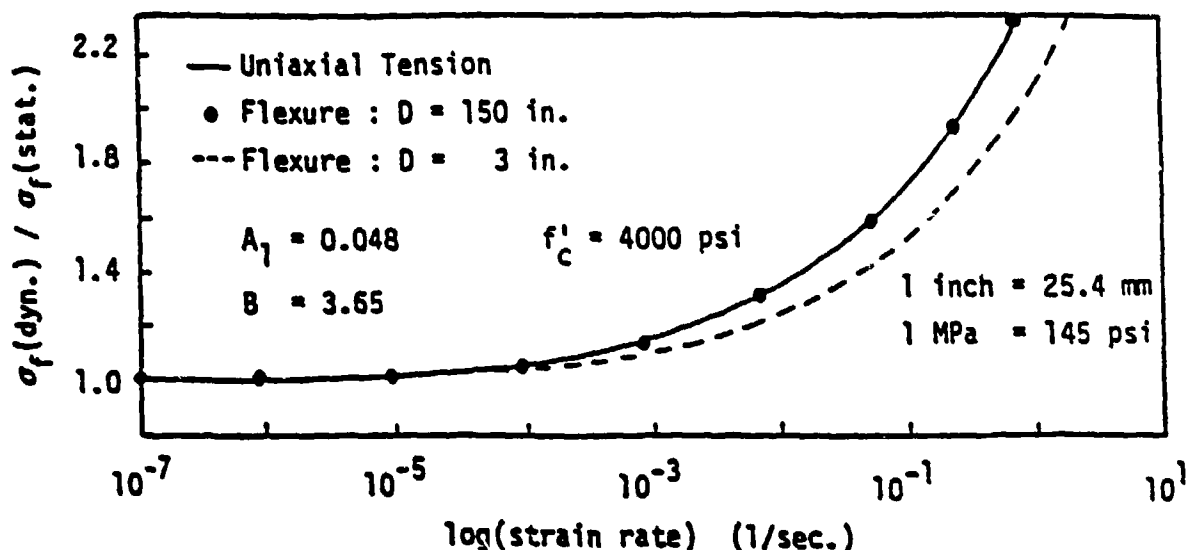


Figure 24. Model predicted size effect on rate sensitivity of flexural strength of concrete (28).

#### 4.2 Constitutive Models

Goldsmith, Polivka and Yang (78) investigated the dynamic behavior of concrete subjected to one dimensional stress pulses. They observed that a solid friction constitutive model was more suitable for describing the dissipation mechanism in concrete than a viscoelastic model. Read and Maiden (79) used a porous constitutive model to describe the dynamic behavior of concrete. The dynamic compaction of preexisting pores was assumed to be mainly responsible for the overall rate sensitivity of the material (79). Bazant and Oh (80) proposed rate sensitive nonlinear constitutive model for concrete in compression. Recently, Oh (81) extended this theory to model the dynamic tensile behavior of concrete.

As discussed earlier, prepeak nonlinearity has been attributed to microcracking and the extent of nonlinearity (microcracking) decreases at high strain rates (17, 26, 49). It appears, therefore, that the continuous damage theory may be appropriate for predicting the mechanical behavior of concrete under both quasistatic and dynamic loading.

One dimensional damage models have been developed for concrete by several researchers (82, 83). They assumed the stress ( $\sigma$ ) vs. strain ( $\epsilon$ ) relation to be of the form:

$$(5) \quad \sigma = E(1 - w)\epsilon$$

In Eq. (5),  $E$  is the initial tangent modulus of elasticity of the undamaged material and  $w$  is the accumulated damage. If it is assumed that nonlinear behavior is solely due to a continuous development of internal microcracks (84, 85)  $w$  represents the microcrack density of a given cross-section.

A damage evolution equation can also be introduced where the damage variable  $w$  is expressed as a function of the strain,  $\epsilon$ . For example  $w$  can be expressed as a linear function of strain:

$$(6) \quad \omega = A\epsilon, \quad A = \text{constant}$$

Combining equations 5 and 6 yields the one dimensional stress-strain relation,

$$(7) \quad \sigma = E(1-A\epsilon)\epsilon$$

A strain-rate dependent damage model can be obtained by introducing a differential equation governing the evolution of damage as follows:

$$(8) \quad k\ddot{\omega} + \dot{\omega} - A\dot{\epsilon} = 0$$

where the first term represents the inertial resistance for microcrack growth (86). This term vanishes for small strain rates and equation 8 reduces to 6.

Combining equation 5 and 8 it can be shown that for high strain-rates the fracture stress dependence on strain-rate is of the form

$$(9) \quad \sigma_f \sim \dot{\epsilon}^{1/2}$$

Note that Eqn. 9 is similar to Eqn. 2 with  $N = 1$ . As discussed in section 4.1, experimental results indicate that for lower strain rates a weaker strain rate dependency is observed for concrete.

The above approach can be used to study uniaxial behavior of concrete and has limited scope for application in multiaxial loading conditions because of the use of a scalar damage variable. A higher order tensorial representation should be adopted for the damage if the model is to exhibit crack induced anisotropy observed in concrete. Suaris and Shah (49, 50) used the vectorial concept of damage to derive constitutive relationships for concrete under impact loading. A few pertinent aspects of the model proposed by Suaris and Shah (49, 50) are given below.

The Helmholtz free energy function (strain energy in absence of thermal effects) ( $\psi$ ) was defined in terms of the coupled invariants of damage and strain. A consistent thermodynamic approach yielded the constitutive equation,

$$(10) \quad \sigma_{ij} = \frac{\partial \psi}{\partial \epsilon_{ij}}$$

and the damage evolution equation,

$$(11) \quad \rho k \ddot{\omega}_i = f_i^D(\epsilon_{ij}, \omega_i, \dot{\omega}_i) - \rho \frac{\partial \psi}{\partial \omega_i}$$

where  $\sigma_{ij}$  = stress tensor,  $\epsilon_{ij}$  = strain tensor,  $\omega_i$  = damage vector,  $f_i^D$  = dissipative part of an intrinsic equilibrated body force,  $\rho$  = density of material and  $k$  = inertia associated with the microcrack growth. Thus Suaris and Shah (49, 50) obtained the generalized rate sensitive constitutive relations for concrete. Using this model, they were able to predict the stress-strain responses in compression and tension, Figs. 25 and 26. Decrease in nonlinearity with increasing strain rates and rate sensitivity in tension, compression, and flexure was also predicted satisfactorily, Fig. 25 and Fig. 8. They were also able to predict the rate effect on biaxial tension-compression failure envelope, Fig. 27. This model appears to be valid up to strain rate of about 10/sec.

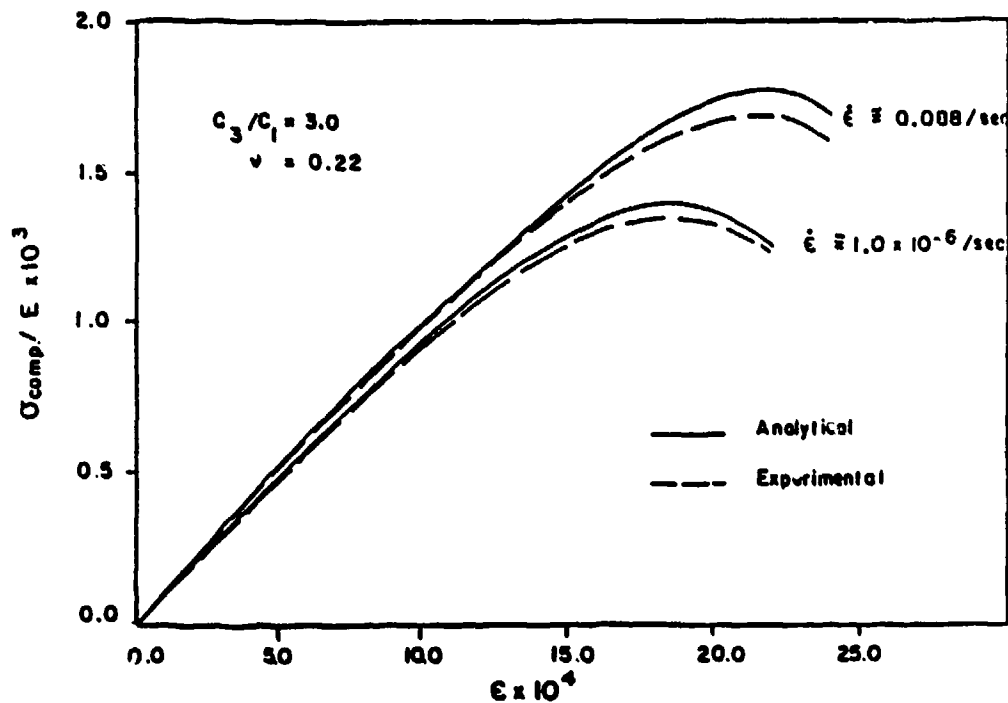


Figure 25. Stress-strain curves in compression at two rates (49, 50).

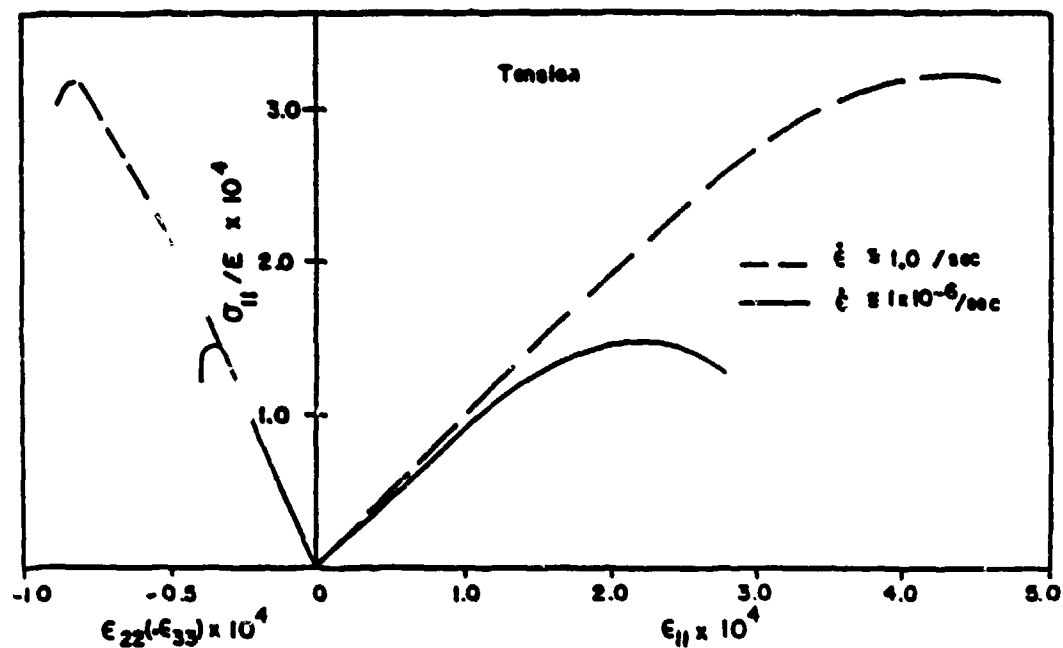


Figure 26. Stress-strain curves in tension at two rates (49, 50).

Recently, Mould and Levine (87) proposed a viscoplastic concrete model to describe the concrete behavior at loading rates varying from pseudo-static to explosive. They reported that this model, when fit to the data from Malvern et al. (50) (strain rates from about 15 to 120/sec.), did not accurately predict the rate sensitivity at lower strain rates ( $< 10^1/\text{sec.}$ ).

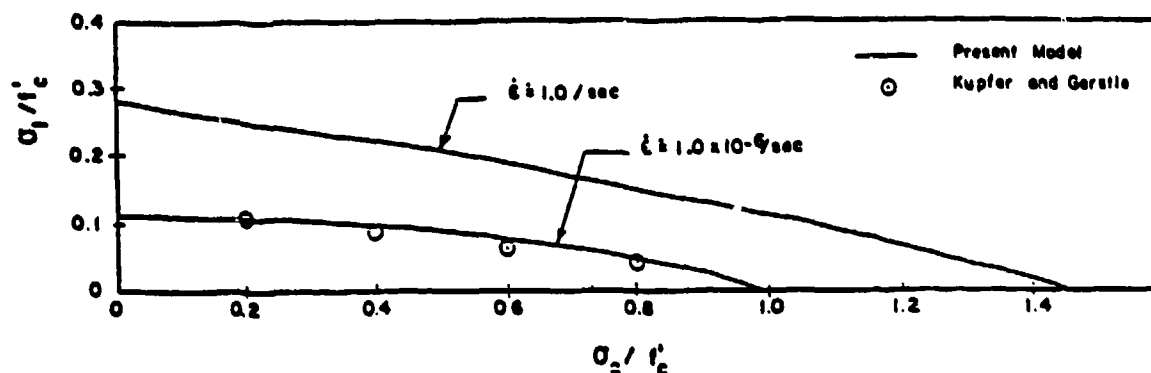


Figure 27. Biaxial tension-compression failure envelope (49, 50).

#### ACKNOWLEDGEMENT

The research reported here was supported by Grant No. DAAG29-82-K-0171 (Program Manager: Dr. George Mayer) from the U. S. Army Research Office to Northwestern University. The authors are also indebted to Dorothy Carlson for her flawless typing of the manuscript.

#### APPENDIX

Table I. High strain rate results in tension for concrete

| References                              | Testing Configuration                       | Test Apparatus for high strain rates      | Maximum Strain Rate (1/sec) |
|---|---|---|-----------------------------|
| Takeda and Tachikawa (34)               | uniaxial tension                            | compressed air driven loading             | 0.05                        |
| Cowell (35)                             | splitting tension                           | hydraulic                                 | 0.20                        |
| Mellinger and Birkimer (36)             | uniaxial tension                            | 'pellet method' -high velocity projectile | 20.00                       |
| Kormeling, Zielinski and Reinhardt (37) | uniaxial tension                            | split Hopkinson bar                       | 0.75                        |
| Tinic and Bruhwiler (38)                | uniaxial tension with effect of compression | constant strain rate                      | 0.01                        |
| Zielinski (39)                          | uniaxial tension with biaxial compression   | split Hopkinson bar                       | 0.50                        |

Table II. High strain rate results in flexure for concrete

| References                       | Testing Configuration | Test Apparatus for high strain rates | Maximum Strain Rate (1/sec) |
|----------------------------------|-----------------------|--------------------------------------|-----------------------------|
| Mindess and Nadeau (40)          | 4 point bend          | instrumented Charpy impact           | 0.20                        |
| Butler and Keating (41)          | 4 point bend          | constant displacement rate           | 0.01                        |
| Zech and Wittmann (42)           | 3 point bend          | instrumented drop weight             | 2.00                        |
| Suaris and Shah (22)             | 3 point bend          | instrumented drop weight             | 1.00                        |
| Gopalaratnam Shah and John (17)  | 3 point bend          | instrumented modified Charpy         | 0.50                        |
| Bentur, Mindess and Banthia (24) | 3 point bend          | instrumented drop weight             | 0.50                        |
| Wecharatna and Roland (43)       | 3 point bend          | instrumented drop weight             | 1.80                        |

Table III. High strain rate results in uniaxial compression for concrete.

| References              | Test Apparatus for high strain rates | Maximum Strain Rate (1/sec) |
|-------------------------|--------------------------------------|-----------------------------|
| Watstein (44)           | drop weight                          | 10.0                        |
| Atchley and Furr (45)   | drop weight                          | 2.0                         |
| Hughes and Gregory (46) | drop weight                          | 20.0                        |
| Cowell (35)             | hydraulic                            | 0.5                         |
| Malvern et al. (32)     | split Hopkinson pressure bar         | 120.0                       |
| Jawed et al. (47)       | split Hopkinson pressure bar         | 1000.0                      |

## REFERENCES

- (1) Shah, S. P. and Swartz, S. E. (Editors), June 1987. Proceedings, SEM-RILEM International Conference on Fracture of Concrete and Rock, Houston, TX, USA.
- (2) Shah, S. P., (Editor), 1985. Application of fracture mechanics to cementitious composites, Proceedings, NATO Advanced Research Workshop, The Hague, Martinus Nijhoff.
- (3) Bazant, Z. P. (Editor), 1985. Mechanics of geomaterials: rocks, concretes, soils, New York, USA, John Wiley and Sons.
- (4) Wittman, F. H. (Editor), 1986. Fracture toughness and fracture energy of concrete, The Netherlands, Elsevier Science.
- (5) Concrete structures under impact and impulsive loading, June 1982. Proceedings, RILEM-CEB-IABSE-IASS - Interassociation symposium, Berlin (West), BAM.
- (6) Mindess, S. and Shah, S. P. (Editors), 1986. Cement based composites: strain rate effect on fracture, MRS Symposium Proceedings, 64.
- (7) Suaris, W., and Shah, S. P., June 1982. Mechanical properties of materials under impact and impulsive loading, Introductory Report for the Interassociation (RILEM, CEB, IABSE, IASS) Symposium on Concrete structures under impact and impulsive loading, Berlin (West), BAM, 33-62.
- (8) Banthia, N. P., March 1987. Impact resistance of concrete, Ph.D. Thesis, Department of Civil Engineering, University of British Columbia, Canada.
- (9) Mutsuyoshi, H., and Machida, A., 1984. Properties and failure of reinforced concrete members subjected to dynamic loading, Transactions of the Japanese Concrete Institute, 6:521-528.
- (10) Chung, L., and Shah, S. P., August 1987. Strain rate effects on bond stresses during earthquake loading, Pacific conference on earthquake engineering, Organized by New Zealand National Society for Earthquake Engineering, Wairekei, New Zealand.
- (11) Mindess, S., 1985. Rate of loading effects on the fracture of cementitious materials, Application of fracture mechanics to cementitious composites, (ed. S. P. Shah), The Hague, Martinus Nijhoff, 617-636.
- (12) Sierakowski, R. L., 1985. Dynamic effect in concrete materials, Application of fracture mechanics of cementitious composites, (ed. S. P. Shah), The Hague, Martinus Nijhoff, 535-557.
- (13) Reinhardt, H. W., 1986. in Cement based composites: strain rate effects on fracture, (eds. S. Mindess and S. P. Shah) MRS Symposium Proceedings, 64:1-13.
- (14) Ramakrishnan, V., Brandshaug, I., Coyle, W. V. and Schrader, E. K., May-June 1980. A comparative evaluation of concrete reinforced with straight steel fibers with deformed ends glued together in bundles, ACI J., 77(3): 135-143.
- (15) Bhargava, J. and Rehnstrom, A., May 1975. High speed photography for fracture studies of concrete, Cement and concrete research, 5:239-248.
- (16) Mayrhofer and Thor, June 1982. Dynamic response of fibre and steel reinforced concrete plates under simulated blast load, in Concrete structures under impact and impulsive loading, Proceedings, RILEM-CEB-IABSE-IASS Interassociation Symposium, Berlin (West), BAM, 279-288.

- (17) Gopalaratnam, V. S., Shah, S. P. and John, R., June 1984. A modified instrumented Charpy test for cement based composites, *J. of Experimental Mechanics*, SEM, 24(2):102-111.
- (18) Gopalaratnam, V. S., and Shah, S. P., 1985. Properties of steel fiber reinforced concrete subjected to impact loading, *ACI J.*, 83(8):117-126.
- (19) Krenchel, H., 1974. Fiber reinforced brittle matrix materials, SP-44, Detroit, ACI, 45-77.
- (20) Johnston, C. D., 1974. Steel fiber reinforced mortar and concrete: A review of mechanical properties, Fiber reinforced concrete, SP-44, ACI, 127-142.
- (21) Abe, H., Chandan, H. C. and Bradt, R.C., 1978. Low blow Charpy impact of silicon carbides, *American ceramic society bulletin*, 57(6):587-595.
- (22) Suaris, W., and Shah, S. P., July 1983. Properties of concrete subjected to impact, *J., Structural Engineering*, ASCE, 109(7):1727-1741.
- (23) Naaman, A. E. and Gopalaratnam, V. S., November 1983. Impact properties of steel fiber reinforced concrete in bending, *International J. of Cement composites and lightweight concrete*, 5(4):225-233.
- (24) Bentur, A., Mindess, S., and Banthia, N. P., 1986. The behavior of concrete under impact loading: Experimental procedures and method of analysis, *Materials and structures*, RILEM, 19(113):371-378.
- (25) John, R., (in preparation). Strain rate effects on fracture of cement based composites, Ph.D. thesis (supervised by S. P. Shah), Department of Civil Engineering, Northwestern University, Evanston, IL, USA.
- (26) John, R. and Shah, S. P., Summer 1986. Fracture of concrete subjected to impact loading, *J. of Cement, Concrete and Aggregates*, ASTM, 8(1):24-32.
- (27) Mobasher, B. and Shah, S. P. (in preparation). Impact behavior of glass fiber reinforced concrete, Department of Civil Engineering, Northwestern University, Evanston, IL, USA.
- (28) John, R. and Shah, S. P., June 1987. Effect of high strength and rate of loading on fracture parameters of concrete, *Proceedings of SEM-RILEM International conference on fracture of concrete and rock* (Eds. S. P. Shah and S. E. Swartz), Houston, TX, USA.
- (29) Kolsky, H., 1949. An investigation of the mechanical properties of materials at very high rates of loading, *Proceedings, Phys. Soc., Sec. B* 62:676-700.
- (30) Zukas, J. A., Nicholas, T., Swift, H. F. Greszczuk, L. B., and Curran, D. R., 1982. *Impact dynamics*, New York, John A. Wiley and Sons.
- (31) Reinhardt, H. W., Kormeling, H. A. and Zielinski, A. J., 1986. The split Hopkinson bar, a versatile tool for the impact testing of concrete, *Materials and structures*, RILEM, 19(109):55-63.
- (32) Malvern, L. E., Tang, T., Jenkins, D. A., and Gong, J. C., 1986. in *Cement based composites: strain rate effects on fracture* (eds. S. Mindess and S. P. Shah) MRS Symposium Proceedings, 64:119-138.

- (33) Suaris, W., and Shah, S. P., Winter 1982. Inertial effects in the instrumented impact testing of cementitious composites, *J. of Cement, Concrete and Aggregates*, ASTM, 3(2):77-83.
- (34) Takeda, J. -I., Tachikawa, H., and Fujimoto, K., June 1982. Mechanical properties of concrete and steel in reinforced concrete structures subjected to impact or impulsive loadings, *Concrete structures under impact and impulsive loading*, RILEM-CEB-IABSE-IASS Interassociation Symposium, Berlin (West), BAM, 83-91.
- (35) Cowell, W., June 1966. Dynamic properties of plain portland cement concrete, Tech. Rep. R447, U.S. Naval Engineering Laboratory, Port Hueneme, CA, USA.
- (36) Mellinger, F. M. and Birkimer, D. L., April 1966. Measurements of stress and strain on cylindrical test specimens of rock and concrete under impact loading. Tech. Rep. 4-46, Dept. of Army, Ohio River Division Laboratory, USA.
- (37) Kormeling, H. A., Zielinski, A. J., and Reinhardt, H. W., May 1980. Experiments on concrete under single and repeated impact loading, Rep. 5-80-3, Stevin Laboratory, Delft University of Technology, Delft, The Netherlands.
- (38) C. Tinic and E. Bruhwiler, 1985. Effects of compressive loads on the tensile strength of concrete at high strain rates, *Int. J. of cement composites and lightweight concrete* 7(2):103-108.
- (39) Zielinski, A. J., 1986. Concrete under biaxial compressive-impact tensile loading, *Fracture toughness and fracture energy of concrete*, (ed. F. H. Wittmann), The Netherlands, Elsevier Science, 479-489.
- (40) Mindess, S. and Nadeau, J. S., 1977. Effect of loading rate on the flexural strength of cement and mortar, *Bulletin of American Ceramic Society*, 56(44):429-430.
- (41) Butler, J. E. and Keating, J., 1980. Preliminary data derived using a flexural cyclic loading machine to test plain and fibrous concrete, *Materials and Structures*, 14(79):25-33.
- (42) Zech, B. and Wittmann, F. H., 1980. Variability and mean value of strength as a function of load, *ACI Journal*, 77(5):358-362.
- (43) Mecharatna, M. and Roland, E., May 1987. Strain rate effects as properties of cement-based composites under impact loading, *Engineering mechanics 6th conference*, ASCE, Buffalo, NY USA, 113.
- (44) Watstein, D., April 1953. Effect of strain rate on the compressive strength and elastic properties of concrete, *ACI Journal*, 49(8):729-744.
- (45) Atchley, B. L. and Furr, H. L., November 1967. Strength and energy absorption capabilities of plain concrete under dynamic and static loading, *ACI Journal*, 745-756.
- (46) Hughes, B. P. and Gregory, R., 1978. Compressive strength and ultimate strain of concrete under impact loading, *Magazine of concrete research* 30(105):189-199.
- (47) Jawed, I., Childs, G., Ritter, A., Winzer, S., Johnson, T., and Barker, D., 1987. High-strain-rate behavior of hydrated cement pasts, *Cement and concrete research*, 17(3):433-440.
- (48) Ahmad, S. and Shah, S. P., Sept-Oct. 1985. Behavior of hoop confined concrete under high strain rates, *ACI J.*, 634-647.

- (49) Suaris, W. and Shah, S. P., June 1984. Rate sensitive damage theory for brittle solids, J. of Engineering mechanics, ASCE, 110(6):985-997.
- (50) Suaris, W. and Shah, S. P., March 1985. Constitutive model for dynamic loading of concrete," J. of Structural engineering, ASCE, 111(3):563-576.
- (51) John, R., Shah, S. P., and Jenq, Y. -S., 1987. A fracture mechanics model to predict the rate sensitivity of mode I fracture of concrete, Cement and concrete research, 17(2):249-262
- (52) Mindess, S., Banthia, A., Ritter, A. and Skalny, J. P., 1986. Crack development in cementitious materials under impact loading, in Cement based composites: strain rate effects on fracture (eds. S. Mindess and S. P. Shah) MRS Symposium Proceedings, 64:217-223.
- (53) Jenq, Y. -S., and Shah, S. P., October 1985. A two parameter fracture model for concrete, J. of Engineering Mechanics, ASCE, 111(10):1227-1241.
- (54) Z. P. Bazant, J. K. Kim and P. Pfeiffer, 1985. Continuum model for progressive cracking and identification of nonlinear fracture parameters, in Application of fracture mechanics to cementitious composites (ed. S. P. Shah), The Netherlands, Martinus Nijhoff, 197-246.
- (55) Hillerborg, A., Modeer, M., and Petersson, P. E., Nov. 1976. Analysis of crack formation and crack growth in concrete by means of fracture mechanics and finite elements, Cement and concrete research, 6(6):773-782.
- (56) Takeda, J. and Tachikawa, H., August 1971. Deformations and fracture of concrete subjected to dynamic load, Proceedings, International conference on mechanical behavior of materials, Vol. IV, Concrete and cement paste, glass and ceramics, Kyoto, Japan, 4:267-277.
- (57) Mlakar, P. F., Vitaya-Udom, K. P. and Cole, R. A., July-August 1985. Dynamic tensile-compressive behavior of concrete, ACI J., 82(4):484-491.
- (58) Suaris, W. and Shah, S. P., May-June 1986. Discussion of Ref. 57, ACI J., 83(3):477-479.
- (59) Takeda, J., Tachikawa, H. and Fujimoto, L, June 1982. Mechanical properties of concrete and steel in reinforced concrete structures subjected to impact or impulsive loads, Proceedings of RILEM-CEB-IABSE-IASS-Interassociation Symposium, BAM, Berlin (West), 83-91.
- (60) Kiger, S. A., and Getchell, J. V., September 1980. Vulnerability of shallow-buried flat roof structures, Technical Report SI-80-7, Report 1, 2 and 3, U. S. Army Engineer Waterways Experiment Station.
- (61) vos, E. and Reinhardt, H. W., September 1980. Bond resistance of deformed bars, plain bars and strands under impact loading, Report 5-80-6, Stevin Laboratory, Department of Civil Engineering, Delft University of Technology, Delft, The Netherlands.
- (62) Evans, A. G., June 1974. Slow crack growth in brittle materials under dynamic loading conditions, International Journal of Fracture, 10(2):251-259.
- (63) Charles, R. J., December 1958. Dynamic fatigue of glass, J. of Applied Physics, 29(12):1657-1662.

- (64) Mihashi, H., and Wittmann, F. H., 1980. Stochastic approach to study the influence of rate of loading on strength of concrete, The Netherlands, Heron, 25(3).
- (65) Kormeling, H. A., 1986. The rate theory and the impact tensile behavior of plain concrete, in Fracture toughness and fracture energy of concrete, (Ed. F. H. Wittmann), The Netherlands, Elsevier Science, 467-477.
- (66) Freund, L. B., 1972. Crack propagation in an elastic solid subjected to general loading: Parts I and II, J. Mechanics and Physics of Solids, 20:129-152.
- (67) Broberg, K. B., 1960. The propagation of a brittle crack, Arkiv for Fysik, 18(6):159-192.
- (68) Grady, D. E. and Kipp, M. E., 1979. The micromechanics of impact fracture of rock, International J. of rock mechanics, mining science and geomechanics abstracts, 16:293-302.
- (69) Diamond, S. and Bentur, A., 1985. On the cracking in concrete and fiber reinforced cements, in Application of Fracture Mechanics to Cementitious Composites (ed. S. P. Shah), The Netherlands, Martinus Nijhoff, 87.
- (70) Swartz, S. E. and Go, C.-G., June 1984. Validity of compliance calibration to cracked concrete beams in bending, Experimental Mechanics, SEM, 24(2):129-134.
- (71) Bascoul, A., Kharchi, F., and Maso, J. C., June 1987. Concerning the measurement of the fracture energy of micro-concrete according to the crack growth in a three points bending test on notched beams, Proceedings of SEM-RILEM international conference on fracture of concrete and rock, (Eds. S. P. Shah and S. E. Swartz), Houston, TX USA.
- (72) Jenq, Y. -S. and Shah, S. P. 1985. A fracture toughness criterion for concrete, Engineering Fracture Mechanics, 21(5):1055-1069.
- (73) Jenq, Y.-S., and Shah, S. P., January 1986. Crack propagation resistance of fiber reinforced concrete, J. of structural engineering, ASCE 112(10):19-34.
- (74) Jenq, Y. -S., June 1987. Fracture mechanics of cementitious composites, Ph.D. Dissertation (Supervised by S. P. Shah), Northwestern University, Evanston, IL, USA.
- (75) Jenq, Y.-S. and Shah, S. P., Submitted for publication, 1987. Mixed-mode fracture of concrete.
- (76) Gopalaratnam, V. S. and Shah, S. P., May-June 1985. Softening response of plain concrete in direct tension, ACI Journal, 82(3):310-327.
- (77) Maji, A. and Shah, S. P., to be published. Process zone and acoustic measurements in concrete, Experimental Mechanics, SEM Paper No. 3609.
- (78) Goldsmith, W., Pulivka, M., and Yang, T., February 1966. Dynamic behavior of concrete, Experimental Mechanics, 65-79.
- (79) Read, H. E., and Maiden, C. J., August 1971. The dynamic behavior of concrete, National Technical Information Service Springfield, VA, No. AD894240.
- (80) Bazant, Z. P. and Oh, B. H., October 1982. Strain-rate in rapid triaxial loading of concrete, Proceedings, ASCE, 108(EM5):764-782.
- (81) Oh, B. H., Jan.-Feb. 1987. Behavior of concrete under dynamic loads, ACI Materials J., 84(1):8-13.

- (82) Loland, K. E., 1980. Continuous damage model for load response estimation of concrete, *Cement and concrete research*, 10:395-402.
- (83) Mazars, J., Mar.-Apr. 1981. Mechanical damage and fracture of concrete structures, *Advances in fracture research* (Ed. D. Francois), 5th International Conference on Fracture, Cannes, 1499-1506.
- (84) Taylor, M. A., 1969. Theory for the determination and failure of cement pastes, mortars and concrete under general states of stress, Ph.D. Thesis, University of California, Berkeley, USA.
- (85) Shah, S. P. and Winter, G., 1968. Inelastic behavior and fracture of concrete, *Causes, mechanism and control of cracking in concrete*, ACI, SP-20, 5-28.
- (86) Passman, S. L., Grady, D. E., and Rundle, J. B., 1980. The role of inertia in the fracture of rock, *Journal of applied physics*, 51(8):4070-4075.
- (87) Mould, J. C. and Levine, H., 1987. A three invariant viscoplastic concrete model, in *Constitutive laws for engineering materials: theory and applications* (Eds. C. S. Desai et al.) New York, USA, Elsevier Science, 707-716.

**Steel Fiber Concrete, Proceedings of U.S.-Sweden Seminar (NSF-STU), Editors: S. P. Shah and A. Skarendahl, Elsevier Applied Science Publishers, U.K., pp. 299-331, October 1986.**

**Strength, Deformation and Fracture Toughness  
of Fiber Cement Composites at Different Rates of Loading**

*by*

**V. S. Gopalaratnam and S. P. Shah**

# **STRENGTH, DEFORMATION AND FRACTURE TOUGHNESS OF FIBER CEMENT COMPOSITES AT DIFFERENT RATES OF FLEXURAL LOADING**

**by V S Gopalaratnam, Asst Prof, University of  
Missouri - Columbia , Columbia, Missouri, USA**

**S P Shah, Prof, Northwestern University,  
Evanston , Illinois, USA**

---

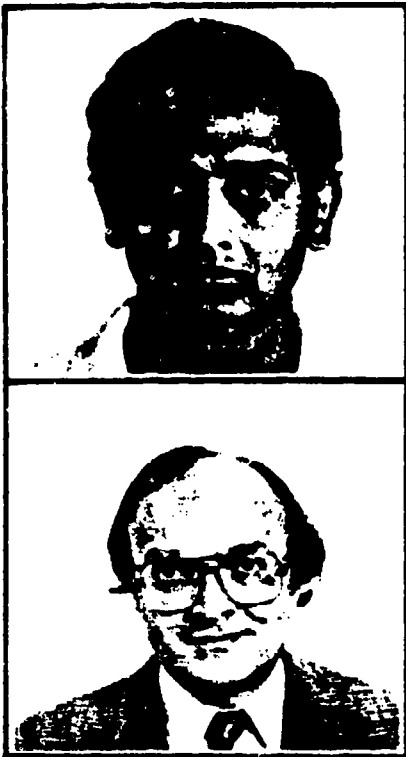
## **ABSTRACT**

Several test methods used for impact tests of fiber reinforced concrete (FRC) are reviewed in the article with a view to evaluate the reliability of the material responses obtained therefrom. Parasitic effects of inertia observed while conducting instrumented impact tests on concrete composites are discussed at length. Based on experience gained during the course of the development of a modified instrumented Charpy test scheme, useful guidelines for selection of the various test parameters are proposed in order to minimize parasitic inertial loads.

The effect of strain-rate on the flexural behavior of unreinforced matrix and 3 different fiber reinforced concrete (FRC) mixes are discussed. Results obtained from the modified instrumented Charpy tests on cement composites compare well with results from several similar investigations that use an instrumented drop-weight set-up.

FRC mixes are more rate-sensitive than their respective unreinforced matrices, showing increases in dynamic (strain-rate of 0.3/s) strength of up to 111% and energy absorption (up to a deflection of 0.1 in.) of up to 70% ( $V_f = 1.5\%$ ) over comparable values at the static (strain-rate of  $1 \times 10^{-6}$ /s) rates. Composites made with weaker matrices, higher fiber contents and larger fiber aspect ratios are more rate sensitive than those made with stronger matrices, lower fiber contents and smaller fiber aspect ratios. Several observations made in the study suggest that the rate sensitivity exhibited by such composites is primarily due to a change in the cracking process at the different rates of loading.

Relative improvements in performance due to the addition of fibers as observed in the instrumented tests are also compared to those from the conventional impact and static tests. Resulting from this comparison, it is proposed that static flexural toughness tests could be used to approximately estimate the dynamic performance of FRC.



•Dr. V.S. Gopalaratnam is Assistant Professor of Civil Engineering at University of Missouri-Columbia. He received his Ph.D. from Northwestern University. His research interests include fracture mechanics and strain-rate behavior of concrete and related composites.

•Dr. S.P. Shah is Professor of Civil Engineering at Northwestern University. After receiving his Ph.D. from Cornell University, he has taught at University of Illinois at Chicago and at Massachusetts Institute of Technology. He was a Guest Professor at Delft Institute of Technology in 1976 and at Denmark Technical University in 1984. His current research interests include: constitutive relations of concrete, application of non-linear fracture mechanics to rocks and concrete, impact loading, fiber reinforced concrete and hysteretic behavior of reinforced concrete structures.

## INTRODUCTION

Despite its extensive use, low tensile strength has been recognized as one of the major drawbacks of concrete. Although one has learned to avoid exposing concrete structures to adverse static tensile loads, these cannot be shielded from short duration dynamic tensile stresses. Such loads originate from sources such as impact from missiles and projectiles, wind gusts, earthquakes and machine vibrations. The need to accurately predict the structural response and reserve capacity under such loading has led to an interest in the mechanical properties of the component materials at high rates of straining.

One method to improve the fracture resistance and the resistance of concrete when subjected to impact and/or impulsive loading is by the incorporation of randomly distributed short fibers. Concrete (or Mortar) so reinforced is termed fiber reinforced concrete (FRC). Moderate increase in tensile strength and significant increases in energy absorption (toughness or impact-resistance) have been reported by several investigators [1-3] in static tests on concrete reinforced with randomly distributed short steel fibers. Studies on the dynamic behavior of FRC are rather limited in comparison. This, despite the fact that the most important property of such composites is its superior impact resistance.

As yet no standard test methods are available to quantify the impact resistance of such composites, although several investigators have employed a variety of tests including drop weights, swinging pendulums and the detonation of explosives. These tests though useful in ascertaining the relative merits of different composites do not yield basic material characteristics which can be used for design.

More recently instrumented impact tests have been developed to obtain reliable and continuous records of the characteristics of brittle materials

when they are subjected to high straining rates [4-10].

Results from such tests could be used to formulate constitutive relations for these composites which would probably lead to more rational design procedures for structures subjected to impact. As in the static analysis of FRC, it is expected that the composite behavior under dynamic loading could be predicted from the knowledge of the behavior of its constituent materials as well as their interaction, at higher rates of loading.

## TYPES OF IMPACT TESTS

A review of some of the test methods and results obtained therefrom, based on tests on fiber reinforced concrete specimens is presented in the following sub-sections. Drawbacks of some of these popular conventional tests are also discussed whenever relevant.

### Charpy Impact Test

Charpy test is a standard impact test recommended for metals (ASTM E29). The energy consumed to totally fracture a notched beam specimen is computed from the rise angle of the pendulum after impact and is used as a measure of the impact resistance of the material. In one such test, Battelle Development Corp. [11] reported increases in Charpy impact energy from 2.2 kJ/m<sup>2</sup> for plain concrete (25x25x102mm beams) to 21.7 kJ/m<sup>2</sup> for FRC (2% by volume of 0.15mm diameter steel fibers). In similar tests with different specimen sizes Krenchel [12] and Johnston [13] observed a similar magnitude of increase in impact resistance achieved with the incorporation of steel fibers. However, Radomski [14] reports of different impact energy values from that reported in [11]. This is probably due to the different test set-up compliances in these studies. Abe et al, [15] while testing rate-insensitive silicon carbide specimens, have shown using an elaborate energy balance, that energy absorbed by the specimen is only of the order of 30% of the total energy recorded in the Charpy test. Bluhm [16] conducted Charpy impact tests on metallic specimens and observed that the stiffness of the pendulum does significantly affect both the peak load and fracture energy recorded.

The differences in the results of some of the earlier studies [11-14] can also be attributed to size dependent characteristics of inhomogeneous materials. Representative results from tests on cement composite specimens of sizes comparable to that recommended for metal specimens (10mm x 10mm x 50mm) cannot, for obvious reasons, be obtained.

In addition to the above machine stiffness and specimen size dependent characteristics of such tests, the conventional Charpy test yields only the total energy absorbed in fracturing a specimen. Properties like ultimate strength, corresponding strains and deformations, influence of the rate of loading, etc. which are invaluable to the development of rational design procedures cannot be ascertained.

### Drop-Weight Test

In the drop-weight type of test a stationary specimen is struck by a

falling weight. The number of blows to produce failure yields a qualitative measure of the impact resistance of the material. The number of variables involved in such tests are larger than that in conventional Charpy type tests. Examples are the specimen size, support configuration, size and shape of the hammer, drop weight and the prescribed failure criteria (first crack, perforation or total fracture, fixed extent of damage, fixed amount of deformation). All the above variables make such a test less meaningful for any purpose other than a qualitative (and/or comparative) measure of the impact resistance of the material being tested. Nanda and Hannant [17] using a "number of blows to no rebound" test found that plain concrete failed after 5 blows while concrete reinforced with 5% steel fibers withstood up to 100 blows. Dixon and Mayfield [18] also recorded an increase in the number of blows to no rebound when concrete was reinforced with 1% by volume of steel fibers.

Jamrozy and Swamy [19] have published results of tests conducted to study the behavior of FRC cubes (200mm) subjected to repeated drop-weight impact loading applied by a 50 kg hammer falling through 300mm. Three types of steel fibers were used: straight round fibers (0.25 x 15mm, 0.25 x 25mm), crimped fibers (0.25 x 25mm) and hooked fibers (0.4 x 40mm). The number of blows to produce first crack was used as a measure of impact resistance. For straight fiber (0.25 x 25mm, volume fraction 1%) reinforced FRC, first crack was found to appear after about 150 blows. Increasing fiber aspect ratio ( $l/d$ ) and volume fraction ( $v_f$ ) was found to increase the impact resistance. They also noted that crimped and hooked fibers performed better under impact loading than smooth fibers.

Bailey et al [20] have reported results of drop weight tests conducted on FRC stair treads to access their impact behavior. Using 1% (volume fraction) of (a) fibrillated polypropylene fibers (50mm long), (b) crimped steel fibers (150mm long) and indented steel fibers (63mm long) they noted that first cracking occurred at approximately the same drop-weight irrespective of whether the tread contained fibers. However, the inclusion of fibers was found to reduce the severity of the subsequent cracking behavior. The American Concrete Institute (ACI Committee 544 on FRC, Ref. 21) recommends a drop-weight type test to evaluate the impact resistance of concrete. A 2½ in. (64mm) diameter hardened steel ball is placed on a cylindrical specimen (6 in. diameter, 2½ in. height, 152 x 64mm). A 10 lb. (4.54 kg) hammer is dropped 18 in. (457mm) onto the ball repeatedly until some prescribed failure criterion (first crack or fixed extent of deformation) is met. Using this procedure Ramakrishnan et al [22] recorded about 100 to 150 blows to first crack for concrete reinforced with hooked-end fibers.

#### Constant Strain Rate Test

Although limited in their capacity to achieve high rates of loading, conventional servo-controlled machines have been used to conduct dynamic tests in the intermediate strain rates.

Butler and Keating [23] have studied the effect of rate of load application on the flexural strength of FRC using a hydraulic ram capable

of moving at different speeds. They tested 200 x 200 x 1500mm beam specimens under four-point bending (1.25% steel fibers, 50mm long and 0.5mm diameter). They observed a 35% increase in the flexural strength of the composite when the stress rate was increased from 0.017 to 170 MN/m/s. This increase is lower than that observed for plain concrete (75% increase) when the stress rate is increased in the same range.

Kobayashi and Cho [24] using a displacement controlled testing machine obtained load-deflection curves for polyethylene fiber (4%, 40mm long and 0.9mm diameter) reinforced concrete beams (100 x 100 x 400mm) at various strain rates. They observed from four-point bending tests that loading velocity affected both the peak load carrying capacity and the corresponding deflection. When the loading rate was increased from 1mm/min to 200mm/min a 50% increase in the composite strength was observed. Less dramatic increase in first crack stress was also reported. Deflections at peak load were smaller at the higher velocities. This increase in stiffness at higher rates was attributed by them to visco-elastic property of the polyethylene fibers.

### Dynamic Tensile Test

Birkimer and Lindemann [25] have reported results of tensile tests conducted on steel and nylon fiber and reinforced concrete specimens. The nylon fibers used were 0.25mm in diameter and the steel fibers 0.43mm. 1% (volume fraction) of these 25.4mm long fibers were used in tests conducted by striking cylindrical specimens at one end with high velocity projectiles. The compression wave generated at the striking end was reflected as a tensile wave when it reached the far end of the cylindrical specimen, causing the specimen to spall. Measuring the fly-off velocity of an impedance matched pellet placed at the far end, enabled the particle velocity to be determined. From this the stresses and strains induced in the specimen were calculated. For strain rates of about 30/s, they recorded a 4 to 5 fold increase in fracture strains/stresses over the corresponding static values (strain rate of about  $10^{-6}$ /s).

Bhargava and Rehnstrom [26] used the "split Hopkinson bar test" to study the dynamic tensile behavior of FRC. The specimens used in the tests were reinforced with 0.2% by volume of polypropylene fibers. Specimens were sandwiched between two very long (5 meters each) aluminum bars. These bars were used to measure the incident and transmitted pulses. The impact strength of the specimen was assumed to have been reached when the transmitted pulse showed no increase with increasing amplitude (impact velocity) of the impact pulse. For observed pulse rise-times of about 50  $\mu$ s the dynamic strength was found to be about 50% greater than the static tensile strength.

### Explosive Test

Explosive tests on FRC slabs have been carried out by Williamson [27]. He observed that shock loading when applied to slabs of plain concrete resulted in the complete disintegration of the specimens. A considerable reduction in spall velocity of the fragments was obtained by him when the matrix was reinforced with 1.75% nylon fibers. The explosive tests conducted on slabs by Robins and Calderwood, [28] also show that inclusion of steel and polypropylene fibers significantly reduces the size and particle velocity of the fragments. Such types of tests are ideally suited

for situations where one would expect a structure to be subjected to rapidly rising pressures resulting from blasts or explosives.

### Instrumented Impact Test

All the conventional tests described earlier offer only insights into relative merits of different fiber cement composites. They lack in their usefulness as they do not provide information on the basic properties of the material such as stress-strain or load deflection relations at high rates of loading. These relations should be independent of the test setup, that is, they must be reproducible on any setup. It is believed that instrumented impact testing, as described in this section satisfies these requirements.

While retaining the conventional mechanisms to apply impact loads, instrumented impact tests permit monitoring of load, deflection, strain and energy histories during the impact event. This allows one to compute basic material properties such as ultimate strength, strain at peak loads, energy absorbed and fracture toughness at the different strain rates.

Hibbert [29] modified a conventional Charpy type test by instrumenting the pendulum striker. He obtained continuous load-time and energy-time histories for plain and fiber reinforced concrete beams (100 x 100 x 500mm). He observed that for all specimens (unreinforced as well as FRC) the peak load under impact loading (impact velocity of 2.85 m/s) was about 10 times that under static loading (displacement rate of 0.05mm/s). This increase is quite high when compared with a less than two-fold increase generally reported by other investigators for similar strain rates (Fig. 1). This high load recorded by him is not representative of true material response but is a consequence of specimen inertia effects. This parasitic effect and solutions to minimize it will be discussed in greater depth elsewhere in this article. Using specially designed supports, Hibbert was able to compute the kinetic energy imparted to the broken halves of the specimen on impact and thus obtain the fracture energy of plain concrete (3.3 kJ/m<sup>2</sup>). This value is an order of magnitude higher than the energy absorbed by plain concrete when fractured under static loading (0.28 kJ/m<sup>2</sup>). For FRC beams he then calculated the energy absorption solely due to fiber debondings, pull-out and fracture, by subtracting the kinetic energy of the specimen and fracture energy of plain matrix from the total energy loss of the pendulum. But, since fracture energy of matrix was overestimated, this procedure resulted in lower energy absorption values for fiber debonding, pull-out and fracture. Hibbert as a result concluded that there is no improvement in energy absorbed due to the fibers in FRC beams under impact, compared to the corresponding value under static loading. Contrary to this conclusion, later studies [4-10] have documented enhanced energy absorption at dynamic rates.

Radomski [30] has used a rotating impact machine for performing instrumented tests on FRC. Impact in his tests is simulated by releasing a striker from a rotating fly-wheel when it has attained the desired velocity. On release, the striker hits a simply supported beam specimen (15 x 15 x 105mm). The load-time response is recorded using piezo-electric gages at one of the specimen supports. The author does not report details of such load histories. However, he observes that measurements of energy absorption obtained from his tests do not correlate with those obtained

with conventional Charpy tests.

More recently Suaris and Shah [6], Gopalaratnam and Naaman [7] and Gopalaratnam and Shah [10] have conducted series of tests on concrete, mortar and FRC specimens using both an instrumented drop-weight set-up and a modified instrumented Charpy set-up. Results from these studies and a series of more systematic tests on FRC will be presented in later sections.

Results compiled by Suaris and Shah [5] from several earlier investigators, on the behaviour of plain concrete at different strain rates is presented in Fig. 1. It is apparent that the rate sensitive behaviour of plain concrete is different in tensile, flexural and compressive modes of loading. Similar trend is to be expected for FRC based on results from some of the impact studies on FRC, cited earlier. Results from static tensile and flexural tests on FRC would suggest similar behaviour as a result of the fact that the behaviour of FRC prior to "first-crack" is not too different from that of plain matrix. In contrast, however, the important contribution of the fibers to the composite behaviour is in the post-cracking regime and hence knowledge of the entire load-displacement behaviour is essential to the accurate quantification of energy absorption under impact loading.

Koyanagi et al [31] have studied the deformation and fracture of mortar and FRC beams (75 x 75 x 660mm) subjected to 3 point bending under static and impact-loading. Instead of recording loads and deflections directly, they have used accelerometers on the striker and specimen in a drop weight type of instrumented impact set-up. Comparing deflections computed from strain gage readings with those obtained from the accelerometers, they observed a good correlation between the two until cracking. Impact force was computed from the mass of the striker and its acceleration. Energy required to fracture the plain mortar specimens or deform the FRC specimens to prescribed deflection was computed by subtracting the kinetic energy of the specimen from the applied impact energy. From reported values of strains, an average strain-rate of 0.09 - 0.2/s was computed for their impact tests. They report of a 50% increase in energy absorbed in the fracturing process under impact loading when compared to static loading. Flexural strength increases from 1030 psi (7.1MPa) to up to 1750 psi (12.1MPa) for plain mortar and 1262 psi (8.7MPa) to 3278 psi (22.6MPa) for FRC have been reported at the static loading rates and impact loading rates respectively. Deflections at peak load reported by them increase by around 50% at impact loading rates compared to the respective values at static rates for both mortar and FRC specimens. Results from their study are compared with those from this investigation elsewhere in this article.

#### INERTIAL EFFECTS IN THE INSTRUMENTED IMPACT TESTS OF BRITTLE MATERIALS

Discussion in this section is restricted to inertial effects in the instrumented impact tests of brittle materials although much of the body of knowledge comes from earlier studies on the impact testing of metals [32-37].

Several investigators have, in the past, recognized that during the initial period of the impact event, the load measured by the striker (tup) and that resisted by the specimen undergoing bending, are not identical

[4-10, 32-37]. This is attributed to specimen inertial effects, which manifest themselves as oscillations on the load-time records. Cotterell [33] observed a linear relationship between inertial load recorded and impact velocity. Inertial oscillations in his tests with mild steel specimens were small compared to bending loads. A mean path correction was used to compute ultimate strength and other material properties. However, for more brittle metals, Venzi, Priest and May [34] have concluded that such a mean-path correction would result in large errors. Server, Wullaert, and Sheckhard [35] have recommended that errors due to inertial oscillations can be neglected after three half-periods of oscillations. While this guide-line has been accepted more or less as a standard practice for metal testing [32], this was shown by Suaris and Shah [4] to be insufficient for the impact testing of asbestos cement composites. They attributed this to the brittleness and the relatively lower strength-to-weight ratios of such composites compared to those of metals. Consequently, they suggested that instances could be realized where inertial loads could overshadow true bending loads sustained by such cementitious composites.

Kalthoff, et al, [36] have shown, using direct optical measurement of the fracture parameter  $K_{Ic}$  of Araldite specimens, that the tup load records can overpredict peak loads in instrumented impact tests by as much as an order of magnitude. They also stated that this overprediction is more pronounced for larger specimens and higher impact velocities. The unusually high peak loads and fracture energies recorded by Hibbert [29] for plain concrete is similar to that reported by Kalthoff, et al., [36]. The influence of inertial loads is likely to be more pronounced in Hibbert's tests because of the larger specimen size used by him.

Suaris and Shah [4] have analyzed this problem and have illustrated by means of a two-degree-of-freedom spring mass-system that the introduction of a rubber pad between the striker and the specimen is an effective way of reducing specimen inertial oscillations. This model has been used in interpreting and evaluating results from the modified Charpy test. The model has also been developed further to provide suitable guidelines for the selection of the various test parameters while conducting instrumented impact tests of brittle materials [8], so that the inertial oscillations can be minimized.

Winkler, et al, [37] too have experimentally observed that the introduction of an aluminum damping pad effectively reduces the peak load recorded by the striker. While testing "pressure vessel" steel specimens. This reduced peak load, according to them, provides improved correlation with crack tip strains directly recorded in the vicinity of the notch.

The testing scheme used in the present study consequently, has been designed with a view to shed more light on the parasitic effects of inertia and to provide some general guidelines on the selection of the various test parameters. A block diagram showing salient features of the modified instrumented Charpy test developed during the course of this study is illustrated in Fig. 2. Details of the test set-up and associated instrumentation is presented in the next section.

## MODIFIED INSTRUMENTED CHARPY SET-UP

### Modifications Effected

A conventional Charpy tester, Tinius Olsen Model 64, was modified and instrumented to facilitate tests on concrete, mortar and FRC specimens at different impact velocities. Among the three primary modifications were: (a) instrumentation of the striker and the two supporting anvils, (b) seating arrangement to accommodate large sized specimens and, (c) low-blow fixture to enable tests at different impact velocities.

It was felt that recording of anvil and striker loads simultaneously was essential to a proper interpretation of inertial loads, and to assess the influence of parameters like test system compliance, specimen size and impact velocity on the test results. The anvils and the striker were designed to serve as compression load cells capable of recording dynamic loads transmitted through them during an impact event. They were made from hardened tool steel (oil hardened, SAE 01, Rockwell C55) to ensure elastic behaviour even under high loads. They were sufficiently rounded at the specimen contact points so as to avoid local compressive damage to the specimen on impact, and at the same time facilitate smooth specimen rotation during bending. Semi-conductor P-N type gages (Kulite M (6) CEP-120-500, gage factor 220, 120  $\Omega$ ) were used in full-bridge configuration within protective recesses provided on either side of all the load cells (2 anvils and the striker). Besides providing a high signal to noise ratio, the configuration also allowed temperature compensation. The dual (P-N) gages were bonded with M-Bond 610, and a post-curing protective acrylic coating M-Coat D (both from Micro-measurements) was later applied. The load cells were calibrated statically using an MTS servo-controlled testing machine, after they were subjected to low-amplitude cyclic pre-loading to eliminate initial gage-seating effects. A 10v D.C. bridge excitation was used for all the load cells. Output from the two anvils were tied in series to monitor total load recorded by the supports.

Commonly recommended size for impact testing of metal specimens is 10 x 10 x 50mm. The heterogeneity of cement based composites necessitates use of larger specimens (76 x 25 x 229mm used here). Consequently, it was necessary to modify the support mechanism of the impact machine. The dimensions of the support and the depth of the specimen did not allow impact to occur when the pendulum reached its lowest position. As a result, the beam and its supports were adequately inclined to ensure a flush contact between the beam and the striker at the moment of impact. While designing the striker, it was ensured that the center of percussion of the pendulum was retained at the center of the striking face so that adverse vibrations on the pendulum were avoided. The larger specimens also did not allow the pendulum to clear the broken halves of the specimen, unlike in a Charpy test. A hydraulic shock absorber mechanism facilitated arresting the motion of the pendulum after the beam had deflected about 50mm, Fig. 3. Peak loads were reached for fiber reinforced concrete specimens, while unreinforced mortar and concrete specimens totally fractured much prior to this deflection. Hence, arresting the pendulum motion did not affect the test results in any adverse manner.

To allow for impacting the specimen at different velocities, a low-blow fixture was designed. This allowed impact velocities in the range

0.5 - 3.0m/s. A safety lock-latching mechanism held the hammer in its raised position and assured a vibration-free release when activated. A photograph showing an overall view of the test set-up including the modified Charpy machine and associated instrumentation is presented in Fig. 4.

### Instrumentation

(a) Digital Storage Oscilloscope: A 4-channel digital oscilloscope (Nicolet 4094) with 2 two-channel differential amplifier plug-in units (4562) of high resolution and frequency response (500 nano seconds per point sampling rate) was used for storing the load, strain and deflection histories. The 16K (points) main-frame storage was augmented by a dual-disk recorder (XF-44) that used 133mm diskettes. Results from 20 tests (20 tracks of 16K each) were stored on these diskettes for permanent records. Hard copies of these records were obtained on a conventional x-y recorder by playing back the stored wave-forms at much slower rates. Fig. 2 shows a block-diagram of the instrumentation.

(b) Strain Measurements: Strains were measured by directly bonding foil gages (Precision Measurements, type F400, 120  $\Omega$ ) at desired locations on the specimen. For the preliminary test strains at quarter-point (and mid-point in some tests) on the tension-face of the unnotched 3 point bend specimen were monitored. Bridge completion network, using dummy gages, was used to provide temperature compensation. Bridge excitation and signal amplification was provided for by a HP-Accudata 218 bridge amplifier. During the later phase of the study, strains at the quarter-point (tension-face) of unnotched plain mortar specimens and notch tip strains (0.5 in., 13mm ahead of the saw cut notch) on the FRC specimens were measured.

(c) Deflection Measurements: Deflections of the beam mid-point were measured using a Schaevitz LVDT (050 MHR). A.C. excitation and output amplification was provided for by a Schaevitz high frequency (20kHz nominal frequency) signal conditioner (CAS-200). A 1:2 hardened steel wedge attached to the beam mid-point (close to mid-point, for notched specimens) drove a plunger that held the LVDT core. The transducer and core assembly was securely enclosed in an aluminum contraption to protect them from possible damage during the impact event. A set-screw arrangement enabled the transducer to be displaced with respect to the core to allow for the initial zeroing operations.

(d) Load Measurements: Detailed description of the dynamic load cell construction was presented earlier. Load outputs from the striker and the support (both anvil outputs tied in series) were fed into one of the plug-in units of the digital scope.

Beam deflection and strain were recorded using the other plug-in unit of the scope. Simultaneous triggering of both the plug-in units was accomplished externally using amplified signal from a fiber-optic block and flag assembly.

### GUIDELINES FOR SELECTION OF TEST PARAMETERS

Before embarking on an elaborate test program it was necessary to thoroughly evaluate the performance of the test set-up developed in this

study. This was successfully accomplished by testing plain concrete specimens for which sufficient reliable data were available from an earlier study [6] on its impact behavior. Results from this preliminary study are detailed in [9]. The guidelines for developing a reliable instrumented impact test scheme for concrete materials is proposed here.

### Period of Inertial Oscillations

The theoretical model used here to evaluate test results obtained from the modified Charpy set-up was originally developed for a drop-weight type impact test by Suaris and Shah [4]. The impact system is represented by a two degree of freedom (d.o.f.) lumped mass system. The test beam is represented as mass  $m_b$  of stiffness  $k_b$ , the hammer-tup assembly by a mass  $m_t$  and the tup-specimen contact zone by an effective stiffness  $k_e$ . The governing equation of motion of the system is given by

$$m_t \ddot{x}_1 + k_e(x_1 - x_2) = 0, \quad m_b \ddot{x}_2 + k_e(x_2 - x_1) + k_b x_2 = 0 \quad (1)$$

where  $x_1$  and  $x_2$  are displacements of the masses  $m_t$  and  $m_b$  respectively. Equation 1 is solved by applying proper initial conditions for  $x_1$ ,  $x_2$ ,  $\dot{x}_1$  and  $\dot{x}_2$ . The two natural frequencies thus obtained, assuming  $m_t \gg m_b$ , are:

$$\omega_1 = \left( \frac{k_b k_e}{m_t(k_e + k_b)} \right)^{1/2}, \quad \omega_2 = \left( \frac{k_e + k_b}{m_b} \right)^{1/2} \quad (2)$$

Generally, the mass of the hammer is much larger than that of the specimen ( $m_t/m_b = 60$ , in this investigation). Consequently,  $\omega_1$  is an order of magnitude smaller than  $\omega_2$ . The frequency of oscillations observed on the load-time traces in instrumented impact tests corresponds closely to  $\omega_2$ .

It is interesting to note that the formula proposed by Server, et al, [35], to empirically calculate the half-period of inertial oscillation ( $\tau$ , given in Eq. 3), is analogous to the half-period computed from the two d.o.f. model ( $\pi/\omega_2$ ). Their formula is given by:

$$\tau = 1.68 (E L W d C)^{1/3} / S \quad (3)$$

where  $E$  = Modulus of elasticity of the specimen,  $L$ ,  $W$ ,  $d$  are the length, width and depth of the specimen,  $C$  the compliance of the specimen and  $S$  is one dimensional longitudinal wave velocity in the specimen  $= \sqrt{E/\rho}$  ( $\rho$  = density of the specimen.)

Server, et al, have suggested that if the time to fracture  $t_f$  is larger than  $3\tau$ , the effects of oscillations beyond this time become negligible. However, unlike metallic specimens, concrete specimens are of lower strength and larger sizes. This results in situations where amplitudes of inertial oscillations may over-shadow true bending loads. To compound the problem, fracture times are also comparatively small for such composites. Consequently the need to know the amplitude of inertial oscillations is the primary motivation for seeking a more elaborate guideline than that proposed by Server, et al.

## Amplitude of Inertial Oscillations

Using the 2 d.o.f. model, the load measured by the tup  $P_t(t)$  and that measured by the anvil  $P_b(t)$  are given by:

$$\left. \begin{aligned} P_t(t) &= k_e v [(A_1 - A_2) \sin(\omega_1 t + \phi_1) \\ &\quad + (B_1 - B_2) \sin(\omega_2 t + \phi_2)] + m_t g \\ P_b(t) &= k_b v [A_2 \sin(\omega_1 t + \phi_1) + B_2 \sin(\omega_2 t + \phi_2)] + m_t g \end{aligned} \right\} \quad (4)$$

where  $v$  = impact velocity,  $\phi_1$  and  $\phi_2$  are constants characterizing the phase shifts corresponding to  $\omega_1$  and  $\omega_2$ ,  $A_1$ ,  $A_2$ ,  $B_1$ ,  $B_2$  are constants chosen to satisfy the initial conditions (all being functions of  $m_t$ ,  $m_b$ ,  $k_e$ , and  $k_b$ ), and  $g$  = acceleration due to gravity.

To analytically predict  $P_t$  and  $P_b$ , it is necessary to know  $v$ ,  $m_t$ ,  $m_b$ ,  $k_e$ , and  $k_b$ . Assuming that the beam vibrates in its first mode, expressions for  $m_b$  and  $k_b$  can be easily obtained. While  $v$  can be experimentally determined,  $m_t$  is normally provided by the manufacturer.  $k_e$ , the effective stiffness of the contact zone can be experimentally determined as described below. In the limiting case where beam deflections are restrained, i.e.,  $x_2(t) = 0$ , Eq. 1, becomes

$$m_t \ddot{x}_1 + k_e x_1 = 0 \quad (5)$$

Using the initial conditions  $x_1(0) = 0$ ,  $\dot{x}_1(0) = v$ , and neglecting the static deflection and weight due to  $m_t$ , peak load recorded by the striker is

$$P_{tmax} = v \sqrt{k_e m_t} \quad (6)$$

Thus,  $k_e$  can be evaluated for both the cases, with and without the rubber pad between the striker and the specimen, once the corresponding peak loads are recorded. This procedure is equivalent to the compliance calibration of the test set-up. Since this model accounts for the stiffness of the test set-up (contact zone) through  $k_e$ , predicted trends of peak load and energy absorbed are in line with observations made by Bluhm [16], Abe, et al, [15], and others. That is, increased values of  $k_e$ , which is a measure of machine stiffness, would yield larger values of recorded peak-loads and energy absorbed.

The ratio of the amplitude of oscillations of the load about the mean can be approximated for the tup and anvil loads as:

$$\left. \begin{aligned} R_t(t) &= \left[ \frac{(B_1 - B_2)}{(A_1 - A_2) \sin(\omega_1 t + \phi_1)} \right] = \frac{m_b}{m_t} \left( \frac{1}{\xi(1 + \xi)^2} \right)^{1/2} \frac{1}{\sin(\omega_1 t + \phi_1)} \\ R_b(t) &= \left[ \frac{B_2}{A_2 \sin(\omega_1 t + \phi_1)} \right] = \frac{m_b}{m_t} \left( \frac{\xi}{(1 + \xi)^2} \right)^{1/2} \frac{1}{\sin(\omega_1 t + \phi_1)} \end{aligned} \right\} \quad (7)$$

where  $\xi = k_b/k_e$ ,  $R_t$  and  $R_b$  are the ratios of the amplitude of oscillations of the load about the mean tup and anvil loads. If fracture times can be estimated a priori, then the error in using tup and anvil loads can be predicted by  $R_t(t_f)$  and  $R_b(t_f)$ , quite precisely. Otherwise, lower-bounds assuming  $\sin(\omega_1 t + \phi_1) = 1$ , can be evaluated to give some rough idea of errors due to oscillations for a particular set of  $m_b$ ,  $m_t$ ,  $k_e$ , and  $k_b$ .

It can be observed from Eq. 7 that for small values of  $\xi$ ,  $R_t$  can be very large. For example, from the results reported by Hibbert [29], where loads were measured only using the tup, a value of around 0.5 was estimated. This can explain the erroneously large values of peak loads recorded by him in the earlier cited impact tests. Characteristic values of  $\xi$  used in the present study with and without the damping pad are 38.5 and 5.8 respectively.

It can be shown that the difference between the tup and anvil loads is given by

$$\Delta P = \{k_e B_1 - (k_e + k_b) B_2\} (\sin(\omega_1 t + \phi_1)) \quad (8)$$

If it is assumed that  $\xi \gg 1$  and  $m_b/m_t \ll 1$  then the maximum value of this difference becomes

$$(\Delta P)_{\max} = |P_t(t) - P_b(t)|_{\max} = v \sqrt{k_e m_b / (1 + \xi)} \quad (9)$$

Both Eqs. 7 and 9 suggest that if  $\xi$  is large and  $m_b/m_t$  is small, the errors in load measurements due to oscillations of the load-time traces can be minimized. A comparison of model predicted load-time traces with experimentally observed results with and without the damping pad showed that predicted trends were accurate [9]. The following sections include details of a systematic experimental program carried out to study the behavior of FRC when subjected to different rates of flexural loading.

## EXPERIMENTAL DETAILS

The scope of the test program is presented in Table 1. Flexural beam specimens (3 in. deep, 1 in. wide and 9 in. long, 76 x 25 x 229mm) were tested so as to obtain 5 different strain rates ( $1 \times 10^{-6}$ /s to about 0.3/s). Four different mix-proportions (unreinforced and reinforced with 3 different amounts of fibers) were used. For each rate of strain and each mix-proportion, 4 flexural specimens were tested. For each mix-proportion, compression tests were conducted at the slowest loading rate using 3" x 6" (76 x 152mm) cylinders.

The composition of matrix and some characteristics of smooth brass coated steel fibers (length = 1 in. diameter = 0.016 in.; 25.4 and 0.41mm) are presented in Table 2. Three different volume fraction of fibers; 0.5, 1.0 and 1.5% were used.

A vertical mixer with a 1 cu. ft. ( $0.03m^3$ ) capacity was used to mix the constituent materials. For the FRC mixes, cement and sand were first dry mixed and then water and fibers were alternately added in several increments and mixing continued until uniform dispersion and desired amounts of reinforcement were obtained.

Cylinders were cast in cardboard molds while beams were fabricated in plexiglas molds. Beams were cast in two 1½ in. (37.5mm) layers with approximately 15 seconds of vibration after each placement. The casting procedure and the dimensions of the beams were such that distribution of fibers was two-dimensionally random (rather than three-dimensionally random). A reasonably uniform dispersion of fiber was evidenced from the rather small scatter in observed behavior within an identical series of specimens.

FRC beam specimens had a 0.5 in. (12.5mm) deep saw cut notch at mid-span. The notch was provided to avoid any appreciable reduction in pendulum velocity (and thus in strain-rate) during impact. Since the energy consumed during fracture was substantially lower for plain mortar beams, no notch was necessary and none was provided. A comparison of the notched and unnotched mortar specimens at the slowest loading rate showed negligible difference in overall response of the beam. Notch when provided was introduced by a circular diamond saw just prior to testing (after the specimens were cured). Microscopic observation (50X) showed no damage ahead of the notch due to the cutting process.

Specimens were demolded after 24 hours and were then stored in a curing room (80°F, 27°C, 98% R.H.) for around 26 days. Subsequently they were stored in laboratory (70°F, 21°C, 50% R.H.) environment for 2 days before testing to facilitate sawing of notches and gluing of strain gages.

## TEST PROCEDURE

### Compression Test

Compression tests were performed in a 120 Kip (534 kN) closed-loop universal testing machine at a strain rate of approximately  $1 \times 10^{-6}$ /s. Average axial displacement was recorded using 2 LVDTs (gage length of 5 in., 127mm). This signal was also used for the feedback control.

### Flexural Test - Static Rates

Three-point-bend tests at the slowest two strain rates:  $\dot{\epsilon}_1 = 1 \times 10^{-6}$ /s and  $\dot{\epsilon}_2 = 1 \times 10^{-4}$ /s were conducted in a closed-loop universal testing machine of a capacity of 40 Kips (178 kN). The central deflection of the beam was used as the feed-back signal. The deflection was measured by a specially designed device consisting of a strain-gage extensometer mounted between a fixed arm and a spring loaded arm of the device. The device was mounted between the tension face of the beam and a fixed cross-bar that held the beam supports. For unnotched mortar specimens, strain gages were glued on the extreme tension face at the quarter-points (points half-way between the supports and the load). The rate of deflection for the test was selected so as to obtain the desired strain-rates at the mid-point (twice the recorded strain rate at the quarter point). The notched beam specimens were tested at these identical deflection rates. Deflections for the notched beams were monitored at the point as close to the center of the beam as possible. Strains were recorded using resistance type foil gages (gage length 0.4 in.; 10mm) mounted at a point 0.5 in. (13mm) ahead of the notch.

### Flexural Test - Dynamic Rates:

Three-point bend-tests for the highest three strain-rates :  $\dot{\epsilon}_3 = 0.09$ ,

$\dot{\epsilon}_4 = 0.17$  and  $\dot{\epsilon}_5 = 0.3/s$  were conducted in the instrumented Charpy impact machine (Fig. 3, 4). Tests were conducted at three different impact velocities; 130, 185 and 245 cm/s. The strain-rates at the load-point (center) at these three velocities was computed as twice those measured at the quarter point of unreinforced, unnotched specimens. The deflection at the center (or close to it for notched FRC specimen) was measured using a Schaevitz LVDT (050 MHR). A-C excitation and output amplification was provided by a Schaevitz high-frequency (20 kHz) signal conditioner (CAS-200).

Load outputs from the two supports and the striker, beam deflection and specimen strain were monitored using a 4-channel digital oscilloscope (Nicolet 4094) (Fig. 2), described earlier.

## TEST RESULTS

### Observations from Flexural Impact Test Results

Typical results obtained from an impact test on a mortar and a FRC specimen are shown in Fig. 5. The values of the load recorded from the instrumented tup, the sum of the two anvil loads, load-point deflection and the measured strain values are plotted with respect to time. The results are for specimens impacted at a velocity of 2.45 m/s. The peak load is reached within about one millisecond. The loads measured by tup and anvil were comparable. The difference at small times apparent in the figure is because of the presence of the rubber pad. Inertial oscillations were present, as expected, but as designed for, their amplitudes around mean values were not significant.

The strain-time plot for the notched specimens was initially linear after which strain increased very rapidly. This occurred just before the peak load. This rapid increase in strain is probably due to crack propagation within the gage length. Note that the linear part of the strain vs. time plot of the unnotched specimens was used for calculations of strain rate (Fig. 5a) and for calculation of modulus of elasticity. For unnotched specimens since the strain was measured away from the critical section, the strain reduces beyond the peak load because of the elastic unloading of the noncritical sections on cracking. For both sets of specimens, deflections continue to increase, at a higher rate, beyond the peak load.

### Observations from the Static Compression Tests

Typical results from compression tests performed at low rates (1  $\mu$ str/s) of loading are presented in Fig. 6 for the various mixes tested. The softening behavior of plain mortar could be well documented as a result of the type of servo-controlled testing.

The following observations can be made from the static compression tests.

(i) Inclusion of fibers in the matrix enhances the compressive strength and the corresponding strains. Plain matrix had a compressive strength of 4414 psi (30.44 MPa) while 1.5% FRC had a strength of 5942 psi (40.98 MPa). For the same aspect-ratio of fibers used (62.5), strength increases were observed to be linearly related to fiber content. Peak

strain of 3750  $\mu$ str. was recorded for the 1.5% FRC specimens compared to 2700  $\mu$ str. for the unreinforced matrix.

(ii) The initial tangent modulus in compression measured experimentally obeys the law of mixture predictions quite well. This value for plain mortar and 1.5% FRC are  $3.97 \times 10^6$  psi (27.38 GPa) and  $4.35 \times 10^6$  psi (30 GPa) respectively.

(iii) The inclusion of fibers has an effect comparable to confining unreinforced concrete. Larger confining pressures yield higher strengths and greater ductility, analogous to larger volume contents. Although the presence of fibers influences the load-deformation behavior in the ascending portion, its major contribution is realized only beyond peak loads. The inset in Fig. 6 shows a normalized plot of stresses and strains (with respect to corresponding value at peak load) which highlight the increased toughness with increased fiber content.

## EFFECTS OF STRAIN RATE

### Unreinforced Mortar

Load-deflection curves for unreinforced mortar specimens subjected to 5 different strain rates are shown in Fig. 7. Increasing the strain rate increases the modulus of rupture, and the deflection at peak load as evidenced in Fig. 7. The average values of modulus of rupture and the energy absorbed to fracture are shown in Table 3. The energy to fracture of unreinforced mortar increases somewhat with increasing strain rate. It should be pointed out that energy to fracture was calculated from the observed load-deflection curves. Since the dynamic loading rates were obtained through a free fall test whereas the static-loading rates were obtained through a displacement controlled test, the energy to fracture may have been underestimated for dynamic loading rates.

It can be seen from Fig. 7 that the initial modulus of elasticity is not influenced by the rate of straining and that the load-deflection curves up to the peak become more linear at higher strain rates. This is further demonstrated in Fig. 8 where the secant modulus at various strain rates (normalized by the corresponding value at the slowest strain rate) calculated at the peak load and at 40% of the peak load are plotted. This plot shows that the load-deflection curves become progressively more linear with increasing strain rate, perhaps indicating that the extent of slow or subcritical crack growth (or nonlinear process zone [38-39]) decreases with increasing strain rate.

### Fiber Reinforced Mortar

The relative values of peak loads (average of 4 specimens, each) at various strain rates (normalized by the corresponding values at the slowest rate) are shown in Fig. 9 for specimens of unreinforced mortar as well as those reinforced with different amounts of fibers. The average values of modulus of rupture and the fracture energy are given in Table 3. From Fig. 9, it can be seen that the effect of strain rate is higher for FRC specimens, the more so the higher the volume fraction of fibers. For example, the modulus of rupture for FRC specimens made with 1.5% fibers at highest strain rate was 2237 psi (15.43 MPa) compared to 1056 psi (7.28

MPa) at the slowest strain rate. For mortar specimens, the values at the highest and slowest rates were 1240 and 747 psi (8.55 and 5.15 Mpa respectively). The higher strain rate sensitivity of FRC specimens is probably due to additional cracking (both transverse matrix cracking and interfacial cracking or debonding) generally associated with fiber reinforced concrete specimens and the observation that the strain rate sensitivity in cement based composites is related to crack growth [5-10].

The strain rate sensitivity of FRC also increases with increasing aspect ratio as shown in Fig. 10 where the results from [7] are plotted. The data are for specimens reinforced with 2% of steel fibers (the same type as used here) and made with fibers of 3 different aspect ratios. For this figure the nondimensionalized strength values are plotted versus strain rate.

Note that the effect of strain rate sensitivity of FRC specimens on fracture energy shows a trend similar to that just discussed for flexural strength (MOR), Table 3. For fiber reinforced specimens fracture energy refers to the energy under load-deflection curve calculated up to a deflection of 0.1 in. (2.5mm). This deflection value is about 10 times the deflection at peak load as observed from Fig. 11 where the results for a set of FRC specimens tested at the different strain rates are presented. The load deflection curve for plain mortar is also shown in Fig. 11 for comparison.

## COMPARISON WITH OTHER RESULTS

### Instrumented Impact Tests

A summary of results obtained from three other investigations [6,31,40] and the present one is shown in Table 4. In this table static properties refer to a strain rate of about  $1 \times 10^{-6}$ /s whereas dynamic properties refer to a rate of about .1 to 1/s, both obtained using a 3 point bending configuration. Wherever possible, mix properties, dimensions of the specimens, modulus of rupture (MOR) computed from peak load using elastic analysis, and the energy absorbed ( $G_f$ ) by unreinforced specimen up to fracture and by steel fiber reinforced specimens (SFRC) up to a fixed value of deflection are reported in the table. From these results it can be seen that: (a) ratio of dynamic to static MOR for unreinforced specimens range from 1.43 to 1.90 and for SFRC specimens from 1.79 - 2.63; (b) ratio of dynamic to static  $G_f$  for unreinforced and reinforced specimens range from 1.35 - 1.56 and 1.52 and 1.86 respectively; (c) the static values of  $G_f$  for unreinforced specimens are between 0.32 and 0.59 lb./in. (56 - 103 N/m) while those for the reinforced specimens are between 7.97 to 15.83 lb./in. (1396 - 2773 N/m); (d) the lower the static MOR, the higher is the influence of strain rate. These observations are similar to those reported in this investigation even though the sizes of specimens, the type of instrumented impact system and the methods of measurements were not identical. This suggests that reliable and reproducible information on material characteristics can be obtained by the type of instrumented impact testing scheme described here.

### Conventional Charpy Tests

Some results from standard Charpy tests for mortar specimens and SFRC

specimens are presented in Table 5. One important observation from these results is that considerably higher values of fracture energy for mortar are reported from standard Charpy test. For example, Krenchel [12], reports a value of 16.53 lb./in. (2900 N/m) from Charpy tests on plain mortar specimens. This value is much larger than those observed from the instrumented impact tests ( $\approx 150$  N/m). In fact, from static flexural test on the same type of mortar, Krenchel reports a value of 44 N/m (up to peak) which is comparable to static values reported in Table 4.

In the Charpy test, the energy value measured includes not only the energy to fracture the specimen, but also the energy absorbed by the testing system and the kinetic energy imparted to the specimen. Abe, et al [15] have shown that for rate insensitive silicon carbide specimens the energy calculated from the Charpy test is much higher than the true fracture energy and that the higher the true fracture energy of the specimen, the smaller is the discrepancy obtained from the Charpy test. This is also seen from Table 5. The results for SFRC specimens reported by Krenchel (20 to 30 kN/m), are comparable to those observed by Suaris and Shah (16.56 kN/m, for deflection up to 0.5 in.) using drop-weight type of instrumented impact testing system [6]. This would mean that the energy measured from the Charpy test will overestimate the true fracture energy, the more so the lower the true fracture energy of the material (for example, for SFRC composites made with low volume fraction and low aspect ratio of fibers).

Johnston [13] reports of about a 3-fold increase in fracture energy measured by the Charpy test when using about 2% steel fibers with an aspect ratio of 100. In light of the results of the present investigation, this unusually low recorded improvement is likely to be due to the parasitic effects of the Charpy testing method - which would overestimate the energy absorption values for the unreinforced matrix.

#### Comparison of Relative Performance of SFRC

The relative improvements in impact resistance, and in static fracture energy measured by several methods are shown in Table 6. A drop-weight test using 6 in. (152mm) diameter, 2½ in. (64mm) high cylinder has been proposed by Schrader [41]. Number of blows required to produce first crack and to induce a fixed amount of diametrical expansion are used as criteria for quantifying impact resistance. Area under the load-deflection curve up to a fixed value of deflection for FRC specimens obtained by testing beams under static loading rates has been suggested as a measure of fracture toughness by Johnston [42] and Henager [43]. This area for FRC specimens when compared to the area up to the peak load of unreinforced matrix (which is sometimes taken as equal to that up to the first cracking load for FRC specimens) is termed toughness index and is taken as an indication of the relative performance of fiber reinforced concrete specimens. The relative performance obtained using a drop-weight method, the standard Charpy test, the static toughness index, and as observed from the instrumented impact tests - for somewhat comparable amounts of reinforcement, aspect ratios and the type of steel fibers are reported in Table 6.

It can be observed that the values of the toughness index are close to the relative performance as measured accurately by the instrumented impact test. This is not surprising since both methods use the area under the

load-deflection curve as a criteria for evaluating the performance of FRC. The other methods generally underestimate the relative performance of fiber reinforced concrete.

Theoretically the area under the complete load-deflection curve should correspond to the energy required to fracture the critical cross-section (under the load-point in a 3-point bend test). However, there are some experimental difficulties in accurately obtaining this value as detailed below.

1. The post-peak load-deflection response is sensitive to the relative stiffness of the testing machine. Testing in a closed-loop mode as performed in this investigation can reduce the parasitic testing-system interaction.
2. If cracks and no linear deformations occur in the regions other than the critical section, then the area under the load-deflection curve will overestimate the true fracture energy of the material, (Jenq and Shah, [44]).
3. Unless the deflections are recorded in such a manner that the local deformations occurring under the load-point and supports are eliminated, the measured energy (area under the load-deflection curve) may overestimate the true fracture energy. This is especially critical for unreinforced specimens or for reinforced specimens up to the first-cracking load. Kobayashi, et al, [45] have shown that due to the load-point deformations, the area of the load-deflection curve up to first-cracking load for FRC composites was as much as 200% larger than its true value.

A similar observation was also made in the present study. The mid-point deflection was measured as a relative displacement between a fixed support and the center of the beam. The average modulus of elasticity calculated from the linear part of the load-deflection curve (after making corrections due to shear deformations) for mortar specimens tested at the slowest rate was  $2.48 \times 10^6$  psi (17.1 GPa). For the same set of specimens, the modulus calculated from the strain measurements (quarter-point, (see Fig. 5) was  $3.97 \times 10^6$  psi (27.4 GPa). This value was identical to that observed from uniaxial compression and uniaxial tension tests, (Gopalaratnam [9]).

These points should be considered when using the area under the load-deflection curve to evaluate the relative performance of FRC.

## CONCLUSIONS

1. The modified instrumented Charpy test described here is useful in studying the dynamic behavior of brittle cement based composites. With the experience gained in this study, it is possible to design a test-system-independent impact test for low-strength brittle materials.

2. Adverse effects due to inertial loads observed in impact testing of tension weak cement composites can be significantly reduced by (a) reducing the impact velocity, (b) increasing the ratio of the tup (hammer) mass to the beam mass, and (c) increasing the ratio of the beam stiffness

to the effective stiffness of the tup-beam contact zone.

3. Mortar, concrete and FRC all exhibit increased flexural strengths at the higher rates of loading. An increase of 65% for mortar and 50% for concrete was observed in this study, when the rate of straining was increased from  $1 \times 10^{-6}$ /s to 0.3/s. The weaker mortar mix exhibits greater rate sensitivity than concrete as observed in the earlier studies. FRC is more rate sensitive than plain matrix, showing improvement in flexural strengths of 79, 99 and 111% over respective static flexural strengths for the 0.5%, 1.0%, 1.5% (fiber volume content) composites (aspect ratio of 62.5) at identical loading rates. In addition to improved strengths at the higher rates of loading, the deflection at ultimate load at these rates were consistently higher than the corresponding values at static loading rates. Up to a 50% increase in these deflection values were recorded for the various plain and reinforced composites tested.

4. Energy absorption during the dynamic fracture of the unreinforced composites increased by 40% over comparative static values. Energy absorption of FRC (generally a couple of orders of magnitude larger than that of the unreinforced composites) up to fixed deflection value (of 0.1 in., 3mm) at the dynamic rate of loading increased by 70-80% over the corresponding static value. For the same aspect ratio of fibers used, composites made with higher fiber content showed larger rate sensitivity, perhaps due to the characteristics of cracking in these composites, and the rate sensitivity associated with such a process.

5. Changes in the cracking process at the static and dynamic rates are perhaps primarily responsible for the rate sensitive behavior of cement composites. Several observations reinforce this hypothesis:

(a) Prepeak non-linearities (and micro-cracking which account for these non-linearities) reduce at the dynamic loading rates. While the initial tangent modulus of cement composites shows no significant change at the different rates of loading, the secant modulus (evaluated at ultimate load) becomes stiffer at the higher rates of loading.

(b) Cement composites exhibit a non-isotropic rate sensitivity with specimens subjected to tension, flexure and compression showing descending order of rate sensitivity at comparable rates of loading.

(c) Weaker matrix mixes are more rate sensitive than stronger ones.

(d) FRC is more rate-sensitive than the unreinforced matrix, with fibrous composites made with higher fiber contents or fibers of higher aspect ratio exhibiting a greater rate-sensitivity.

6. Static flexural toughness tests on FRC provide a conservative estimate of the impact strength and toughness of such composites. Until a standard impact test for FRC comes into effect, results from the static flexural toughness test can be used to interpret the dynamic behavior of the composite.

#### ACKNOWLEDGEMENT

The research reported here is being supported by a grant (DAAG-29-82-K-0171) from the U.S. Army Research Office to Northwestern University. The authors gratefully acknowledge Mr. John Schmidt for his

assistance in the development of instrumentation for the project. The authors are also indebted to Denise Cable for her flawless typing of the manuscript.

#### REFERENCES

1. Shah, S.P., and Rangan, B.V., "Fiber Reinforced Concrete Properties," ACI Journal, Vol. 68, No. 2, Feb. 1971, pp. 126-135.
2. Hannant, D.J., "Fibre Cements and Fibre Concretes," John Wiley and Sons, Ltd., 1978.
3. Swamy, R.N., Mangat, P.S., and Rao, C.V.S.K., "The Mechanics of Fiber Reinforcement of Cement Matrices," Publication SP44, ACI, Detroit, 1974, pp. 1-28.
4. Suaris, W., and Shah, S.P., "Inertial Effects in the Instrumented Impact Testing of Cementitious Composites," ASTM Journal of Cement, Concrete and Aggregates, Vol. 3, No. 2, Winter 1981, pp. 77-83.
5. Suaris, W., and Shah, S.P., "Strain-Rate Effects in Fibre Reinforced Concrete Subjected to Impact and Impulsive Loading," Composites, Vol. 13, No. 2, April 1982, pp. 153-159.
6. Suaris, W., and Shah, S.P., "Properties of Concrete Subjected to Impact," Journal of Structural Engineering, (ASCE), Vol. 109, No. 7, July 1982, pp. 1727-1741.
7. Naaman, A.E., and Gopalaratnam, V.S., "Impact Properties of Steel Fiber Reinforced Concrete in Bending," International Journal of Cement Composites and Lightweight Aggregates, Vol. 5, No. 4, Nov. 1983, pp. 225-233.
8. Gopalaratnam, V.S., Shah, S.P., and John, R., "A Modified Instrumented Charpy Test for Cement Based Composites," Experimental Mechanics, June 1984, pp. 102-111.
9. Gopalaratnam, V.S., "Fracture and Impact Resistance of Steel Fiber Reinforced Concrete," Ph.D. Thesis, Northwestern University, 1985.
10. Gopalaratnam, V.S., and Shah, S.P., "Properties of Steel Fiber Reinforced Concrete Subjected to Impact Loading," Submitted for Publication.
11. Battelle Development Corp., "Two-Phase Concrete and Steel Material," USA Patent No. 3429094, Feb. 1969.
12. Krenchel, H., "Fiber Reinforced Brittle Matrix Materials," Publication SP44, American Concrete Institute, Detroit, 1974, pp. 45-77.
13. Johnston, C.D., "Steel Fiber Reinforced Mortar and Concrete - A Review of Mechanical Properties," Publication SP44, American Concrete Institute, Detroit, 1974, pp. 127-142.

14. Radomski, W., "Application of the Rotating Impact Machine for Testing Fiber Reinforced Concrete," *International Journal of Cement Composites and Lightweight Concrete*, Vol. 3, No. 1, Feb. 1981, pp.3-12.
15. Abe, H., Chandan, H.C., and Brandt, R.C., "Low Blow Charpy Impact of Silicon Carbides," *Bulletin of the American Ceramic Society*, Vol. 57, No. 6, 1978, pp. 587-595.
16. Bluhm, J.E., "The Influence of Pendulum Flexibilities on Impact Energy Measurements," *ASTM STP 167, American Society for Testing and Materials*, 1955, pp. 84-92.
17. Nanda, V.K., and Hannant, D.J., "Fibre Reinforced Concrete," *Concrete Bldg. and Concrete Prods.*, XLIV, No. 10, October 1969, pp. 179-181.
18. Dixon, J., and Mayfield, B., "Concrete Reinforced with Fibrous Wire," *Concrete*, March 1971, pp. 73-76.
19. Jamrozy, Z., and Swamy, R.N., "Use of Steel Fibre Reinforcement for Impact Resistance and Machinery Foundations," *International Journal of Cement Composites*, Vol. 1, No. 2, July 1979, pp. 65-76.
20. Bailey, J.H., Bentley, S., Mayfield, B., and Pell, P.S., "Impact Testing of Fiber Reinforced Concrete Stair Treads," *Magazine of Concrete Research*, Vol. 27, No. 92, September 1975, pp. 167-170.
21. ACI Committee 544, "Measurement of Properties of Fiber Reinforced Concrete," *ACI Journal*, Vol. 75, No. 7, July 1978, pp. 283-289.
22. Ramakrishnan, V., Brandshaug, I., Coyle, W.V. and Schrader, E.K., "A Comparative Evaluation of Concrete Reinforced with Straight Steel Fibers with Deformed Ends Glued Together in Bundles," *ACI Journal*, Vol. 77, No. 3, May-June 1980, pp. 135-143.
23. Butler, J.E., and Keating, J., "Preliminary Data Derived Using a Flexural Cyclic Loading Machine to Test Plain and Fibrous Concrete," *Materials and Structures*, June 1980, Vol. 14, No. 79, pp. 23-33.
24. Kobayashi, K., and Cho, R., "Flexural Behaviour of Polyethylene Fibre Reinforced Concrete," *International Journal of Cement Composites and Lightweight Concrete*, Vol. 3, No. 1, Feb. 1981, pp. 19-25.
25. Birkimer, D.L., and Lindemann, R., "Dynamic Tensile Strength of Concrete Materials," *ACI Journal*, Jan. 1971, pp. 47-49.
26. Bhargava, J., and Rehnstrom, A., "Dynamic Strength of Polymer Modified and Fibre-Reinforced Concretes," *Cement and Concrete Research*, Vol. 7, 1977, pp. 199-207.
27. Williamson, G.R., "Response of Fibrous Reinforced Concrete to Explosive Loading," *Technical Report 2-48, U.S. Army Corps of Engineers, Ohio River Division Laboratories*, Jan. 1966.
28. Robins, P.J., and Calderwood, R.W., "Explosive Testing of Fibre Reinforced Concrete," *Concrete*, Jan. 1978, pp. 76-78.

29. Hibbert, A.P., "Impact Resistance of Fibre Concrete," Ph.D. Thesis, University of Surrey, 1977.
30. Radomski, W., "Application of the Rotating Impact Machine for Testing Fiber Reinforced Concrete," International Journal of Cement Composites and Lightweight Concrete, Vol. 3, No. 1, Feb. 1981, pp. 3-12.
31. Koyanagi, W., Rokugo, K., Uchide, Y., and Iwase, H., "Energy Approach to Deformation and Fracture of Concrete under Impact Load," Transaction of the Japan Concrete Institute, Vol. 5, 1983, pp. 161-168.
32. Electric Power Research Institute, "Instrumented Precracked Charpy Testing," Proceedings of the C.S.N.I. Specialist Meeting, Edited by R.A. Wullaert, California, Nov. 1981.
33. Cotterell, B., "Fracture Toughness and the Charpy V-Notch Test," British Welding Journal, Vol. 9, No. 2, Feb. 1962, pp. 83-90.
34. Venzi, S., Priest, A.H., and May, M.J., "Influence of Inertial Load in Instrumented Impact Tests," Impact Testing of Metals, ASTM STP 466, American Society for Testing and Materials, 1970, pp. 165-180.
35. Server, W.L., Wullaert, R.A., and Sheckhard, J.W., "Evaluation of Current Procedures for Dynamic Fracture Toughness Testing," Flaw Growth and Fracture, ASTM STP 631, 1977, pp. 446-461.
36. Kalthoff, J.F., Winkler, S., Klemm, W., and Bienert, J., "On the Validity of  $K_{Id}$ -Measurements in Instrumented Impact Tests," Proceedings, 5th International Conference on Structural Mechanics in Reactor Technology, Berlin, 1969, G4/6, 1-11.
37. Winkler, S., Kalthoff, J.F., and Gerscha, A., "The Response of Pressure Vessel Steel Specimens on Drop Weight Loading," Proceedings 5th International Conference on Structural Mechanics in Reactor Technology, Berlin, 1979, pp. G4/6, 1-9.
38. Wecharatana, M., and Shah, S.P., "A Model for Predicting Fracture Resistance of Cement Composites," Cement and Concrete Research, Vol. 13, 1983, 819-829.
39. Ballarini, R., Shah, S.P., and Keer, L.M., "Crack Growth in Cement Based Composites," Engineering Fracture Mechanics, Accepted for Publication.
40. Zech, B., and Wittmann, F.H., "Variability and Mean Value of Strength as a Function of Load," ACI Journal, Vol. 77, No. 5, Sept.-Oct. 1980, pp. 358-362.
41. Schrader, E.K., "Impact Resistance and Test Procedure for Concrete," ACI Journal, Vol. 78, No. 2, March-April 1981, pp. 141-146.
42. Johnston, C.D., "Definition and Measurement of Flexural Toughness Parameters for Fiber Reinforced Concrete," Cement, Concrete and Aggregates CCAGDP, Vol. 4, No. 2, Winter 1982, pp. 53-60.

43. Henager, C.H., "A Toughness Index for Fibre Concrete," Testing and Test Methods of Fibre Cement Composites," RILEM Symposium 1978, pp. 79-86.
44. Jenq, Y.S., and Shah, S.P., "A Fracture Toughness Criterion for Concrete," Engineering Fracture Mechanics, Accepted for Publication.
45. Kobayashi, K., and Umeyama, K., "Method of Testing Flexural Toughness of Steel Fiber Reinforced Concrete," Japanese Society of Civil Engineers, Proceedings, May 1980, pp. 251-254.

Table 1: Details of the Experimental Program

| Mix <sup>1</sup> | Fiber Content<br><br>$v_f$ (%) | Flexural Tests <sup>2</sup>                               |                  |                     |              |              |              |              | Compression Tests <sup>3</sup><br>Number of Specimens<br>$\epsilon_1$ |
|------------------|--------------------------------|---|------------------|---------------------|--------------|--------------|--------------|--------------|---|
|                  |                                | Net Cross Section<br>Depth x Width<br>in. x in. (mm x mm) | Span<br>in. (mm) | Number of Specimens |              |              |              |              |   |
|                  |                                |   |                  | $\epsilon_1$        | $\epsilon_2$ | $\epsilon_3$ | $\epsilon_4$ | $\epsilon_5$ |   |
| 1                | 0.0                            | 3 x 1, (76 x 25)  | 8, (203)         | 4                   | 4            | 4            | 4            | 4            | 4   |
|                  |                                | 5/2 x 1, (64 x 25)  | 8, (203)         | 4                   | -            | -            | -            | -            |   |
| 2                | 0.5                            | 5/2 x 1, (64 x 25)  | 8, (203)         | 4                   | 4            | 4            | 4            | 4            | 4   |
| 3                | 1.0                            | 5/2 x 1, (64 x 25)  | 8, (203)         | 4                   | 4            | 4            | 4            | 4            | 4   |
| 4                | 1.5                            | 5/2 x 1, (64 x 25)  | 8, (203)         | 4                   | 4            | 4            | 4            | 4            | 4   |

1 Matrix 1:2:0:0.5 (C:S:A:W, by weight), Fibers  $\ell = 1$  in. (25 mm),  $d = 0.016$  in. (0.4 mm).

2  $\epsilon_1 = 1 \times 10^{-6}$ /s,  $\epsilon_2 = 1 \times 10^{-4}$ /s,  $\epsilon_3 = 0.09$ /s,  $\epsilon_4 = 0.17$ /s,  $\epsilon_5 = 0.3$ /s.

Flexural tests at  $\epsilon_1$  and  $\epsilon_2$  were conducted using a closed loop machine under displacement control.

Flexural tests at  $\epsilon_3$ ,  $\epsilon_4$ , and  $\epsilon_5$  were conducted using the modified instrumented Charpy set-up.

3 Compression tests were conducted on 3 x 6 in. (76 x 152 mm) cylinders.

Table 2 : Some Physical and Mechanical Properties of the Constituent Materials.

|               |   |  |
|---------------|---|--|
| Mortar Matrix | <p><b>Composition*</b></p> <p>Cement, lb/ft<sup>3</sup> (kg/m<sup>3</sup>)</p> <p>Sand, lb/ft<sup>3</sup> (kg/m<sup>3</sup>)</p> <p>Water, lb/ft<sup>3</sup> (kg/m<sup>3</sup>)</p> <p><b>Mechanical Properties (Static Loading)</b></p> <p>Tensile Strength <math>\sigma_p</math>, psi (MPa)</p> <p>Compressive strength <math>f'_c</math>, psi (MPa)</p> <p>Modulus of elasticity <math>E_c</math>, x 10<sup>6</sup> psi (GPa)</p> <p>Modulus of rupture MOR, psi (MPa)</p> | <p>43.0 (690.3)</p> <p>86.0 (1380.6)</p> <p>21.5 (345.2)</p> <p>405 (2.8)</p> <p>4414 (30.4)</p> <p>3.97 (27.4)</p> <p>747 (5.2)</p> |
| Steel Fibers  | <p><b>Physical Characteristics</b></p> <p>Smooth brass coated steel fibers</p> <p>Length <math>l</math>, in. (mm)</p> <p>Diameter <math>d</math>, in. (mm)</p> <p>Volume fractions used in the mix, <math>v_f</math> (%)</p> <p><b>Mechanical Properties (Static Loading)</b></p> <p>Ultimate tensile strength <math>\sigma_u</math>, ksi (MPa)</p> <p>Modulus of elasticity <math>E_s</math>, x 10<sup>6</sup> psi (GPa)</p>   | <p>1.000 (25.4)</p> <p>0.016 (0.41)</p> <p>0.5, 1.0, 1.5</p> <p>90-120 (621-828)</p> <p>29.0 (200)</p>                               |

\* Type I Ordinary Portland Cement and River Sand Maximum Size 5 mm used

Table 3 : Average<sup>1</sup> Material Properties at Different Strain Rates

| Material | Fiber Content<br>$v_f(\%)$ | Property <sup>2</sup>                    | Strain Rate <sup>3</sup> (1/s)          |   |                            |                            |                            |
|----------|----------------------------|--|---|---|----------------------------|----------------------------|----------------------------|
|          |                            |  | $\dot{\epsilon}_1$                      | $\dot{\epsilon}_2$                      | $\dot{\epsilon}_3$         | $\dot{\epsilon}_4$         | $\dot{\epsilon}_5$         |
| Mortar   | 0.0                        | MOR, psi (MPa)<br>$G_f$ , lb/in (N/m)    | 747(5.15)<br>0.43(75)                   | 800(5.52)<br>0.42(73)                   | 1113(7.68)<br>0.52(92)     | 1153(7.95)<br>0.56(97)     | 1240(8.55)<br>0.58(101)    |
| FRC      | 0.5                        | MOR, psi (MPa)<br>$G_f^*$ , lb/in (kN/m) | 806(5.56)<br>8.01 <sup>4</sup> (1.40)   | 864(5.96)<br>8.09 <sup>4</sup> (1.42)   | 1334(9.20)<br>12.09(2.12)  | 1392(9.60)<br>12.89(2.26)  | 1450(10.00)<br>13.54(2.37) |
|          | 1.0                        | MOR, psi (MPa)<br>$G_f^*$ , lb/in(kN/m)  | 864(5.96)<br>9.77 <sup>4</sup> (1.71)   | 989(6.82)<br>10.06 <sup>4</sup> (1.76)  | 1603(11.06)<br>15.24(2.67) | 1670(11.52)<br>15.93(2.78) | 1718(11.85)<br>17.20(3.01) |
|          | 1.5                        | MOR, psi (MPa)<br>$G_f^*$ , lb/in (kN/m) | 1056(7.28)<br>14.32 <sup>4</sup> (2.50) | 1181(8.15)<br>15.18 <sup>4</sup> (2.66) | 2054(1416)<br>21.20(3.71)  | 2150(14.83)<br>21.83(3.82) | 2237(15.43)<br>24.50(4.29) |

1. Average of four specimens for each reported value of MOR and  $G_f$

2. Modulus of rupture (MOR) computed using elastic theory and net beam depth. Fracture energy ( $G_f$ ) computed as area under the load deflection curve (for fracture of plain mortar and up to a central deflection of 0.1 in. for FRC) for unit net cross-sectional area.  $G_f^*$  is represented as  $G_f^*$  for FRC because area is computed only up to a deflection of 0.1 in.

3.  $\dot{\epsilon}_1 = 1.0 \times 10^{-6}/s$   $\dot{\epsilon}_3 = 0.09/s$   $\dot{\epsilon}_5 = 0.3/s$

$\dot{\epsilon}_2 = 1.0 \times 10^{-4}/s$   $\dot{\epsilon}_4 = 0.17/s$

4. Stopped test at  $\delta = 0.075$  in.,  $G_f^*$  up to  $\delta = 0.1$  in. estimated by extrapolating P- $\delta$  curve between  $\delta = 0.075$  in. and  $\delta = 0.1$  in.

Table 4. Results from Instrumented Impact Tests on Mortar, Concrete and FRC

| Reference            | Set-up<br>(in. x in.)       | Specimen Size                          |              | Mix Proportions                      |                        | Static Properties |                  | Impact Properties |                          |                 |
|----------------------|-----------------------------|--|--------------|--------------------------------------|------------------------|-------------------|------------------|-------------------|--------------------------|-----------------|
|                      |                             | Net Cross-<br>Section<br>Depth x width | Span<br>(in) | Material                             | C:S:A:W<br>(By weight) | MOR<br>(psi)      | $G_f$<br>(lb/in) | Strain<br>Rate    | $MOR_d/MOR_s$            | $G_{fd}/G_{fs}$ |
| Zech and<br>Wittmann | Instrumented<br>Drop Weight | 0.79 x 0.79                            | 7.9          | Mortar                               | 1:4.7:0:0.57           | 1813              | -                | 1.00              | 1.50                     | -               |
|                      |                             |  |              | Mortar                               | 1:8.2:0:0.90           | 1030              | -                | 1.00              | 1.90                     | -               |
| Suaris<br>and Shah   | Instrumented<br>Drop Weight | 3 x 1.5                                | 15           | Mortar                               | 1:2:0:0:5              | 1060              | 0.43             | 0.27              | 1.67                     | 2.35            |
|                      |                             |  |              | Concrete                             | 1:2:3:0.5              | 1430              | 0.59             | 0.27              | 1.43                     | -               |
|                      |                             |  |              | SFRC*<br>$v_f = 1\%$<br>$z/d = 100$  | 1:2:0:0.5              | 1370              | 15.83            | 0.27              | 2.02                     | 1.86            |
| Koyanagi<br>et al.   | Instrumented<br>Drop Weight | 3 x 3                                  | 24           | Mortar                               |                        | 1030              | 0.59             | 0.20              | 1.10(1.74 <sup>+</sup> ) | 1.56            |
|                      |                             |  |              | SFRC*<br>not reported                |                        | 1262              | 7.97             | 0.20              | 2.63                     | 1.52            |
| Present              | Instrumented                | 3 x 1                                  | 8            | Mortar                               | 1:2:0:0.5              | 747               | 0.43             | 0.30              | 1.65                     | 1.35            |
|                      |                             |  |              | Concrete                             | 1:2:2:0.5              | 1400              | 0.32             | 0.30              | 1.50                     | 1.47            |
|                      |                             | 2.5 x 1                                | 8            | $v_f = 0.5\%$<br>$z/d = 63$          | 1:2:0:0.5              | 806               | 8.01             | 0.30              | 1.79                     | 1.69            |
|                      |                             |  |              | SFRC*<br>$v_f = 1.0\%$<br>$z/d = 63$ | 1:2:0:0.5              | 864               | 9.77             | 0.30              | 1.99                     | 1.76            |
|                      |                             |  |              | SFRC*<br>$v_f = 1.5\%$<br>$z/d$      | 1:2:0:0.5              | 1056              | 14.32            | 0.30              | 2.11                     | 1.71            |

1 in. = 2.54 cm. 1 psi = 0.0069 MPa. 1 lb/in = 175.2 N/m.

\*  $G_f$  for all FRC specimens is reported up to a 0.1 in. mid-point deflection.

+ When sufficient potential energy available in the impact.

Table 5 : Results\* from Conventional Charpy Tests on Mortar and FRC

| Reference           | Specimen Size           |           | Mix Proportions                       |                     | Impact Velocity (m/s) | Pendulum Energy | Impact Resistance (kJ/m <sup>2</sup> ) |
|---------------------|-------------------------|-----------|---------------------------------------|---------------------|-----------------------|-----------------|--|
|                     | Cross-Section (mm x mm) | Span (mm) | Material                              | C:S:A:W (By Weight) |                       |                 |  |
| Battele Devp. Corp. | 25 x 25                 | 102       | Mortar                                | -                   | -                     | -               | 2.2                                    |
|                     |                         |           | SFRC<br>$v_f=2\%$ , $d=0.15\text{mm}$ | -                   | -                     | -               | 21.7                                   |
| Krenchel            | 40 x 40                 | 140       | Mortar                                | 1:2:0:0.45          | 3.5-4.0               | 50              | 2.9                                    |
|                     |                         |           | SFRC<br>$v_f=2\%$ , $l/d=100$         | 1:2:0:0.45          | 3.5-4.0               | 50              | 20.0                                   |
|                     |                         |           | SFRC<br>$v_f=0.9\%$ , $l/d=170$       | 1:2:0:0.45          | 3.5-4.0               | 50              | 30.0                                   |
| Radomski            | 15 x 15                 | 50        | Mortar                                | 1:3:0:0.60          | 5.2                   | 300             | 23.2                                   |

1mm = 0.0394 in., 1m/s = 3.28 ft/s, 1 J = 0.737 ft-lbs, 1 kJ/m<sup>2</sup> = 5.7 lb/in.

\* Johnston, based on conventional Charpy impact tests on 22 x 22 x 100mm specimens reports of relative impact resistance by fiber inclusion of between 2 - 10 times that of the unreinforced matrix (1:2.4:0:0.5) depending upon the reinforcing parameters. Details of the reinforcing parameters or absolute fracture energy values from these tests are, however, not reported.

Table 6: Relative Increase in Energy Absorption Capacity Due to the Incorporation of Fibers Measured by Conventional Tests and Instrumented Impact Tests

| Ramakrishnan et al. <sup>1</sup>  | First Crack     |                   | Ultimate Failure |                   |
|-----------------------------------|-----------------|-------------------|------------------|-------------------|
|                                   | Number of Blows | Relative Increase | Number of Blows  | Relative Increase |
| Mortar<br>1:3.66:0.46             | 10              | 1.0               | 13               | 1.0               |
| SFRC<br>$V_f = 1\%$<br>$L/d = 70$ | 48              | 4.8               | 155              | 11.9              |

| Krenchel <sup>2</sup>              | Charpy Impact Resistance |                 |
|------------------------------------|--------------------------|-----------------|
|                                    | kJ/m <sup>2</sup>        | Relative Impact |
| Mortar<br>1:2:0:0.45               | 2.9                      | 1.0             |
| SFRC<br>$V_f = 2\%$<br>$L/d = 100$ | 20.0                     | 6.9             |

| Static Flexural Toughness   | Energy Absorbed | Toughness Index |
|---|-----------------|-----------------|
|   |                 |                 |
| Heneggar <sup>3</sup><br>SFRC<br>$V_f = 1.5\%$<br>$L/d = 61$          | -               | 30.4            |
| Ramakrishnan et al. <sup>4</sup><br>SFRC<br>$V_f = 1\%$<br>$L/d = 70$ | -               | 16.0            |

| Present Study <sup>5</sup>                      | Static Flexural Toughness |                   | Instrumented Impact Toughness |                   |
|---|---------------------------|-------------------|-------------------------------|-------------------|
|   | kJ/m <sup>2</sup>         | Relative Increase | kJ/m <sup>2</sup>             | Relative Increase |
| Mortar<br>1:2:0:0.5                             | 0.075                     | 1.0               | 0.102                         | 1.0               |
| SFRC <sup>6</sup><br>$V_f = 1\%$<br>$L/d = 63$  | 1.711                     | 22.8              | 3.013                         | 29.5              |
| Suaris and <sup>6</sup> Shah                    |                           |                   |                               |                   |
| Mortar<br>1:2:0:0.5                             | 0.075                     | 1.0               | 0.177                         | 1.0               |
| SFRC <sup>6</sup><br>$V_f = 1\%$<br>$L/d = 100$ | 2.773                     | 37.0              | 5.158                         | 29.1              |

<sup>a</sup>Toughness computed up to 0.1 in. deflection.

1. Ramakrishnan et al.

2. Krenchel, M.

3. Heneggar, C.

4. Ramakrishnan, et al.

5. Present Study

6. Suaris and Shah

ACI recommended drop weight test in a compressive configuration on 6" diameter, 1.5" height cylinders (152 x 38 mm). Conventional Charpy test on flexural specimens, cross-section 40 x 40 mm, span 140 mm, impact velocity 3.5 - 4 m/s, Pendulum energy 50J.

Third point loading cross-section 102 x 102 mm, span 305 mm, loading rate 0.5 - 1 mm/min, matrix composition 1:2.4:0.47,  $\sigma_{HOR} = 6.13$  MPa, ACI Toughness Index up to  $\delta = 1.9$  mm.

Third point loading cross-section 76 x 76 mm, Span 305 mm, Matrix Composition 1:3.66:0.46, ACI Toughness Index up to  $\delta = 2.5$  mm.

3 point flexural tests at static strain rate of  $1 \times 10^{-7}$  and impact strain rate of 0.3/s.

3 point flexural tests at static strain rate of  $0.67 \times 10^{-6}$  and impact strain rate of 0.27/s.

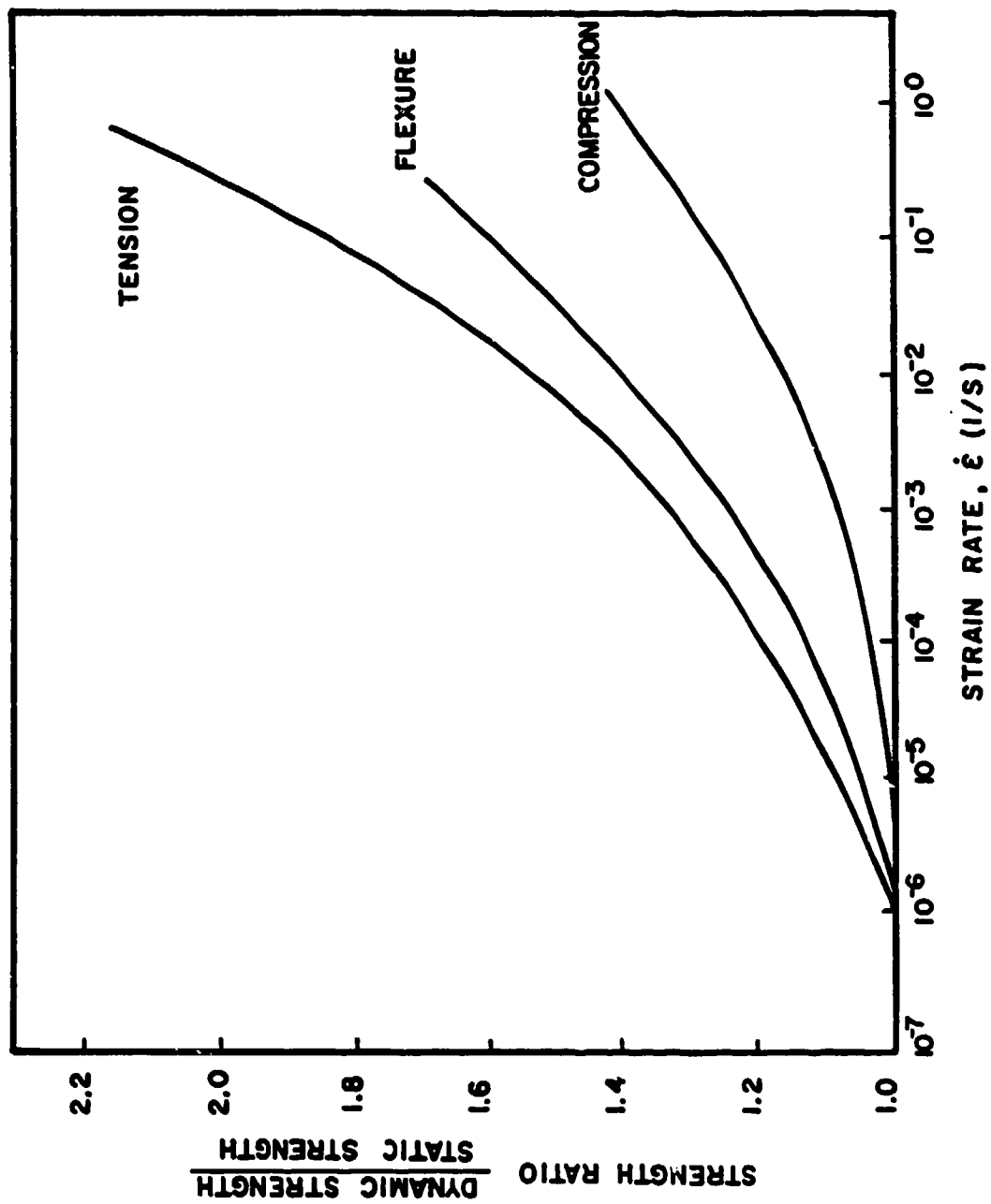


Fig. 1. Strain Rate Behavior of Plain Concrete in the Different Simple Response Modes. Ref. 5.



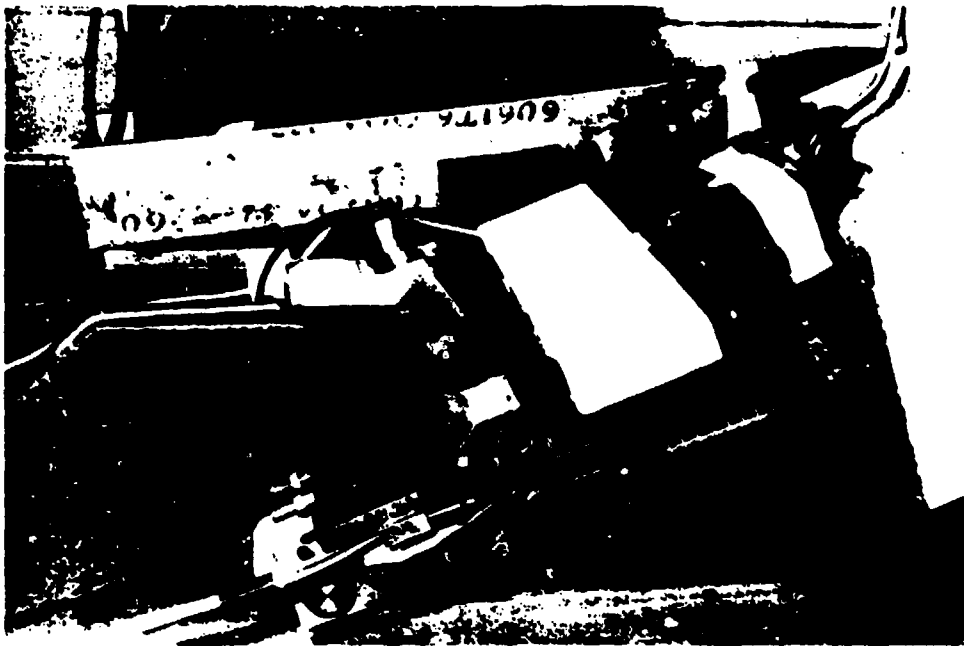


Fig. 3. Close up of the modified supports and the loading configuration, showing the instrumented anvils, striker, dynamic displacement measuring device, and the shock absorber mechanism.



Fig. 4. An overall view of the modified Charpy impact machine and associated instrumentation.

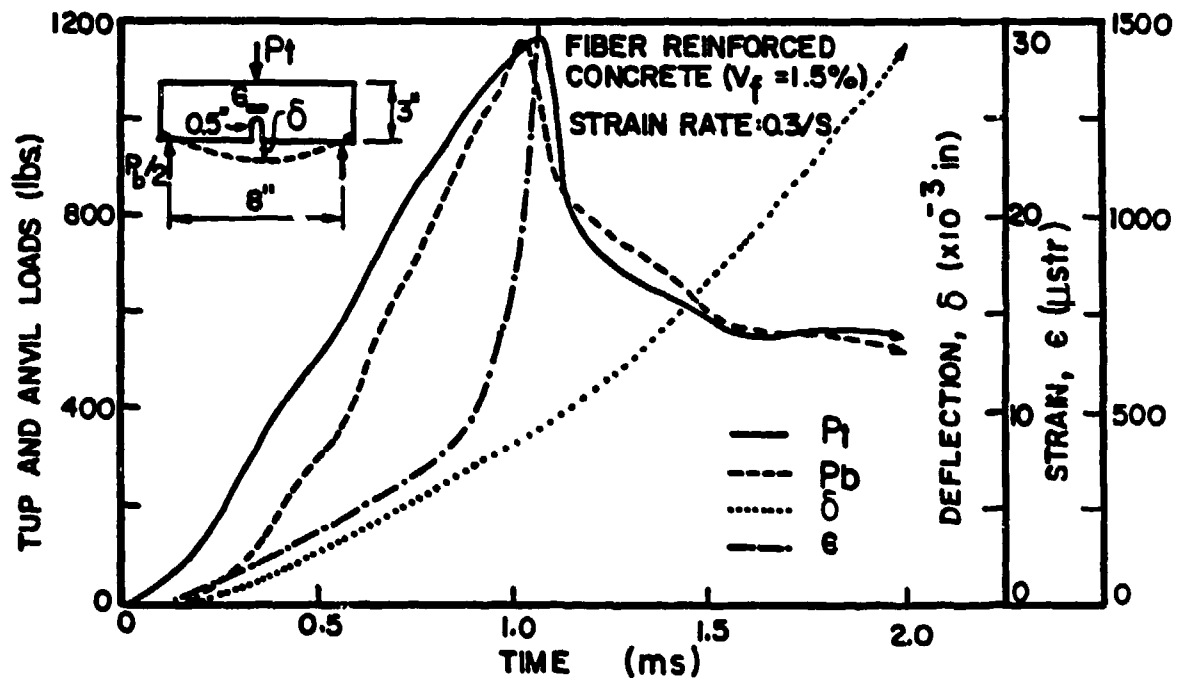
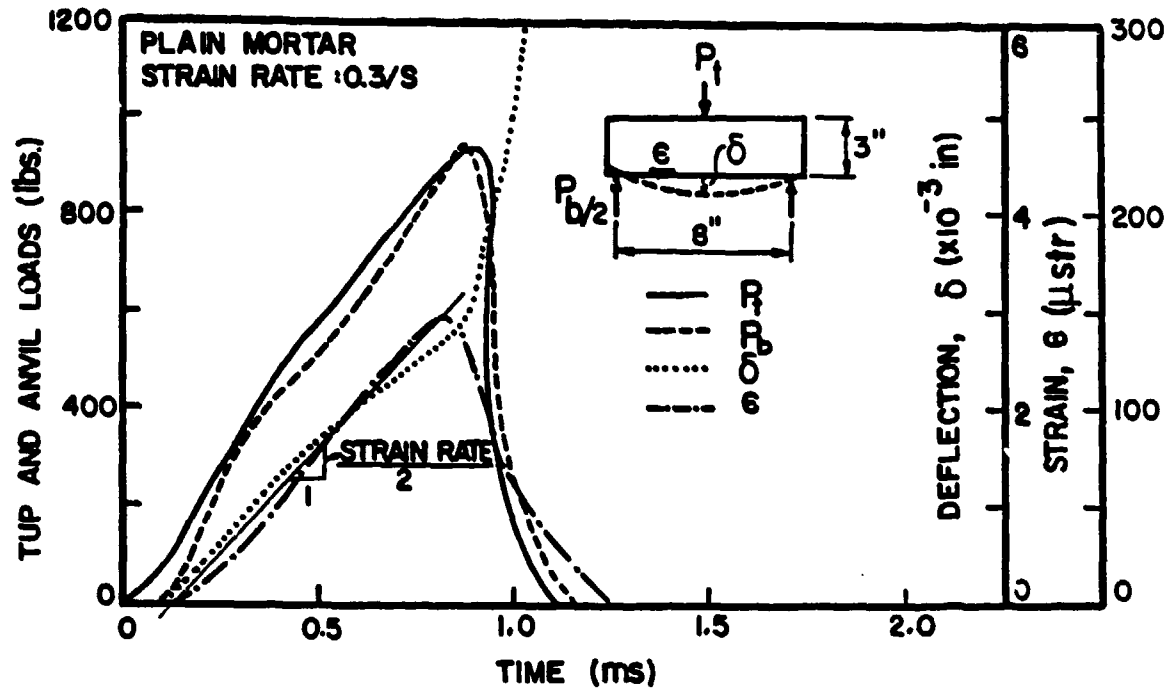


Fig. 5. Typical histories of load (tup and anvil), midpoint deflection and beam strain recorded during an impact event at strain rate of 0.3/s.

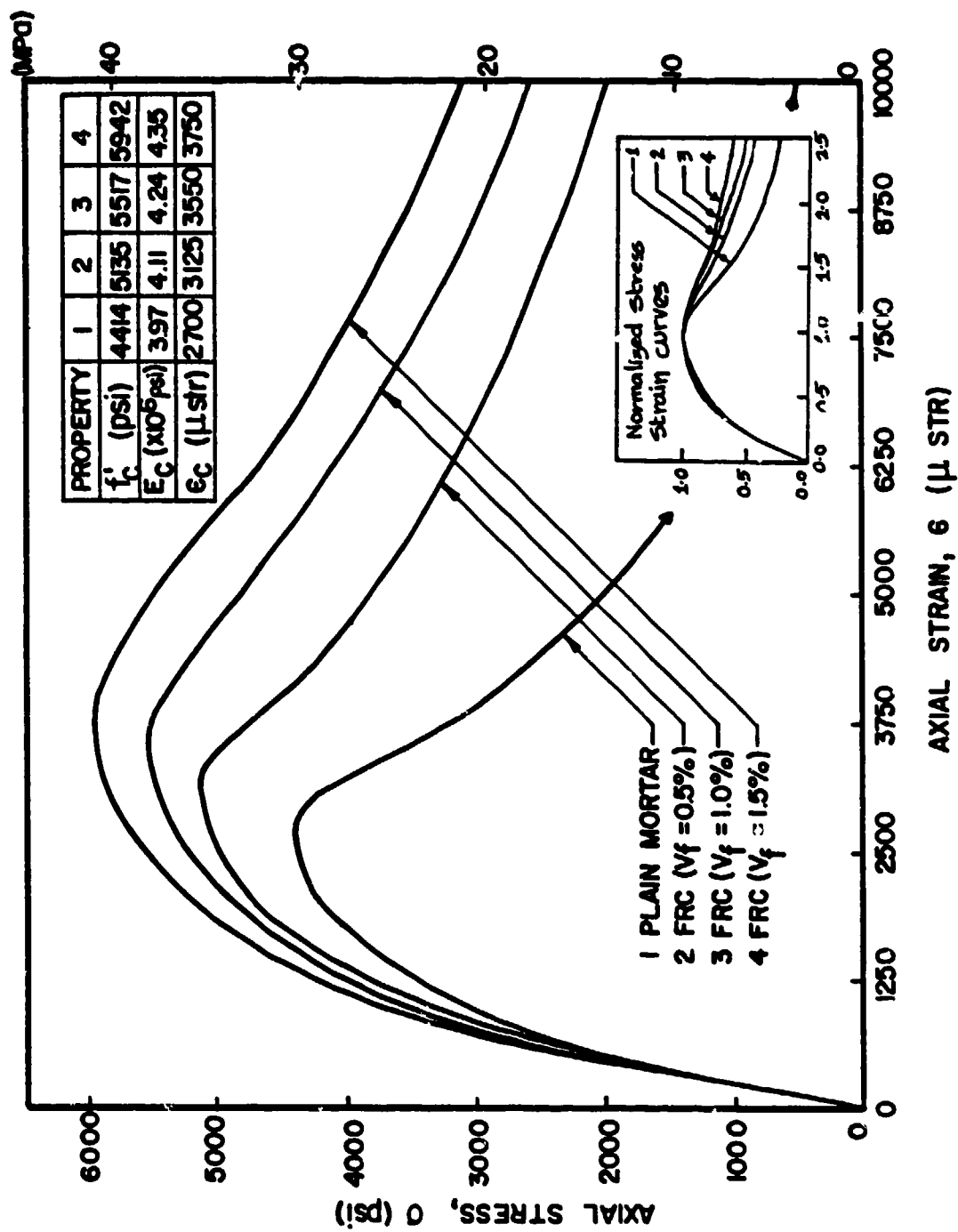


Fig. 6. Results from static uniaxial compression tests on plain mortar matrix and FRC specimens. Inset shows normalized (with respect to peak stress and strain values) stress-strain curves to highlight the effect of the incorporation of fibers.

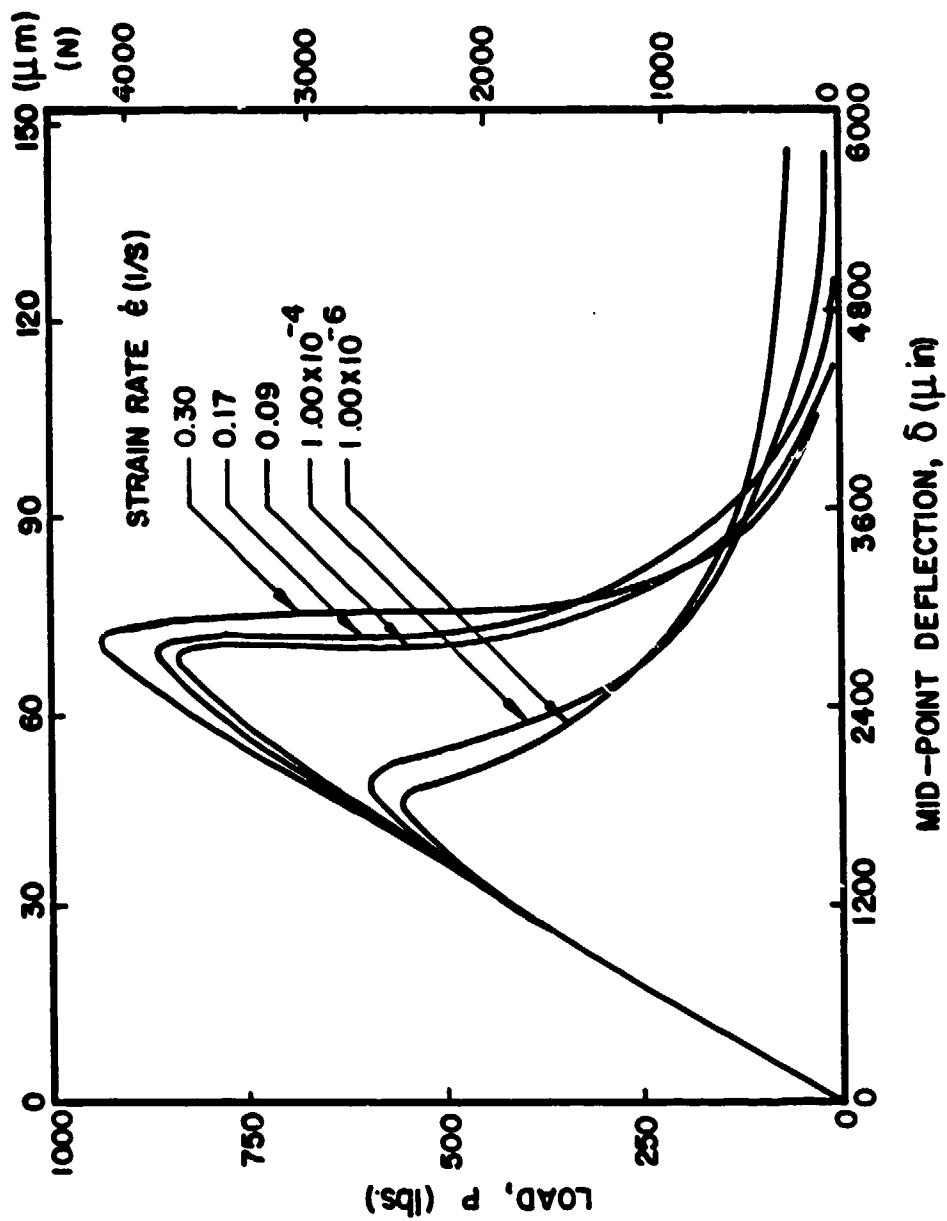


Fig. 7. Typical load-deflection response of unnotched plain mortar matrix beams at different rates of loading

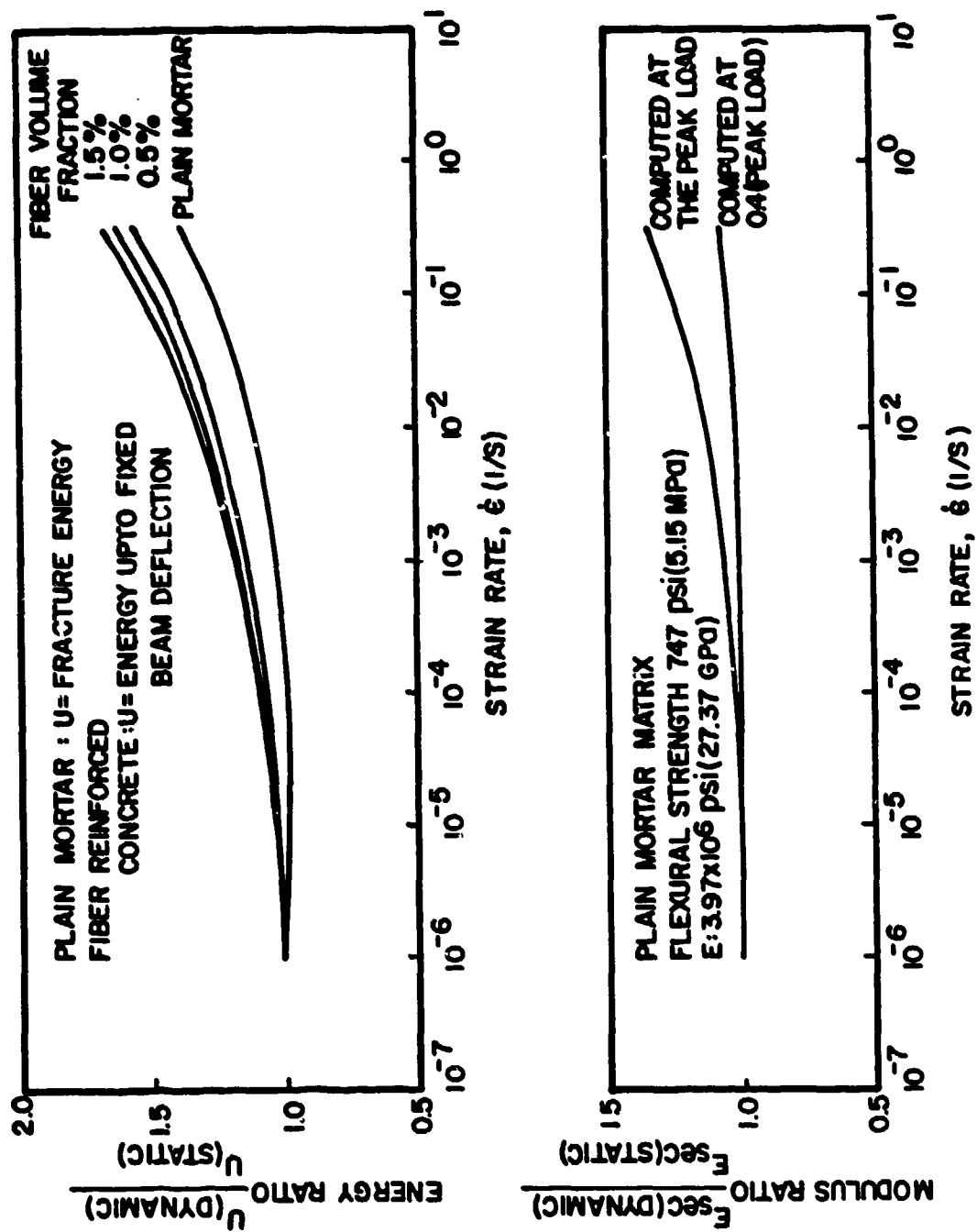


Fig. 8. Effect of strain rate on the elastic moduli and energy of plain mortar matrix.

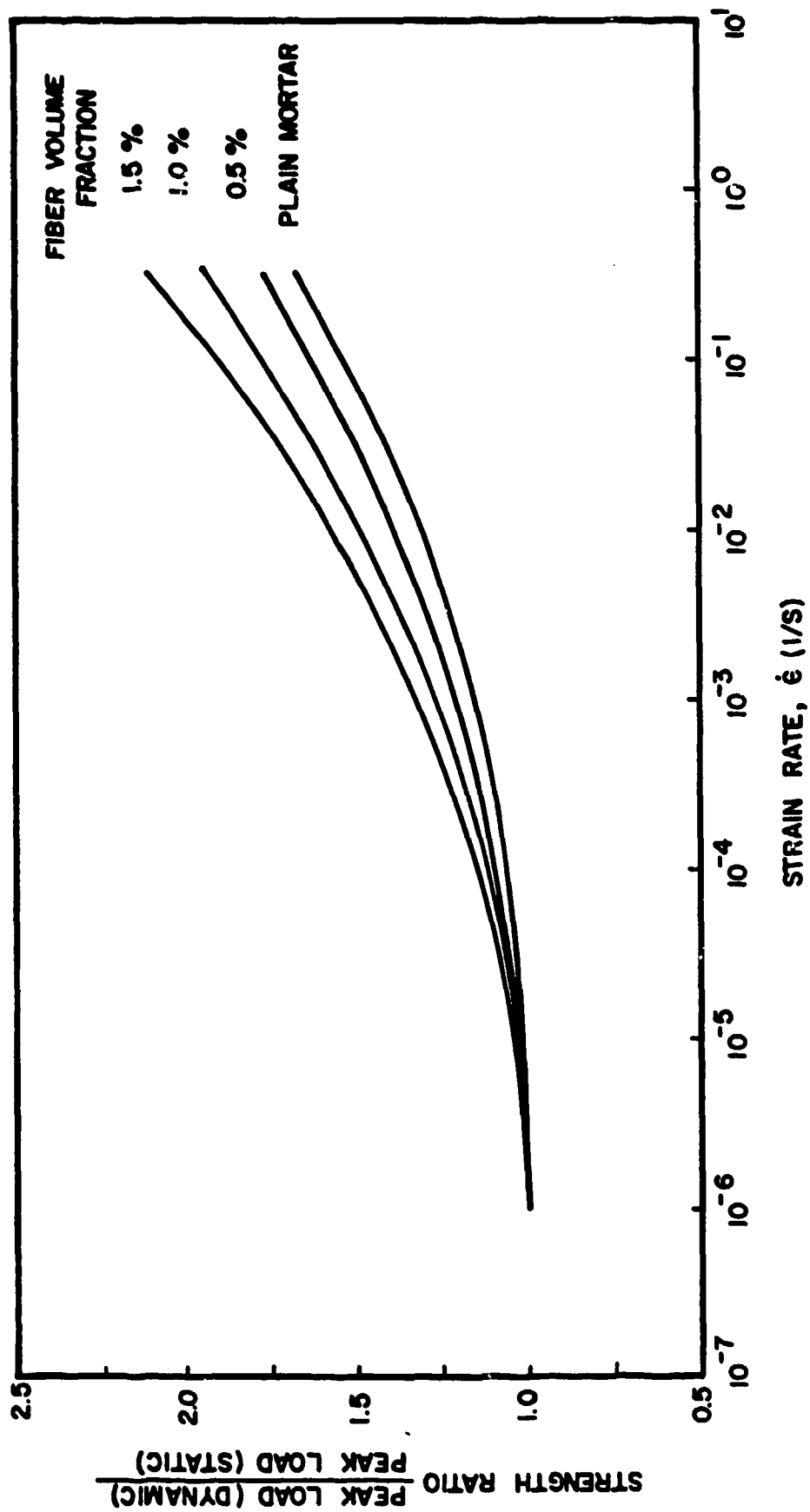


Fig. 9. Effect of strain rate on the flexural strength of unreinforced and fiber reinforced mortar specimens. The influence of fiber content ( $l/d=63$ ) is highlighted in this figure.

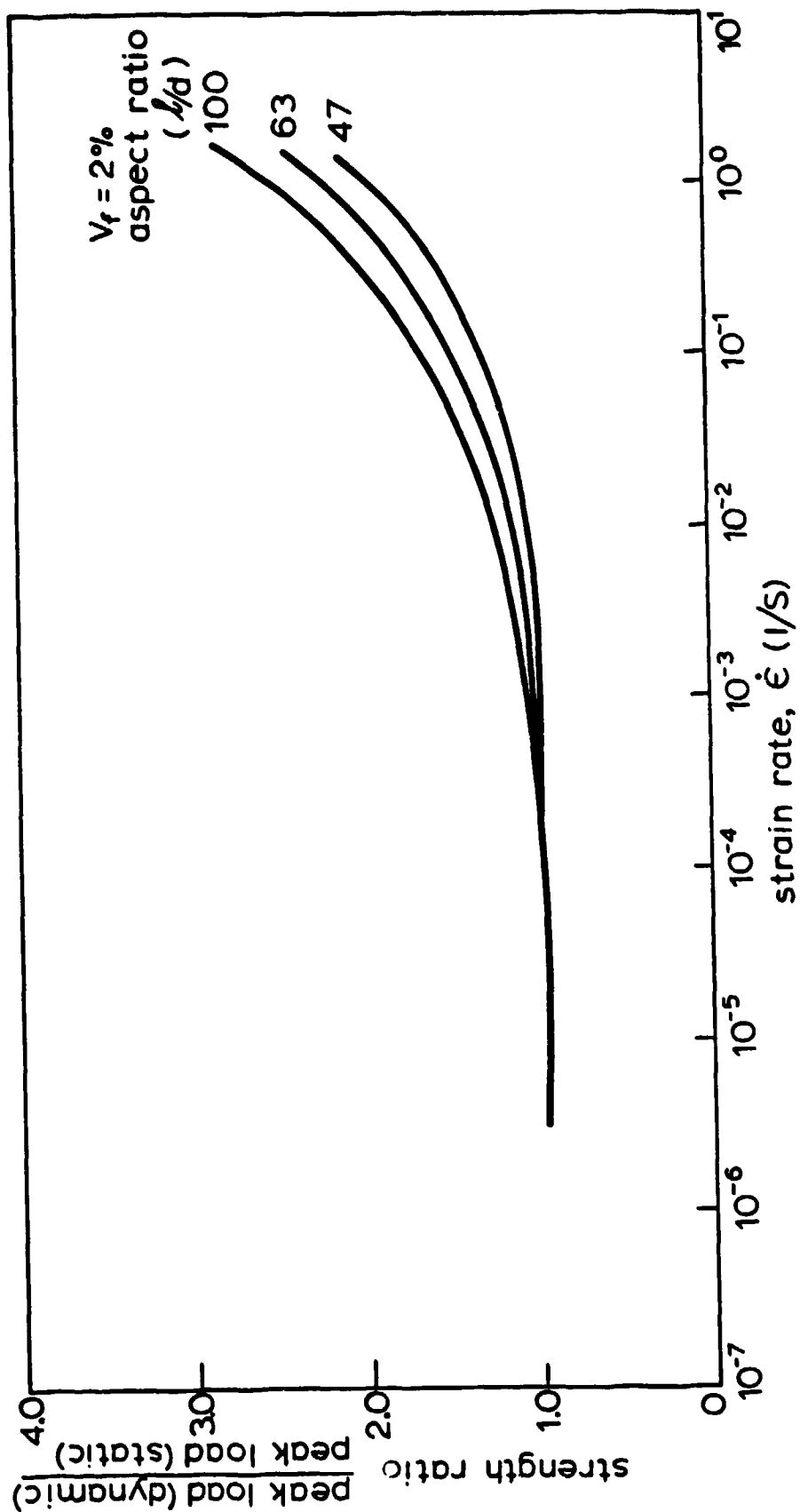


Fig. 10. Effect of strain rate on the flexural strength of unreinforced and fiber reinforced mortar specimens. The influence of fiber aspect ratio ( $V_f=2\%$ ) is highlighted in this figure. Test results from Ref. 7 have been used.

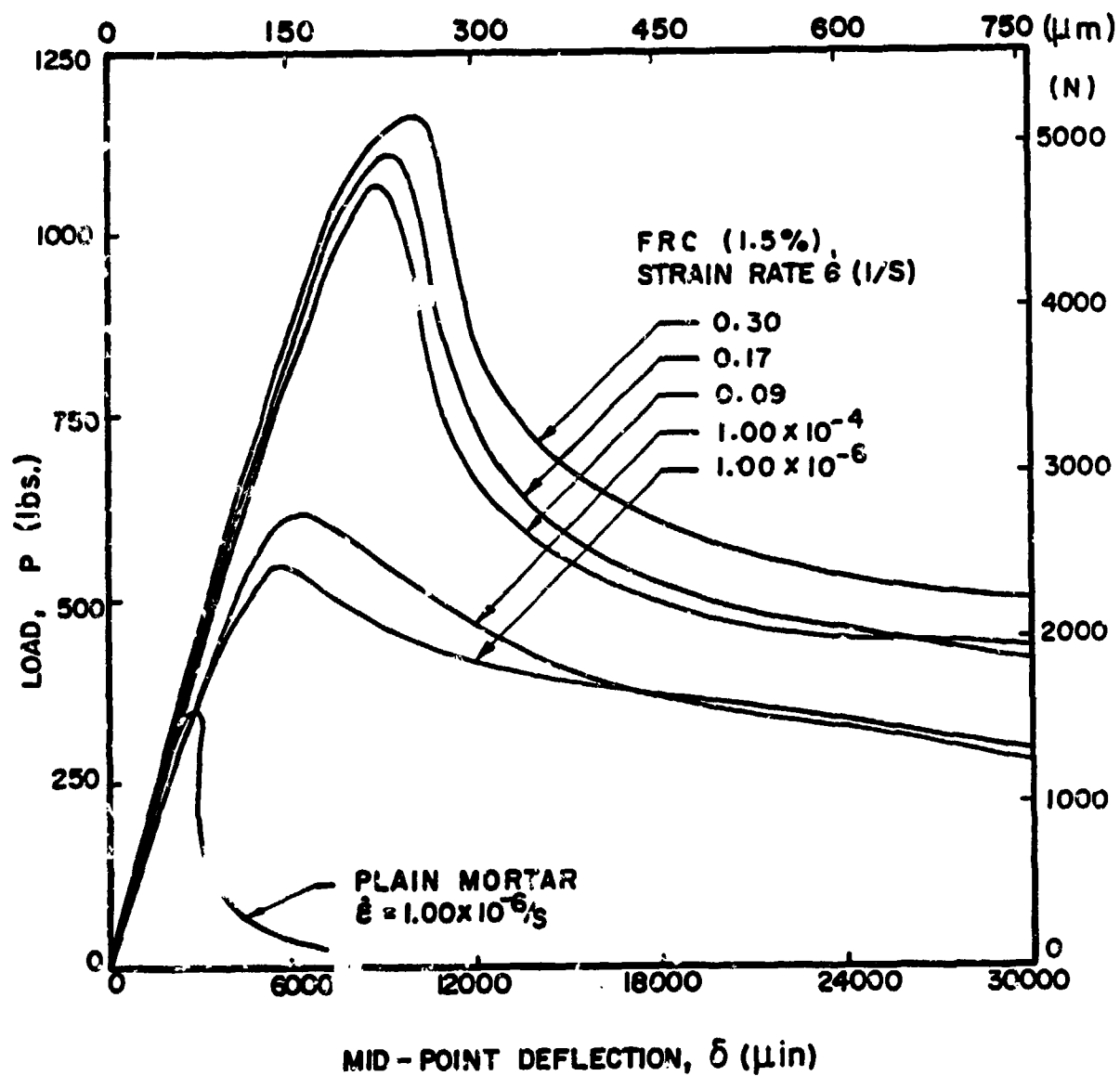


Fig. 11. Typical load-deflection response of notched FRC beams (notch depth = 0.5 in., width = 0.1 in.) at the different rates of loading. ( $V_f = 1.5\%$ ,  $l/d = 63$ )